School
Of
Mechanical Engineering

Thermo-mechanical Analysis of Non-pneumatic Rubber Tyres.

Stephen Harwood

"This thesis is presented as part of the requirements for the award of the Degree of Master of Engineering

of the

Curtin University of Technology"

January 1999

To Veronica

My partner

My wife

My typist

Abstract

This thesis is concerned with the design, analysis and optimisation of semi-solid or non-pneumatic tyres. More specifically, the thesis is intended to show how the FEA software package Abaqus can be used to determine whether or not an 'AirBoss' tyre meets performance criteria in regards load/deformation criteria and if there is a likelihood of failure through overheating of the tyre during service.

The work is intended to clearly explain the nature of natural rubber from a molecular description through to phenomenological descriptions used to solve for stresses, strains, creep and relaxation phenomena and temperature generation through hysteresis losses within the structure of the rubber compound.

The thesis examines practical ways to obtain data for use in the analysis and describes test equipment (both 'off-the-shelf' and purpose built) to obtain the required information.

The objective is to progress, step by step, through the stages of analysis beginning with information to predict static loading conditions for the tyre. Viscoelastic behaviour, such as creep and relaxation are predicted and then tested to determine the correlation and refine test data before proceeding to the next stage of analysis.

Ultimately, a prediction is made as to the temperature distribution throughout a section of the non-pneumatic tyre. A testing rig is described which has been built to test the analysis and enable a comparison to be made between FEA prediction and 'real life'.

Candidates Statement

To the best of my knowledge, this thesis does not contain any material which has been accepted for the award of any other degree or qualification at any educational institution. Material previously written or published by any other person has been acknowledged by due reference.

The proprietary software packages Abaqus from Hibbitt, Karlsen and Sorensen and I-Deas software from Structural Research Dynamics Corporation have been used for design and analysis of the tyre and test-pieces described in this thesis. It is not the author's intention to suggest that these software packages are preferred over others that are available. It is simply the case that these were the tools available to the author at the time of this investigation.

The tyre which is the subject of the investigation has been chosen because it is patented and in production. It may have been a more authentic approach to follow a new design tyre from first stages to final design. This approach was not taken due to consideration of the intellectual and commercial property of AirBoss Tyres Proprietary Limited.

Stephen Harwood

Acknowledgements

The author expresses thanks to the following parties for their assistance in producing this thesis:

Dr. Kian K Teh,
Senior Lecturer Department of Mechanical Engineering
Curtin University of Technology
Perth, Western Australia.

For supervising this project, giving direction to the project and for guiding the author in production of papers and reviewing papers and manuscripts.

The Management of AirBoss Tyre Pty Ltd
2 Norlin Street
Kewdale WA

For providing encouragement and advice and for providing financial assistance including; testing equipment, hardware and software facilities, fees and costs incurred in attending Conferences within Australia and overseas.

CONTENTS

LIST OF FIGURES

List of Symbols

M	.....	Mass, Molecular mass
W	.....	Weight
N	.....	Number of moles
R	.....	Extended chain length
K	.....	Spring constant (newtons per metre)
K	.....	Degree Kelvin
δ	.....	Amount of deflection (metres)
δ	.....	Loss angle
τ	.....	Time constant, period (seconds)
IRHD	.....	International Rubber Hardness Degrees
λ_i	.....	Ratio of stretched length to unstretched length in direction i
σ	.....	Stress (MPa)
I_i	.....	Strain Invariant related to direction i
C_{ij}	.....	Strain energy constant
W	.....	Energy rate (Watts)
m	.....	length (metre)
J	.....	Energy (Joule)
s	.....	Time (second)
T	.....	Circular frequency (Rads.s^{-1})
T_U	.....	Uniaxial stress (MPa)
T_B	.....	Biaxial stress (MPa)
T_S	.....	Shear stress (MPa)
U	.....	Strain energy (joules)
ε	.....	Strain
r	.....	Strain amplitude
ν	.....	Poisson's Ratio
E	.....	Elastic modulus (MPa)
G_R	.....	Relaxation modulus (MPa)
G_O	.....	Glassy modulus (MPa)
kgf	.....	kilogram force
t	.....	time (seconds

LIST OF TABLES

Publications

The following technical papers were produced for publication during the course of this thesis:

S Harwood

"The Compilation and Input of Rubber Data for the Abaqus HYPERELASTIC Option"

Presented at the COMPUMOD Tenth Australasian Users Conference, Melbourne, 1996 and printed in the conference proceedings.

S. Harwood

"The Use of FEA to Predict Heat Build-up in Semi-solid Tyres"

Presented at the 2nd International Conference on Numerical Methods in Engineering. Universiti Putra, Serdang, Malaysia. and printed in the conference proceedings.

INTRODUCTION

THE USE OF RUBBER AS AN ENGINEERING MATERIAL

Natural rubber has been used as an engineering material for over one hundred and fifty years. The process of vulcanisation developed or discovered by Charles Goodyear in 1839 gave to the world a material with unmatched versatility. As shock absorbers, rubber components range in size from the patented 'Inca-block protection' in wrist watches to bollards weighing many tonnes and able to absorb and cushion the docking impact of ocean going ships weighing tens of thousands of tonnes. As vibration dampers, rubber ranges in size from 'buttons' under the feet of sensitive electronic equipment to isolation mounting supports for bridges and multi-storey buildings.

Rubber is a 'hyperelastic' material. In a suitable form, it can be stretched to 1000% of its original length and, when released, return strongly to its undeformed shape. Rubber is corrosion resistant, withstands attack from many chemicals and is impervious to gases and water. Many of the material's properties are modified or enhanced by the addition of chemicals and fillers. Rubber's ability to accommodate impact loads, to deform in order to adopt the contour of the object deforming it and its high coefficient of friction, make it the obvious and unrivalled choice for tyres for well over a hundred years.

Although rubber has no real counterpart in the tyre realm, it has some drawbacks when it is used in the manufacture of solid tyres. Rubber's ability to generate heat due to stress and strain and the degradation of the rubber once the temperature of the rubber exceeds a certain critical point, impose a limit on the amount of work that an item made of rubber can do. Heat generated in the middle of thick sections of rubber can prove problematic, as rubber is such a poor conductor of heat. These virtually insulated pockets of heat can become the point of 'blow-out', a phenomenon similar to the dramatic collapse of a pneumatic tyre due to sudden loss of air pressure.

In the design of rubber components, this property of heat generation must be taken into account. Where it is likely to be a problem, the design must be modified, either to reduce the amount of heat likely to be generated or to promote the dissipation of the heat as it is generated.

THE FINITE ELEMENT METHOD IN ENGINEERING

The finite element method is a numerical method which can be used for the solution of complex engineering problems. The method depends on being able to reduce a complex component or domain into a number of simple elements which are then solved simultaneously. The success of the method depends on the availability of a high speed computer to solve the matrices of equations in a practical time. The method was first developed in 1956 for the analysis of aircraft structural problems [Spyrakos (1994)]. Within a decade the method had been used with success on a wide variety of engineering problems including heat transfer and temperature distribution, electrical potential distribution, fluid flow, vehicle crash simulation, underwater shock problems and a great many more. Many texts are available on this numerical method; Zienkiewicz & Taylor (1989, 1990), Cook, Malkus & Plesha (1989) and others.

In the forty years since its inception, the finite element method has been developed to a point where software to construct the model and solve for stresses, strains and other parameters is available, at reasonable cost, for personal computers. Results are displayed graphically as coloured contours on the model and the model can be displayed as the deformed shape it will adopt under the applied loads.

AIRBOSS TYRES

AirBoss Tyres Limited was established in 1985 as Altrack Limited. The Company has grown from a concept developed by the (now) Chairman of the Company to

being a range of patented designs. Although the designs vary, the basis of the AirBoss non-pneumatic tyre design remains the same. The AirBoss tyre is an otherwise solid tyre which incorporates voids or holes within the structure. The prime purpose of the voids is to increase the amount of deflection which the tyre undergoes for a given load. This increased deformability of the tyre, compared to a solid tyre, gives a cushioned ride which, in many cases, approaches that of a pneumatic tyre.

The job of the AirBoss Design Engineer is to produce tyre designs which fit within the AirBoss umbrella, meet performance criteria set down for the particular tyre (Australian and international standards set out specifications for most tyres) and give optimum performance. The tyres must meet or exceed minimum standards in respect to; wear life, fatigue life and driver comfort. The optimisation of the tyre design has relied on many tools during development of the knowledge base. Currently, a major tool used in design and optimisation of the AirBoss tyre range is 'high-end' finite element analysis software.

The objective of this thesis is to examine the use of the finite element method (specifically, the software package, Abaqus) in the analysis of non-pneumatic tyres made of natural rubber. The analysis is to provide results in two areas; the deflection of the tyre under a given load (including the stresses and strains developed within the tyre due to the applied load) and the temperature likely to be reached under heavy usage of the vehicle fitted with the non-pneumatic tyres.

This thesis proceeds through chapters 1 to 6 from a description of natural rubber, additives and the process of vulcanisation, a description of rubber by way of mechanical analogies, a background of AirBoss tyre development to date, methods of obtaining data for use with Abaqus FEA software and the way in which the data is compiled for submission to Abaqus Solver. The thesis concludes with a prediction of temperature distribution within an AirBoss tyre and a comparison between this prediction and results obtained from a purpose-built test rig.

Chapter 1

NATURAL RUBBER AND COMPOUNDS.

1.1 INTRODUCTION

Natural rubber is harvested from the rubber tree (Hevea Brasiliensis) as latex, a whitish liquid that is tacky to touch. The latex is in the form of an emulsion made up of small (5 μm) spheres of rubber suspended in a water base. The harvested liquid is an emulsion of droplets of the natural polymer polyisoprene in a sheath of protein. Within these globules the rubber is in the form of very long chain hydro-carbon molecules, ranging in length from 10,000 to 50,000 carbon atoms along the main chain [Nagdi (1993)].

Once the water has been evaporated, the basis of natural rubber is left. Use has been made of latex in this fashion, however, the real usefulness of the rubber is realised only after it has undergone the vulcanisation process. Vulcanised rubber has properties that set it apart from all other solid materials.

The properties of rubber are enhanced by compounding the natural rubber with various additives. Fillers reinforce the rubber compound and can impart other beneficial properties to it (such as abrasion resistance). Chemicals are added to prevent the compound from curing too quickly or at too low a temperature while others accelerate the curing process once it is subjected to the temperature designated as its curing or vulcanising temperature [Hofmann (1988)].

1.2 EARLY THEORIES ON THE NATURE OF RUBBER

There is a very wide gap in the elastic properties between those of rubber and an ordinary solid. This difference ranges from a factor of about 100,000 in rigidity and about 1,000 to 10,000 in extensibility [Nagdi (1993)]. The first theories to attempt an explanation of these differences postulated some sort of open structure which would permit large displacements in the bulk of the rubber whilst requiring only small strains in structural elements. Examples of such structures are coil springs, lattices and cellular structures.

In the early part of this century, rubber was thought to consist of a lattice-like structure making up the outer sheath of the latex globule. The latex within the globules and between them was described as a 'hydrocarbon fluid'. This model accounted for the apparent incompressibility of the rubber (a high bulk modulus, similar to that of many fluids) and the high degree of deformability, brought about by the cellular network of the sheath deforming in the direction of applied force [Gent (1992)].

Another model consisted of a spiral configuration of the molecule of the rubber hydrocarbon with the tendency to retract being due to residual forces between neighbouring turns of the spiral, associated, in the main, with the carbon-carbon double bonds. If one considers the polyisoprene molecule folded on itself and held in this configuration by forces acting between the hydrogen atoms, then an extension of 300% in moving from the closely packed to the fully extended form is possible . In addition, a further extension of the bulk rubber can introduced by the turning of the extended molecule in the direction of strain bringing the maximum extensibility up to 600% [Treloar (1958)] This model is close to the current picture of the molecular structure of rubber with a more or less irregular, kinked form of molecular chain resulting from rotations about single bonds. This model, shows the importance of the molecules turning to align with the direction of strain.

The flexibility of the polymer chain is maintained by Brownian motion of the atoms throughout the rubber. The structure of the polymer vibrates in a random manner proportional to the temperature. This continual movement ensures that frictional forces between the entangled chains are minimised (Although there is evidence to indicate that friction is a factor in explaining the behaviour of rubber [Turner (1988)]).

The current, generally accepted, theory is based on thermal energy changing as the structure is strained. Vibrations of atoms along the chain will have greater amplitude in a direction perpendicular to the direction of pull, since forces restricting or inhibiting movement in this direction are weak intermolecular forces while the force in line with the extended chains are primary valence forces. The effect of this dissimilarity will be to produce a repulsive pressure between parallel or extended chains. This repulsive pressure will tend to draw the ends of the chains together and so may be considered as equivalent to a longitudinal tension. Under the influence of the lateral, repulsive pressure, the stretched rubber will retract until an irregular, statistically determined arrangement of the molecules and their parts is brought about. Once this statistically random structure is re-established, there will no longer be a resultant, directional effect [Gent (1958)].

1.3 THE CHEMICAL COMPOSITION OF RUBBER.

Although the solution of thermo-mechanical problems in rubber, using finite element analysis, is not derived directly from knowledge of the structure at a molecular level, it is nonetheless valuable to have such an understanding. Many of the early models of the rubber structure were constructed from a macro view of the behaviour of elastomers. The fact that many of these models are not unlike our current understanding of the structure indicates that much of the behaviour of rubber

components can be predicted, in a qualitative way at least, by keeping in mind the general chemical structure of the substance.

The general formula for natural rubber is $[C_5H_8]_n$ The single unit is isoprene and the chain of repeating units is polyisoprene. The repeating, monomer unit contains five carbon atoms and eight hydrogen. There are two possible configurations for the monomer; cis,1,4 isoprene and trans,1,4 isoprene. In the cis configuration, carbon atoms numbers 1 and 4 are on the same side of the double bond, as shown in figure 2.1 below. In the trans configuration, these two atoms are on opposite sides. Natural rubber is virtually 100% cis,1,4,polyisoprene [Osswald & Menges (1995)].

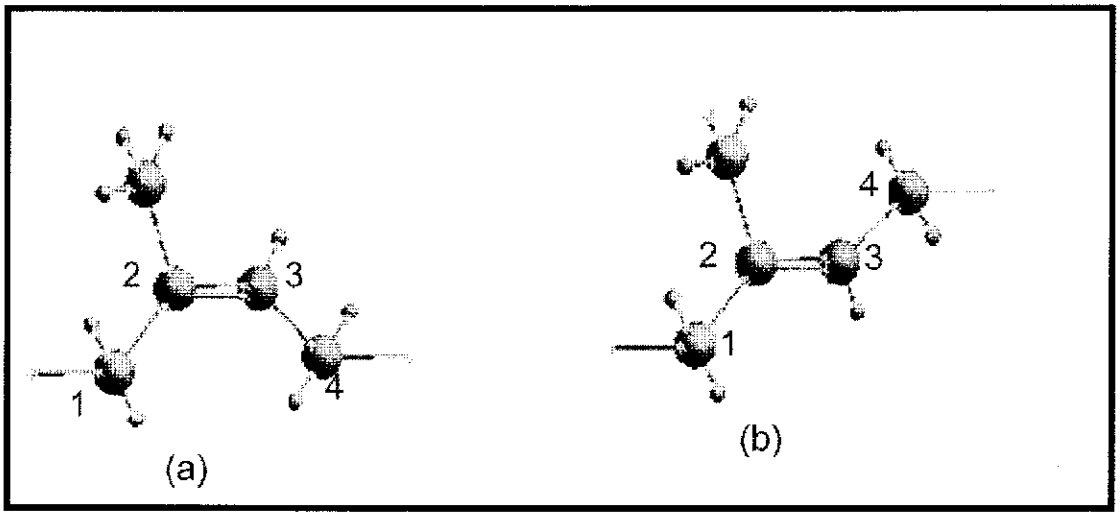

Figure 1.1 Isoprene

(A) CIS 1,4 configuration (b) TRANS 1,4 configuration

Source: Osswald & Menges (1995), Material Science of Polymers.

Once the latex has been reduced and allowed to coagulate, it takes on some of the properties normally associated with rubber. If a piece is stretched and then released, it will retract. A ball made of latex will rebound strongly if dropped to the floor. However rubber in this state is of little or no engineering value. If a piece is stretched and held, it will quickly neck and break. If it is made to support a load then, over a period of time the rubber will flow, allowing the load to sink through it. For rubber to

become an engineering material is must undergo the process of cross-linking by vulcanisation.

The carbon-carbon covalent bond makes an angle of approximately 109.5 degrees. The angle between the double bond and the adjacent carbon-carbon bond is close to 125 degrees. The double bond does not permit rotation so the distance between atoms 1 and 4 is fixed, apart from variations in interatomic distance due to internal energy changes. The single bond does allow free rotation (subject to the 109.5 degree angle being maintained) [Bhowmick & Stephens (1988)].

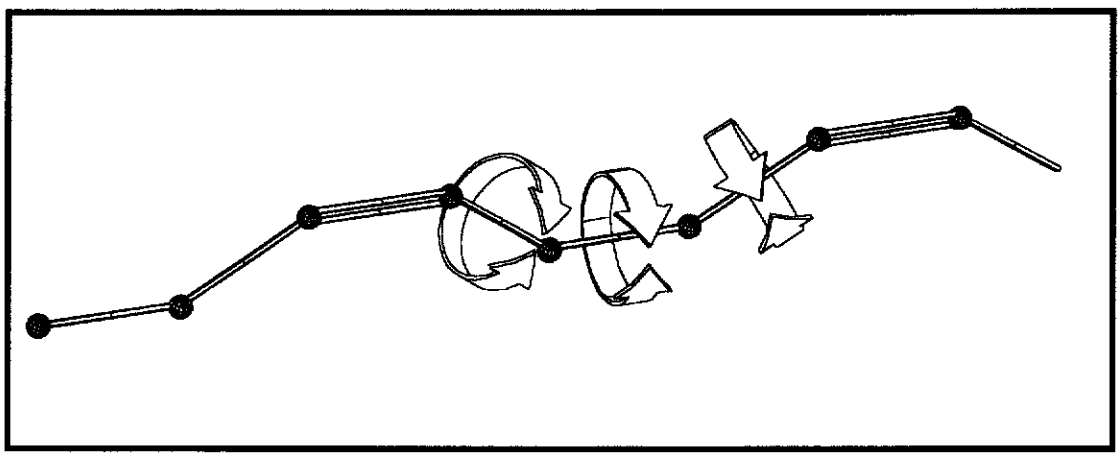

Fig 1.2 Possible rotations in the molecular chain.
Rotation about the single C-C bond is unhampered, but no rotation is possible about the double bond.
Source: Crandall, Dahl & Lardner (1978), An Introduction to the Mechanics of Solids.

The orientation of the molecular chain can be regarded as statistically random as can the mass of the chains. Two useful numbers arise from this random distribution of chain orientation and size;

The average molecular mass (which can be interpreted as average chain length)

$$M=W/N \qquad (1.1)$$

Where W is the weight of a sample and N is to number of moles in the sample.

In Natural rubber, the average molecular mass is, approximately, 5,000,000 atomic units, since there are four carbon atoms on the main chain for each repeating unit and an average of 30,000 repeating units on a chain. Each unit having an atomic mass of 68 gives the above average mass. The distribution is approximately normal with a standard deviation of 10,000 atomic units [Mark, Erman & Eirich (1978)].

The mean square end to end distance of a molecular chain. If the chain were fully extended, the length (R) would be

$$4*n*l \tag{1.2}$$

(four times the number of repeating units times the distance between carbon atoms on the backbone). Since the rotation about the single bonds is unrestricted, the distance between ends becomes a statistical matter. For a collection of chains which do not interfere with each other Aklonis (1972) derives the expression below

$$r^2 = \frac{1}{p}\sum_{i=1}^{p} r_i^2 \tag{1.3}$$

Where r_i refers to the end-to-end distance of the i^{th} chain and p to the number of chains.

For a system of chains where every configuration of chain has an equal probability, the mean square end-to-end distance becomes;

$$r^2=n*l^2 \tag{1.4}$$

Since uncured or 'green' rubber exhibits many of the properties associated with cured elastomers, There must be some forces acting within the structure to give it the

properties of an elastic solid. These two characteristics are weak atomic or Van der Waals forces acting between more active sites on adjacent chains and physical entanglements of the chains.

If one were to picture a rod of uncured rubber being stretched and clamped and the structure necking until rupture occurs, then one might picture the internal mechanism being that of molecular chains straightening in the direction of strain and sliding past each other while, at the same time, Van der Waals bonds breaking and (perhaps) being reformed at other sites as the flow-to-rupture process continues.
Although uncured rubber is very rarely used as an engineering material, weak atomic forces and chain entanglements are a significant feature of vulcanised rubber components and can impart desirable or undesirable characteristics to the component [Rosen (1971)].

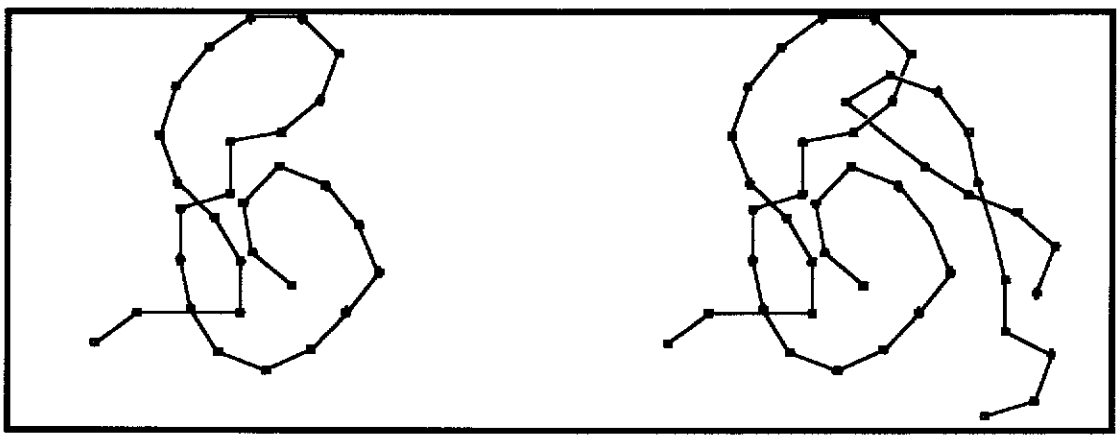

Figure 1.3 Isoprene as freely jointed rigid-linked chains
Left, isoprene monomers as links in a freely jointed chain
Right, entanglements in freely jointed chains

Source: Mark, Erman & Eirich (1978), Science & Technology of Rubber.

1.4 THE VULCANISATION PROCESS

Vulcanisation takes place by mixing sulphur with the green rubber (carbon black or silicon granules are added at the same time as filler material) and subjecting the compound to elevated temperature. Usually, prior to the vulcanisation process, the compound is masticated to raise the temperature and render the compound even less rubber-like. The masticated compound behaves like plasticine or putty. In this state the rubber compound is shaped into the desired component, often by squeezing it into a mould tool and holding it in this manner whilst applying heat. Vulcanisation takes place at temperatures of 130°C and above.

Vulcanisation or cross-linking takes place when sites on the polymer chain become active and can accept or donate electrons to free radicals provided by the vulcanising agent. The cross linking process is completed when the carbon-carbon double bond site on a neighbouring chain is broken and joined to the radical site. The most common procedure for vulcanisation of natural rubber is to add .05 % sulphur to the uncured rubber together with accelerators such as organic peroxides, shape the compound into its final form and then heat. Once cross linking has taken place, the rubber component cannot be reshaped. The chemical process for cross linking by sulphur is shown schematically bellow.

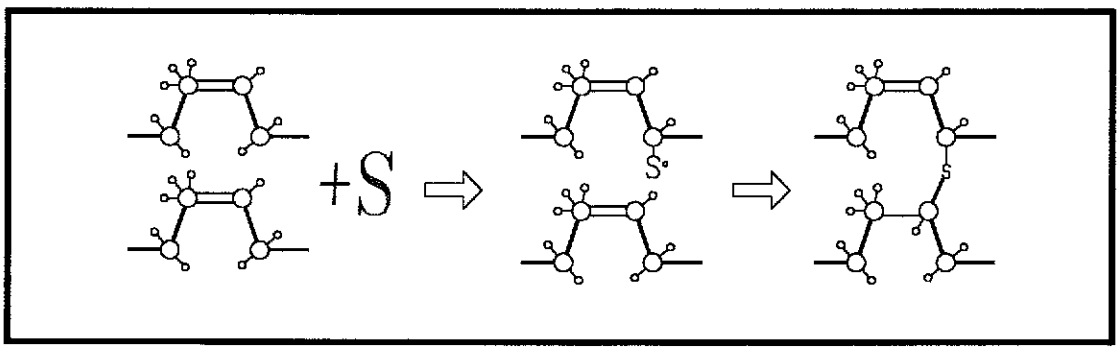

Figure 1.4 Cross-linking via free radicals

Source: Mark, Erman & Eirich (1978), Science & Technology of Rubber.

The cross-linking via free radicals takes place when a sulphur donor displaces a carbon atom to become an active site on one chain followed by breaking of the C-C double bond on an adjacent chain and subsequent cross linking.

This cross-linking takes place at the applied temperature, which categorises rubber as a thermo-setting polymer. Thermoplastics become solid when they cool. They can be remelted (and reshaped) by applying heat. Vulcanised rubber and thermo-setting plastics cannot be returned to their pre-vulcanised state.

On average, only about one in 3000 potential crosslink sites are actually linked. If the link density is increased (by adding more sulphur to the mix, say) the rubber become stiffer. If the majority of sites are linked the rubber becomes ebonite, a material that is akin to hard wood.

Figure 1.5 below is a schematic drawing of three potential states of rubber compound;

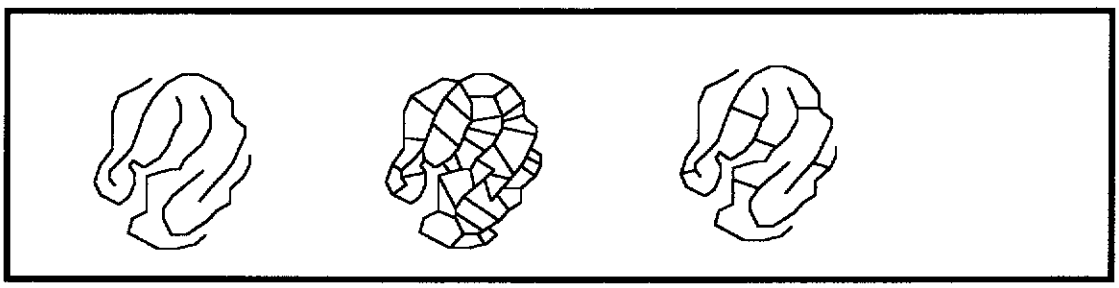

Figure 1.5 Three possible degrees of cross-linking. From left to right

- Uncured rubber, no cross-linking (only chain entanglements).
- Rubber with greater than 5% sulphur. The greater than optimum number of links make the material hard and relatively inflexible. (Ebonite)
- With this small percentage of sites fixed, the rubber component takes on the properties normally associated with rubber.

Source: Mark, Erman & Eirich (1978), Science & Technology of Rubber.

The cross linked structure is a three dimensional matrix. As can be seen from figure 1.6 (below), cross-linking can result in three chain configurations;

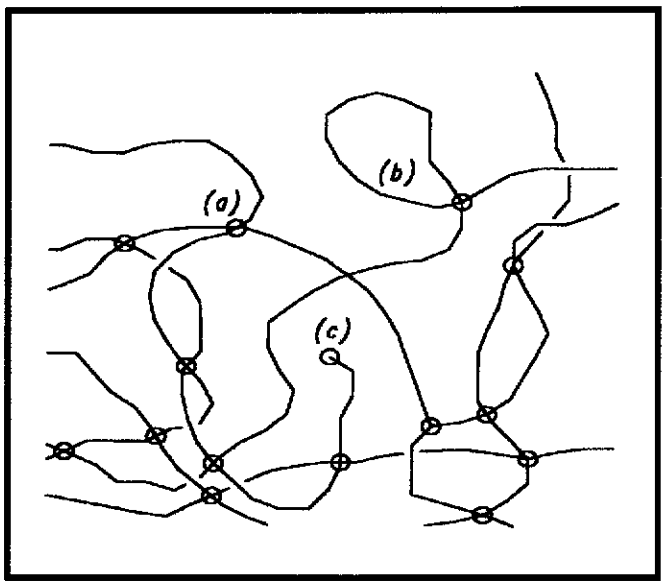

Figure 1.6 Results of various cross link positions

(a) Chains linked at sites along the length of their chains.

(b) Looped chain

(c) An orphaned chain end

Source: Hofmann (1988), Rubber Technology Handbook.

We now have an image of a compound made up of macromolecules of polyisoprene, linked at various points to other macromolecules. The vulcanised compound contains many more sites where the movement of adjacent chains is impeded by weak atomic forces acting between active regions of the neighbouring molecules. A third impediment to flow within the rubber is the physical entanglements of the macromolecules. The final feature of vulcanised rubber which is needed to explain its properties is the inclusion of particulate fillers.

1.5 THE USE OF PARTICULATE FILLERS.

Virtually all components made from natural rubber are reinforced with particulate fillers. In the vast majority of cases this reinforcing filler is carbon black (In this study, carbon black is the only filler used in the rubber compounds. However, zinc oxide which is discussed later, acts as a filler but is added to compounds for other reasons). It is not uncommon for fillers to increase the ultimate properties of vulcanised rubber (tear and cut resistance, abrasion resistance etc) by up to tenfold.

The degree of reinforcement provided by a filler depends on a number of variables, the most important of which is the development of a large polymer-filler interface. This large interface can be furnished only by particles of colloidal dimensions. Spherical particles of one micrometre in diameter have a specific surface area of six square metres per cubic centimetre. In practice such a particle would be too large to be useful for most reinforcing applications.

Carbon black is produced by the incomplete combustion of hydrocarbons or by thermal cracking. Although it is useful to think of filler particle size in terms of the diameter of individual spheroids, in fact, the carbon black is invariably in the form of agglomerations of these particles consisting of fifty to a hundred spheroids.

By virtue of their morphology the aggregates are bulky and occupy an effective volume considerably larger than that of the carbon itself. The bulkiness of the aggregates is the property commonly called 'structure.' "High Structure" refers to a high degree of bulkiness and a high capacity to absorb oils and "Low Structure" refers to the converse.

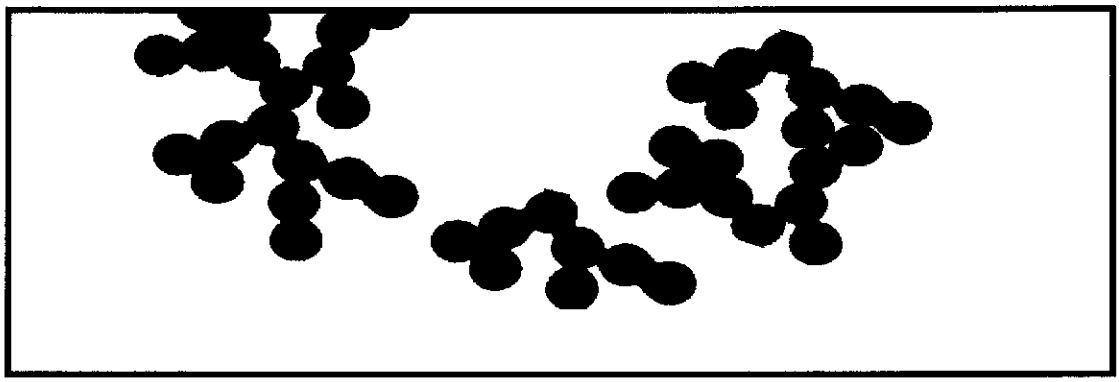

Figure 1.7. Schematic of carbon black agglomerates consisting of fused primary particles..

Source: Gent (1992), Engineering with Rubber, How to Design Rubber Components.

A practical scale of structure can be constructed in terms of the results of various tests which involve absorption of some vehicle (commonly iodine or nitrogen) from an aqueous solution. The "iodine number" is a measure of the surface area of the filler which is available for bonding with rubber compound. The Nitrogen Adsorption number is a more accurate measure of the surface area of the carbon black but it includes the area of small voids in the particles which cannot be entered by rubber compound and so remain as micro-voids within the final structure. The Iodine Number is given as the amount of iodine adsorbed (in grams per kilogram of carbon black). The Nitrogen Adsorption Number is given as surface area per kilogram. Knowledge of surface area per gram plus the average particle size gives a good indication as to the manner and degree to which a chosen carbon black filler will modify rubber properties.

The American Society of Testing Materials has established a carbon black classification system based essentially on particle size and structure. Table 1.1 below shows the range of ASTM numbers and the corresponding average particle diameter as well as the surface area per gram.

Range of ASTM numbers	Nominal average particle size (nanometres)	Nitrogen Adsorption Number M^2 /Kg $*10^3$
900-999	201-500	7 – 9
800-899	101-200	15 – 20
700-799	61-100	28 – 32
600-699	49-60	35 – 42
500-599	40-48	40 – 45
400-499	31-39	52 – 73
300-399	26-30	88 – 115
200-299	20-25	99 - 110
100-199	11-19	105 – 120
000-099	1-10	110 – 150

Table 1.1 ASTM Carbon Black designations and typical properties

Source: American Society for Testing Materials Annual Book 1993.

1.5.1 PHYSICAL & CHEMICAL INTERACTIONS AT THE FILLER SURFACE

Although fillers can impart beneficial properties to the vulcanised compound, even if there is no chemical bonding at the filler – rubber interface, chemical bonding leads to the unique combination of mechanical properties which make carbon black the best overall reinforcing agent known.

Carbon black surfaces contain functional groups capable of reacting with polymer molecules to form grafts during processing and vulcanisation. Numerous reactions of hydrocarbon polymers with carbon black have been demonstrated. Several possible mechanisms exist by which grafts can be formed. Some examples are;

- Carbon blacks chemisorb olefins at vulcanisation temperatures. The degree of chemisorption is increased in the presence of sulphur.

- Shear-generated polymeric free radicals have been shown to graft to the carbon black during mixing.

- Hydrogen can be exchanged between rubber and bound hydrogen situated at the edges of the large aromatic ring molecules that make up the layer planes of carbon black.

The addition of fillers also increase the elastic modulus of rubber. This change in the value of modulus may be advantageous or disadvantageous depending on specific requirements and application.

Although other chemicals are added to rubber compound, they do not affect the properties of concern in this work to any significant degree. Agents to increase the rate at which curing takes place or to enhance the ease with which it can be processed prior to vulcanisation are important additives as are additives to reduce the likelihood of attack from oxygen or oils. However, the effect of the chemicals on hysteretic heat generation or upon the elastic properties is not great.

For the rubber compounds under consideration here, we now have a near-complete picture of the structure of rubber. Several compounds have been trialled to find the optimum performer for non-pneumatic tyres, these have included synthetic-natural rubber blends as well as all-natural rubber. The compounds of 100% natural rubber have proven superior, for non-pneumatic tyres, in every case. The process of finding the optimum compound is now a choice between compounds containing various concentrations of carbon black filler and various structures of filler

Chapter 2

MECHANICAL ANALOGIES OF RUBBER .

2.1 INTRODUCTION

The early views of the structure of rubber were of a collection and arrangement of spring elements and linked chains with various degrees of rotational freedom or some other mechanism which would explain the properties of rubber in terms of easily visualised mechanical units. Much of the current understanding of rubber is also based on this approach. The three main mechanical analogies used to describe the behaviour of rubber are; an arrangement of coil springs, dashpots and sliding blocks. Properties of rubber such as its ability to generate heat internally due to straining can be explained in terms of irreversible work done in moving dashpots.

There are applications where the rubber component can be thought of as a completely elastic element (an elastic band, a catapult, a rubber ball and so on). However, there are several characteristics of rubber that demand a more complex model to describe it.

- If a rubber-band-like piece of vulcanised rubber is stretched and clamped at its ends in such a way that the force exerted by the piece can be monitored, it will be seen that, over a period of time, that force will diminish until a final, steady force is established.

- In a similar manner, if a weight were to be suspended from a rubber test piece, such that a constant force is acting upon the piece, it would be observed that the elongation of the test piece would increase (at a diminishing rate) until a final, stable, elongation is attained.

- If a piece of rubber is squashed (say clamped in a vice) and left in the deformed state for some hours, when it is released, it will not return completely to its original shape but, instead, take on a permanent 'set'.

- A rubber component, deformed and released repeatedly will become warm to touch.

All the above phenomena have been explained in terms of mechanical models consisting of various permutations and combinations of springs, dashpots, links and sliding blocks.

2.2 MECHANICAL MODELS OF RUBBER

The two most often used models are the Voigt and the Maxwell elements. The elements of these models are arrangements of springs and dashpots as shown in figure 2.1 below.

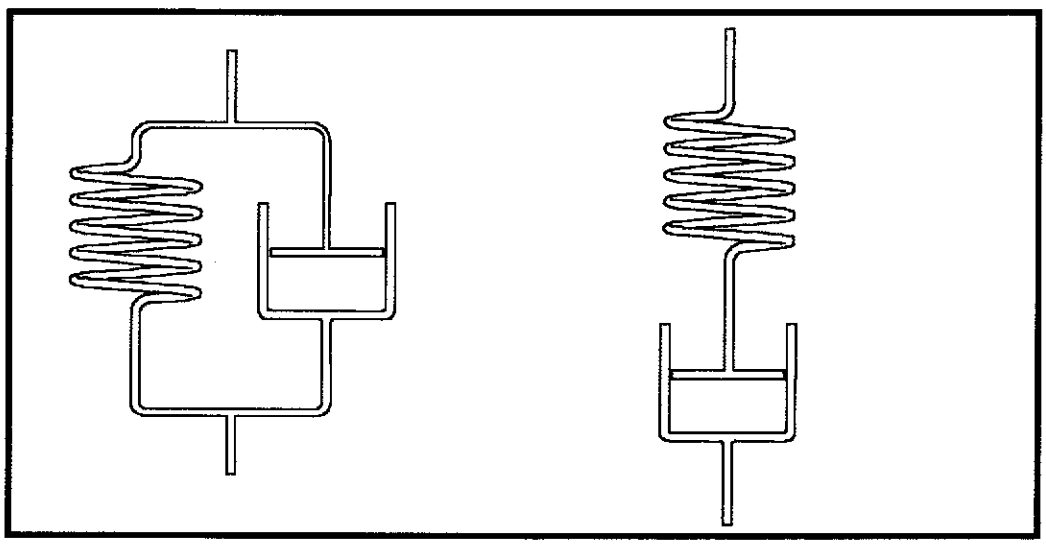

Figure 2.1 Mechanical models of vulcanised rubber
Left, Voigt Element, right, Maxwell element
Source: Ward & Hadley (1993), Mechanical Properties of Solid Polymers

Both elements go part of the way to describe the behaviour of rubber. If rubber were entirely an elastic material, then an instantaneously applied stress would produce an instantaneous strain which would not change further. Figure 2.2 shows a schematic of a piece of rubber undergoing instantaneous strain and a graph of the force to maintain that strain diminishing over time.

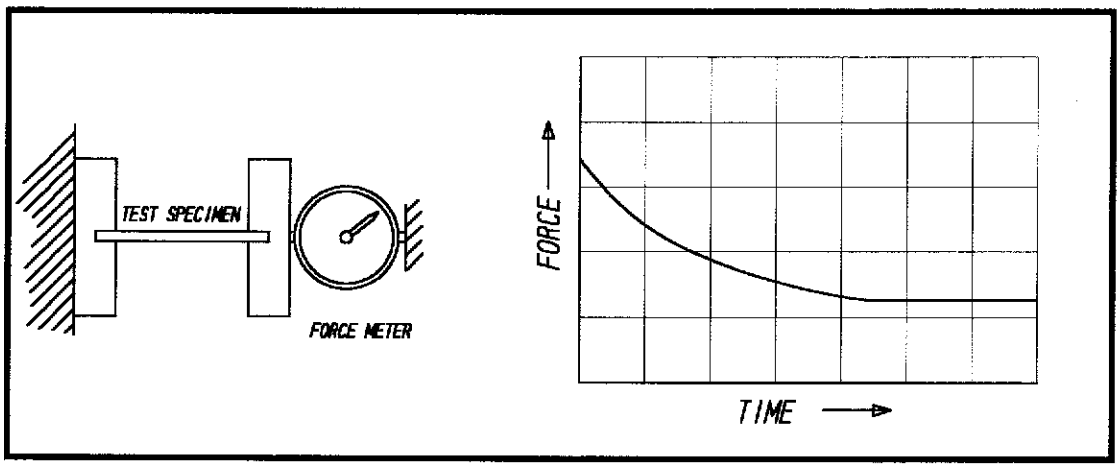

Figure 2.2 Plot of force required to maintain constant strain versus time

Source: Ward & Hadley (1993), Mechanical Properties of Solid Polymers.

One could imagine the Voigt element being strained and clamped. The spring stretches instantly followed by movement in the dashpot allowing the spring to relax.

If a force is suddenly applied to the Maxwell element, the result would be as shown in figure 2.3 below.

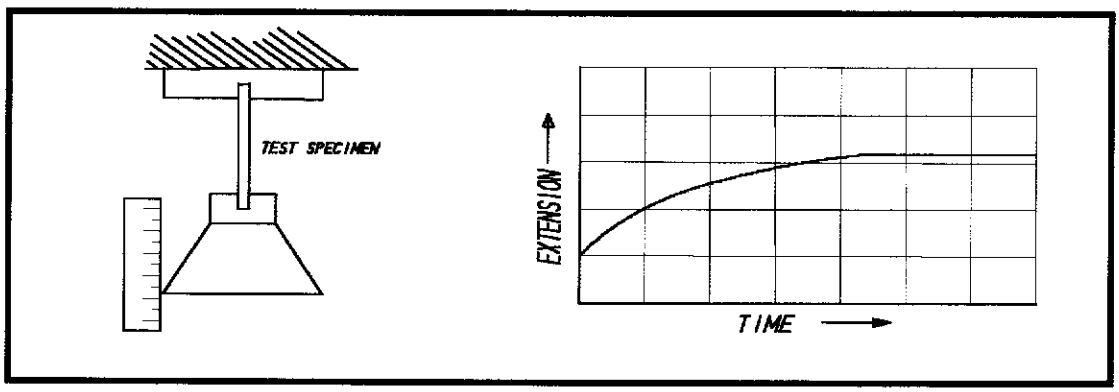

Figure 2.3 Plot of test-piece elongation with constant load versus time

Source: Reference Ward & Hadley (1993), Mechanical Properties of Solid Polymers

With the model of figure 2.3, the applied force does not move instantly but 'creeps' due to the dashpot, until the spring force matches that of the applied force.

The majority of the mechanical characteristics of natural rubber can be explained as combinations of the maxwell and Voigt elements. A simple combination of the two will be used to derive material constants for use with Abaqus Finite Element software.

2.3 THE METHOD OF HEAT GENERATION IN RUBBER COMPONENTS.

When rubber components are repeatedly deformed, they produce heat. Heat generated in this way is hysteretic. Hysteretic heat generation can be explained by the mechanisms already discussed in Chapter 1. In terms of the molecular structure of rubber, the heat is a result of flow within the network. When the rubber is deformed, strain energy initially stored within an element of rubber is sufficient to cause weak bonds between neighbouring molecular chains to break and allow the chains to slide past each other. This internal movement, which takes place in the direction of strain, is akin to laminar, viscous flow. When the strain is reversed, a similar amount of flow occurs in the opposite direction. Since irreversible work has been done in causing flow to take place, that work appears as heat.

A similar and, possibly, easier way to visualise the method of heat generation is to consider the spring, and dashpot arrangement comprised of the Voigt and Maxwell elements shown in figure 2.4 below.

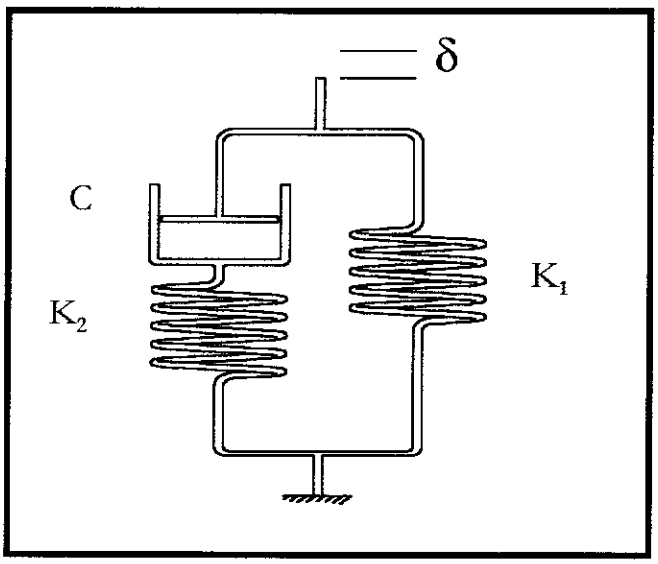

Figure 2.4 a combination of Maxwell and Voigt elements.

Source: Ward & Hadley (1993), Mechanical Properties of Solid Polymers.

When an element of rubber is deformed, the spring component stores the energy. The energy stored in the spring is;

$$0.5*K*\delta \qquad (2.1)$$

where K is the spring constant (newtons per metre)

δ is the amount of deflection (metres) which the spring element undergoes.

The dashpot element cannot store energy. Energy that is expended upon the system to displace the dashpot must be stored within the system in some other form and that form is heat energy which leads to a rise in temperature.

If the element shown at figure 2.4 is displaced an amount δ at time t=0, a graph of force versus elapsed time would be as appears in figure 2.5 below.

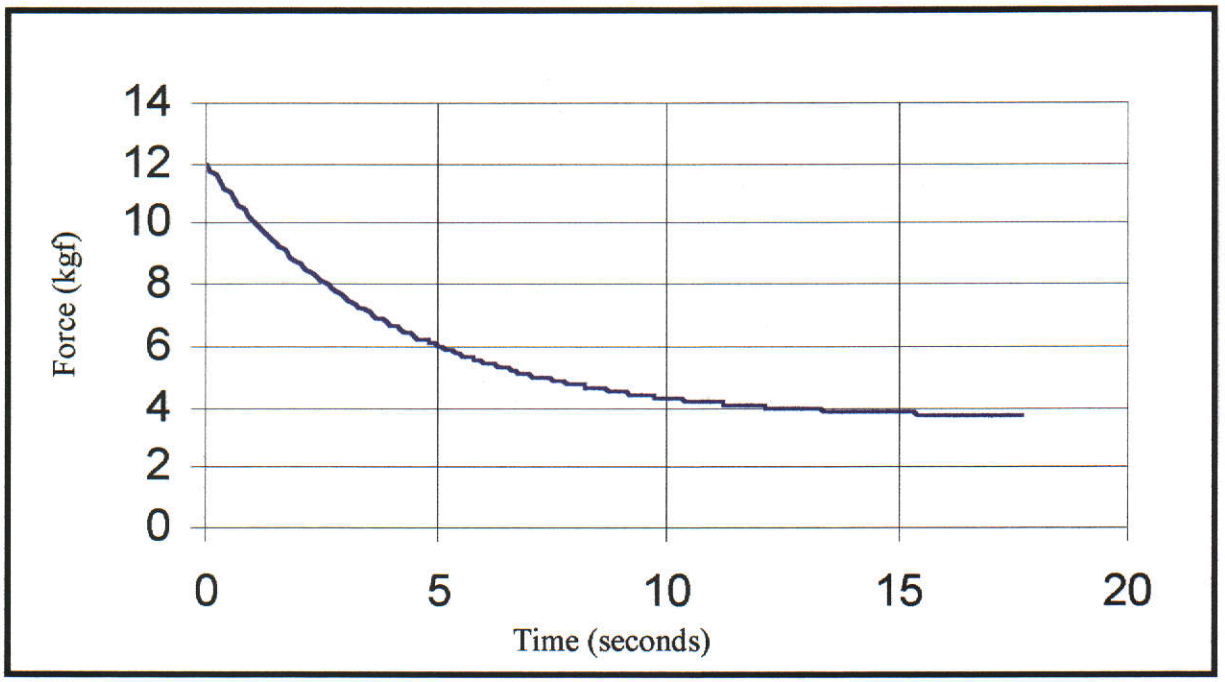

Figure 2.5 Force decaying with time for the Maxwell Voigt element

Source: Ward & Hadley (1993) Mechanical Properties of Solid Polymers

In the case of a suddenly applied displacement of δ, the dashpot continues to move until the spring in line with the dashpot has regained its undeformed length. The energy expended in moving the dashpot is then 0.5*K*δ The energy initially stored in the in-line spring is converted into heat energy due to the viscous losses in the dashpot. This is analogous to the losses within the structure of a rubber component due to similar, viscous flow.

If the rubber component which the spring/dashpot element represents has unit cross-sectional area then, with the constant strain parameter, the elastic modulus is proportional to the value of the force.

The graph of figure 2.5 would be similar if the spring and dashpot arrangement were replaced by a test piece made of vulcanised rubber. If it is assumed that the cross

sectional area remains constant and that the length of the test piece divided by the cross sectional area and by the deflection has the constant value of unity, then the force is equal to the value of elastic modulus. Three important parameters can be read from the graph;

- The instantaneous or 'glassy' modulus, $K_1 + K_2$ (Force at time = 0)
- The long term or fully relaxed modulus is K_1 (Force for large value of time)
- The decay constant, which governs the rate at which the elastic modulus decreases can be derived from the expression which describes the curve, namely

$$K_R(t) = K_1 + K_2 * e^{-t/\tau} \qquad (2.2)$$

If the values above were derived experimentally, then the value of τ can be derived by a 'best fit' method.

Graphs of force versus deflection for the Maxwell element and for the Voigt element subjected to a constant strain rate (velocity) are shown below. The shaded portion under the graph represents the total energy (stored and lost) within each element.

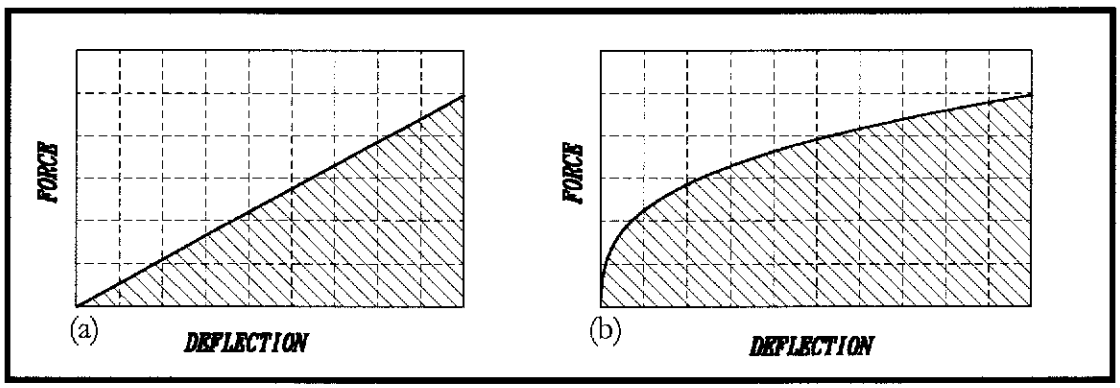

Figure 2.6 Force/deflection (energy) in (a)Maxwell and (b) Voigt elements

Source: Mark, Ermann & Eirich (1978), Science and Technology of Rubber.

If the combined Maxwell-Voigt element shown at figure 2.4 is subjected to a sinusoidally varying strain of amplitude r and circular frequency T (rads.sec^{-1}) then a plot of force versus time would appear as shown in figure 2.7

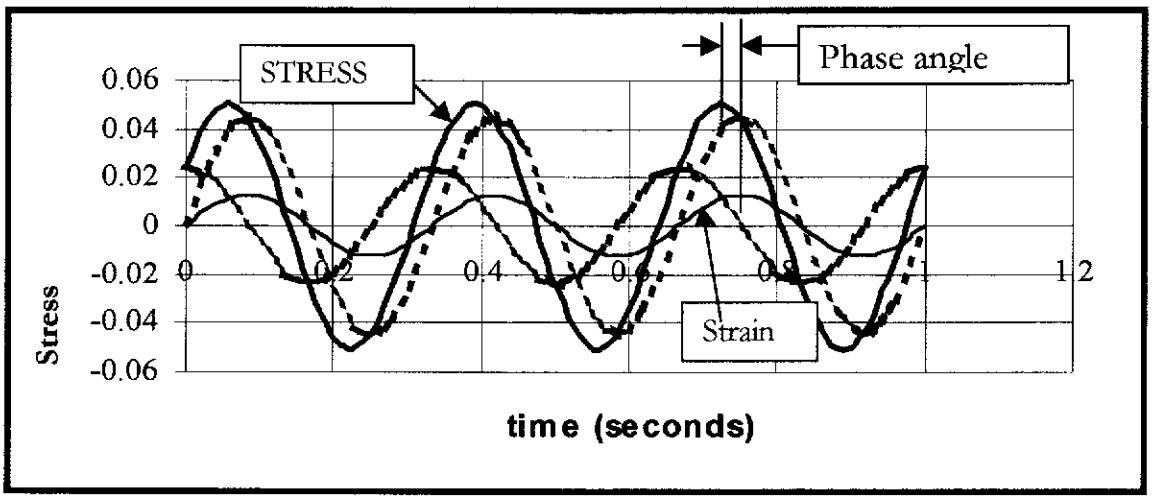

Figure 2.7 Stress response to an applied sinusoidal strain.

Dotted lines represent decomposition of response into in phase and out-of-phase components.

Source: Mark, Erman & Eirich (1978), Science and Technology of Rubber.

The graph shows four sets of data; the sinusoidally applied strain (lowest peak-to-peak curve), the resulting force (or stress). The two dotted curves are the components of the resultant force broken into two components; the in-phase (the force due to the spring elements) and the out-of-phase component which lags the applied strain by 90°

The out-of -phase component of force is the force due to the dashpot. The energy expended in moving the dashpot is 'lost' while the energy expended in moving the springs is stored and returned to the system.

The in-phase and out of phase components of the stress/strain curves give rise to the 'dynamic modulus', which is the vector sum of the storage and loss moduli as shown in Figure 2.8. The figure shows the dynamic or complex modulus which is the vector addition of the storage modulus (arising due to the spring like nature of rubber) and

the loss modulus (due to the dashpot or laminar viscous nature of rubber). The loss angle (arctangent of the ratio of loss modulus to storage modulus) is a value often quoted in the description of a compound.

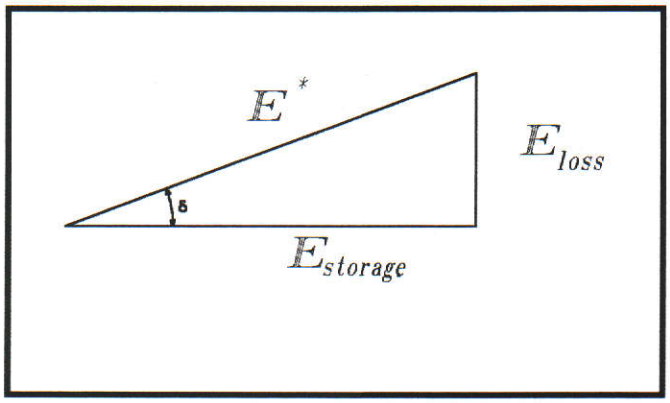

Figure 2.8 The vector addition of the storage and loss moduli gives the complex elastic modulus.

Source: Ward & Hadley (1993), Mechanical Properties of Solid Polymers.

Table 2.1 below shows the variation of loss angle and several other material parameters with carbon black loading for several natural rubber compounds. The loss or phase angle varies with temperature. The values below are for 25°.

Carbon black Loading (pph)	IRHD	Loss angle (degrees)	Resilience	Shear modulus (Mpa)
0	43	0.8	88%	0.47
15	48	2	83%	0.53
20	52	3	81%	0.55
55	56	5.8	70%	0.79
60	66	7.2	68%	0.95
85	77	9.7	56%	1.12

Table 2.1 Variation of keys parameters with carbon black loading

Source: American Society of Testing Materials Annual Book 1993

- Hardness is determined by resistance of the surface to deformation by an indentor of specified dimensions and specified load. The scale of hardness is from zero (infinitely soft) to 100 (bone hard). The scale is either IRHD (International Rubber Hardness Degrees) or Shore Hardness. The scales are equivalent.

- Resilience is expressed as the percentage of energy returned during a single rebound test. The test used to derived the values below is a 'Lupke Pendulum', a swinging arm with a striker of specified mass which is dropped to impact with a rubber test piece. The height to which the pendulum returns is the resilience. The resilience could also be measured by dropping a ball made of the rubber from a height of (say) one metre and then measuring the height to which it rebounds. If the ball returned to a height of one metre (100% resilient). It could be pictured that the compound consisted entirely of spring elements.

- Shear modulus for rubber is analogous to the shear modulus for steel and other elastic materials. However the shear modulus for rubber varies with the amount of strain. Therefore the moduli of rubbers can only be specified completely by giving the amount of strain at which the shear modulus applies. For the table above, the amount of strain is 50%.

Figure 2.9 below shows a graph of the variation of major parameters with carbon black loading.

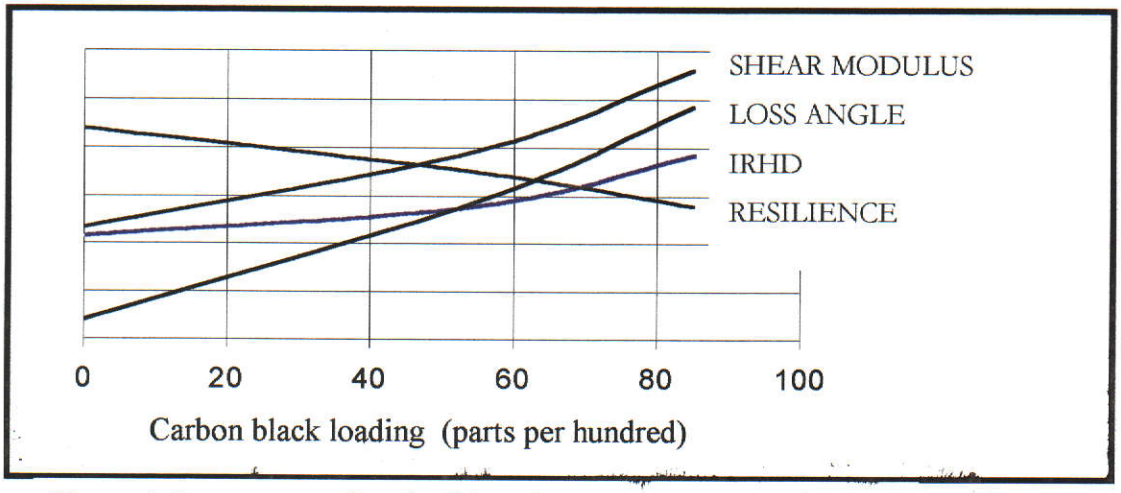

Figure 2.9. Graph of data from table 2.1

It is of interest to compare the IRHD hardness measurement with the shear modulus. The scatter plot below (figure 2.10) is taken directly from the Natural Rubber Engineering Data Sheets.

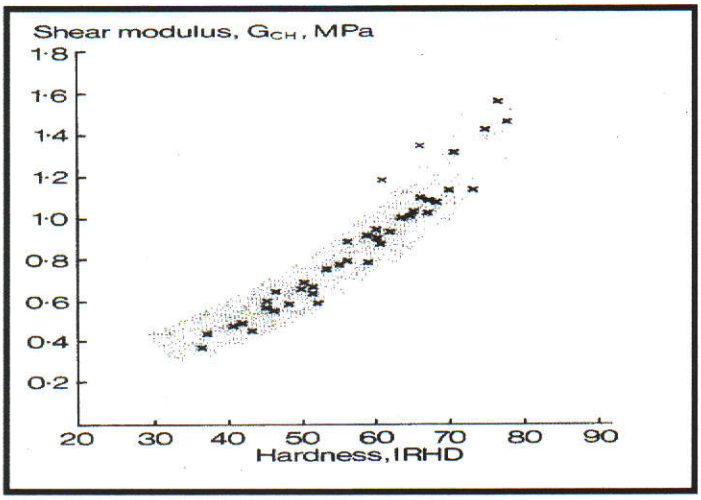

Figure 2.10 Scatter plot of hardness Vs shear modulus

Source Malaysian Rubber Research Institute Engineering Data Sheets

The value of shear modulus is the basis of material properties for analysis of rubber components under static loads. The value of shear modulus can be approximated from the above plot if the hardness value is known. The value of hardness can be determined by the hand held Durometer pictured in figure 2.11 below. The Durometer gives a direct readout of the IRHD hardness).

Figure 2.11 Hand held Durometer

Source: AirBoss Tyres Limited and Teclock Instruments

Chapter 3

AIRBOSS TYRES

3.1 INTRODUCTION

AirBoss Tyres Limited has its head office and R&D Centre located in Kewdale, Western Australia. AirBoss design and manufacture non-pneumatic tyres. Currently, a range of AirBoss tyres is available to suit the following types of vehicles;

- Skid steer loaders
- Loader backhoes
- Forklift trucks
- Scissor lift platforms
- Site dumpers
- Ride on mowers
- Trenching machines

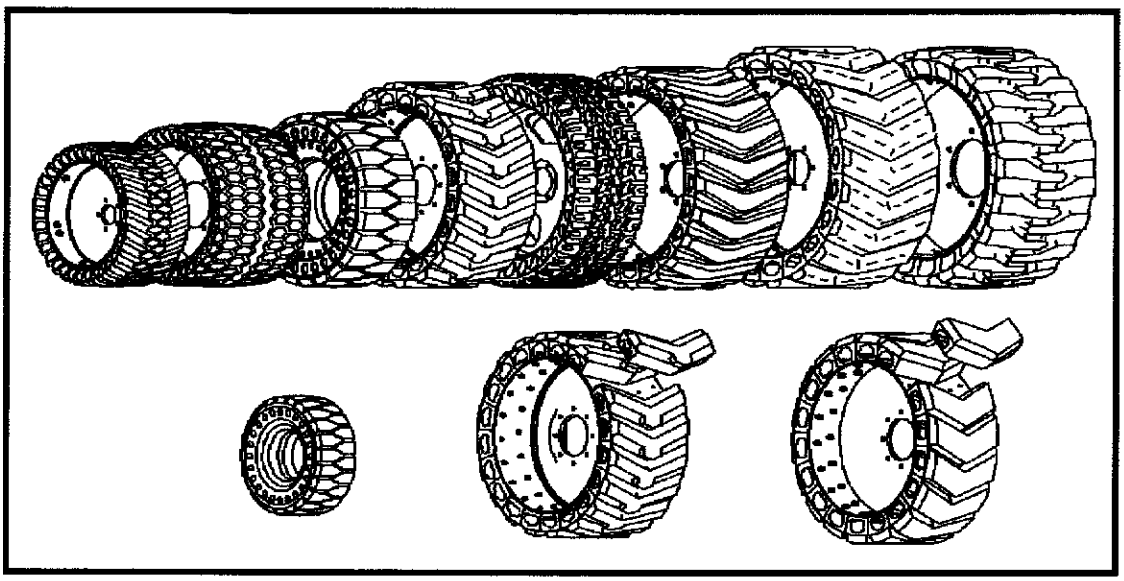

Figure 3.1 AirBoss tyre range

Source AirBoss Tyres Limited

AirBoss semi-solid tyres have found success in applications where punctures pose a serious handicap to production or a significant risk to personnel. Such applications as building demolition sites, scrap metal yards and rubbish tips are areas where a pneumatic tyre can be written off within an hour.

One alternative is to use solid rubber tyres which, while overcoming the puncture problem, give a very harsh ride. The concept of the AirBoss semi-solid tyre is that it is a solid or non-pneumatic tyre that has holes or voids incorporated into the body of the tyre. These holes increase the amount of deflection for a given load on the tyre. In this way the tyre gives a more cushioning effect than a solid tyre. The design objective is to produce tyres which give a ride approaching the comfort of a pneumatic tyre whilst being able to withstand staking and catastrophic rubber loss without being rendered unusable. Naturally, it is a requirement that the tyre has a similar life to that of its pneumatic or solid equivalent. The graph below shows data taken from three tyres subjected to a load-deflection test.

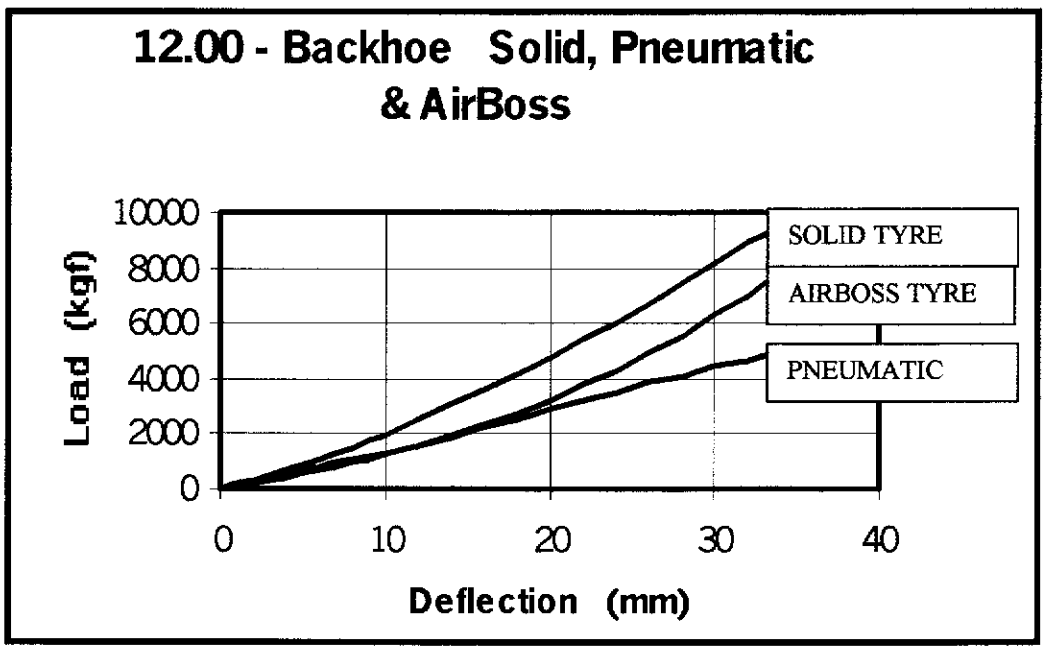

Figure 3.2: Load versus deflection curves for AirBoss tyres, solid and Pneumatic tyres.

The pneumatic tyre requires the lowest force to deflect the tyre a given amount. It can be seen that the relationship between load and deflection is almost linear for this tyre. This might be expected since the deflection is inhibited by pressurised air which is subject to the gas law: volume is "inversely proportional to pressure". Over the fairly small range of pressure changes brought about by varying loads on pneumatic tyres, pressure increase is proportional to load increase and deflection of the tyre is proportional to volume change. The near-linear load deflection characteristic of the tyre and the amount that the tyre deflects in response to a sudden change in load (say, hitting an irregularity in the road surface) are responsible for the superior comfort of the pneumatic tyre.

The full solid tyre is extremely robust in service. However it is also a very heavy tyre and the most uncomfortable for vehicle operators.

The AirBoss tyre is a compromise. As can be seen from the figure 3.2 above, the load deflection curve (hence the degree of driver comfort) lies between that of the pneumatic and solid tyres. At light loadings, the curves are very similar. As the load increases, the stiffness of the tyre rises quickly.

3.2 GENISIS OF AIRBOSS TYRES

AirBoss Tyres Proprietary Limited was established (as Altrack Limited) in 1987. The concept of the AirBoss tyre was the brainchild of the (now) Chairman of AirBoss, Alan Burns. Some years earlier, Mr Burns had been a surveyor in the mining and minerals industry.

Surveying in Western Australia, as in most mining states, often involves travelling large distances over virgin bush-land to remote locations. A major cause of vehicle breakdowns is tyre damage. After bush-fires, many shrubs remain as nothing more than the root system and a few inches of wood sticking out of the ground. These 'stakes' often puncture and tear the side-wall, rendering the tyre irreparable. The usual precautions are to take up to eight spare tyres and then, when there are no spares left, head gingerly for home-base.

Strategies employed to overcome the possibility of becoming stranded in difficult terrain involve some method of making the tyres puncture proof. Many of the puncture proof tyres have other drawbacks that make them less than ideal;

- Solid tyres have one distinct advantage, they work. They are the strongest of all tyres and are almost indestructible. They are also the heaviest of all tyres. It is virtually impossible to manhandle them into position to fit them to the vehicle (because solid tyres are not legal for highway service, all four tyres must be changed at the point where the vehicle leaves the road). Solid tyres have little 'give'. They do not readily deform to cushion the ride. For this reason, they are uncomfortable and even worse, the harsh ride can result in damage to the running gear of the vehicle.

- Foam filled tyres make the tyre immune to fairly minor damage. The foam is in the form of an aerated rubber which, while lighter than solid rubber, makes the tyre difficult to handle. If the foam filled tyre is damaged by staking, the tear that usually results allows the foam to ooze out and the tyre soon becomes unusable.

- Cushion solids, with a resilient rubber encased in a wear resistant rubber, give a good ride. However, they tend to be expensive and heavy.

The first AirBoss tyres were designed for four-wheel-drive vehicles. The prototypes soon led to the 'segmented' tyre which has proved successful for slow-moving, off-road equipment such as backhoe loaders, skid-steer loaders, graders and so on. Today, the emphasis is on development of one-piece tyres which will cater for the industrial, off-road and possibly some on-road applications.

Figure 3.3 shows the development of AirBoss tyre design from the original prototype (looped conveyor belting, bolted to a fabricated rim) to the segmented tyre.

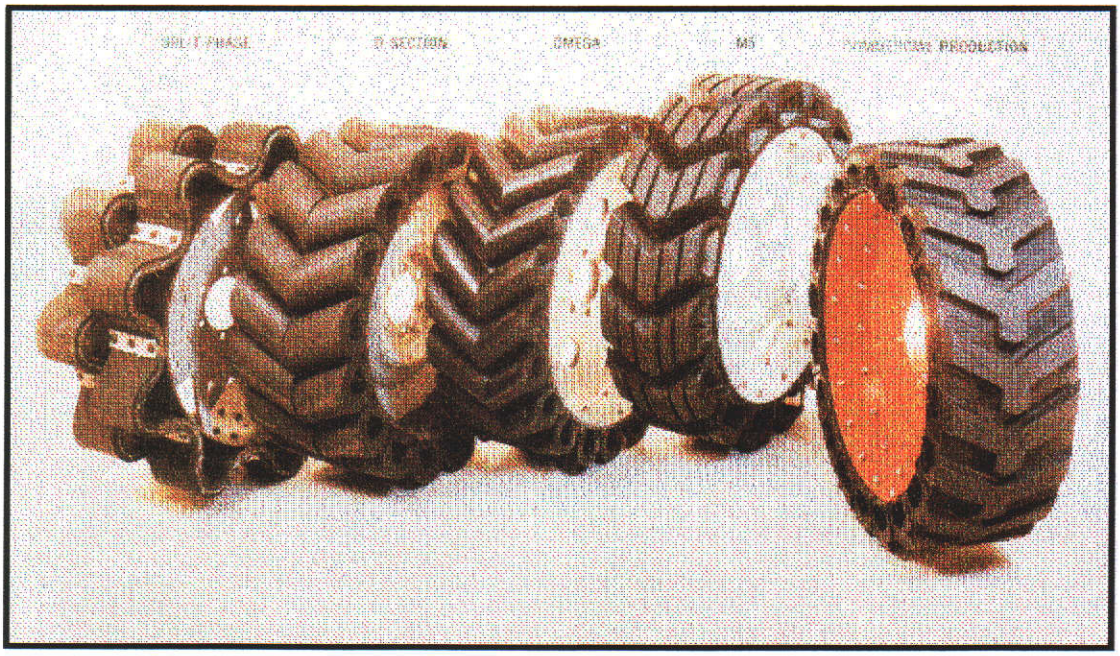

Figure 3.3 Early prototype tyres

The tyre on the right of figure 3.3 is the first commercial AirBoss tyre. The tyre was first developed for the skid-steer loader market. One of the main attractions of a tyre built up from a series of chevron shaped segments is that individual segments can be replaced as necessary. If one segment is torn and damaged beyond being useable, that one segment can be replaced rather than the entire tyre. The segment and the procedure for replacing a single segment appear below.

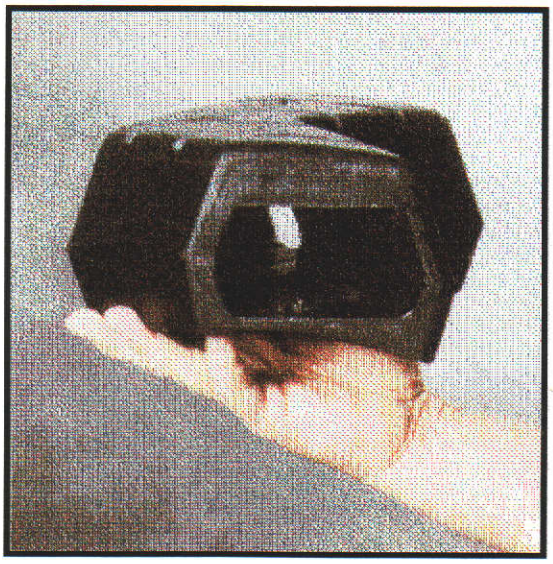

Figure 3.4

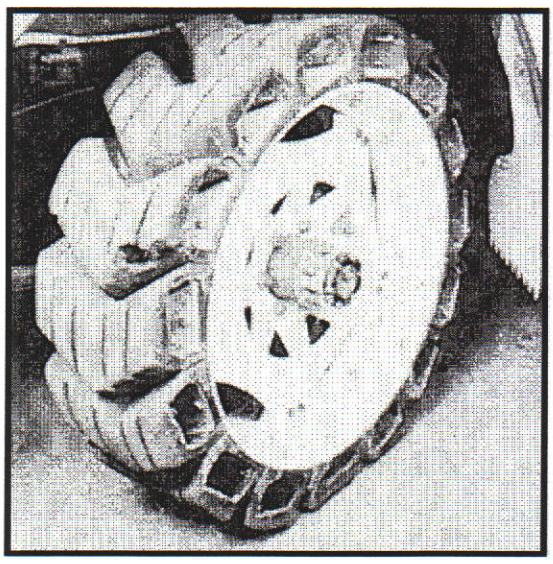

Figure 3.5

Figure 3.6

Figure 3.7

Figure 3.8

Figure 3.9

Figures 3.5 to 3.9 show the stages of repairing a segmented tyre with a single damaged segment.

Fig 3.5	Rotate the wheel to expose the damaged segment.
Fig. 3.6	Remove fastening bolts and retaining plates.
Fig. 3.7	Withdraw damaged segment
Fig. 3.8	Fit new segment and retaining plate.
Fig. 3.9	Refit fastening bolts and tighten.

Although the various designs of segmented tyre were well accepted for use on slow-moving off road vehicles, there was little prospect of this type of tyre being used on-road. The possibility of a segment breaking loose at moderate or high speed and becoming a projectile and a hazard for other vehicle users was deemed too great. There was also a clear indication from users that a one-piece tyre would be preferable in many circumstances.

The one piece concept was first used to create a series of industrial tyres for use on popular sized fork lift trucks. The wide acceptance of these tyres led to the creation of one-piece tyres for other applications and designs for two on-road tyres.

Figures 3.10 and 3.11 show a tyre developed for use on scissor lift platforms. Although tyres in this application are not particularly prone to punctures, the outcome of a puncture could be severe. If an operator was working on the elevated platform and a puncture did occur, the scissor-lift could tilt to an angle which could cause it to topple. Because of this possibility, the puncture proof tyre has gained popularity in the elevated platform market.

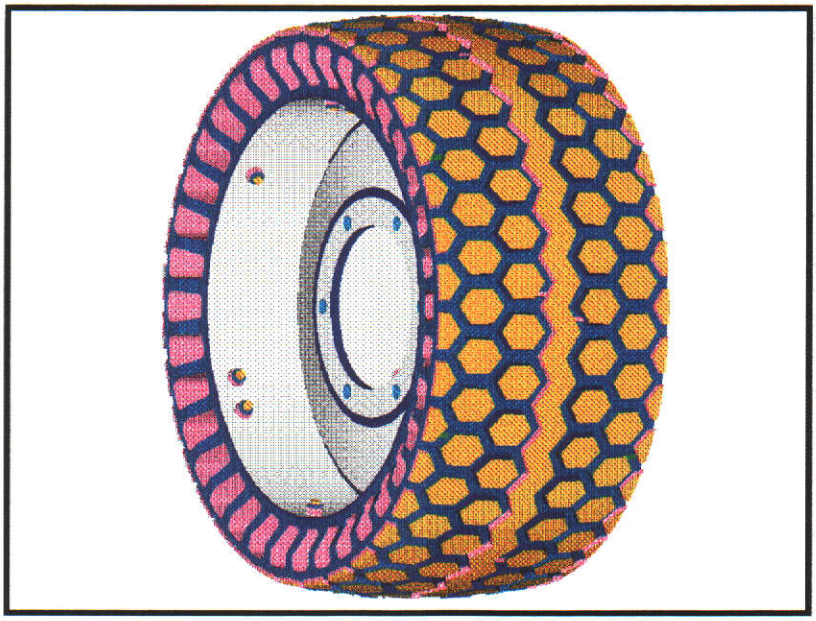

Figure 3.10 One-piece tyre for scissorlift platform

Figure 3.11 Tyres fitted to scissorlift platform.

The one-piece AirBoss concept has led to a tyre to suit a four-wheel-drive vehicle such as the Toyota Landcruiser or Landrover. Figure 3.12 is a model of a 7.50 – 16 tyre for a Toyota Landcruiser. At this time, the tyres are not legal for road use, however they are in use on mine sites and other off-road situations. There is the possibility that this design of tyre may be approved for on-road use.

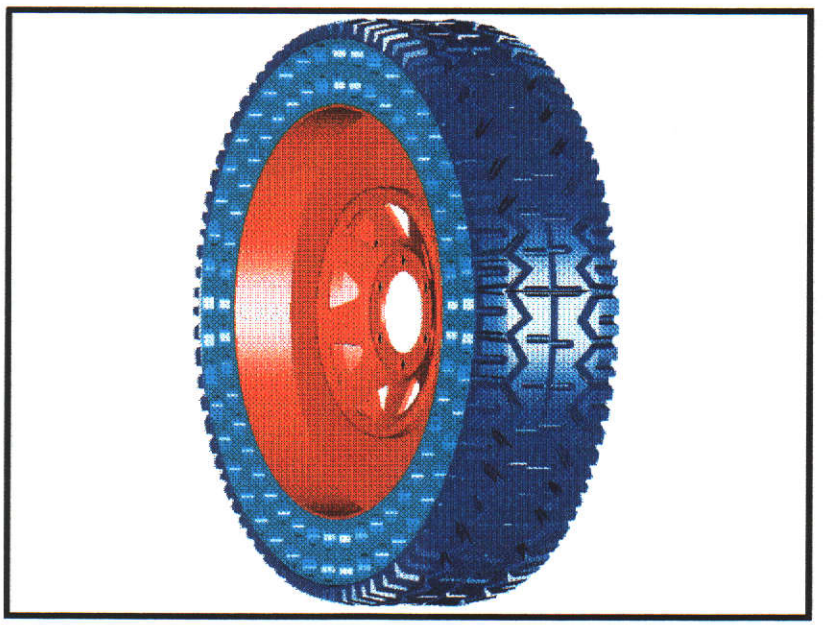

Figure 3.12 7.50 - 16 4WD tyre.

Also under development, at this time, is an AirBoss tyre for a town car. Many passenger car manufacturers are abandoning the spare tyre. Punctures tyres are not a common occurrence in metropolitan areas. This state of affairs arises due to the

generally excellent state of metropolitan roads and the advent of steel belted radial tyres. In any event, a flat tyre within city precincts is more of an annoyance than a threat. A service such as the R.A.C. could be equipped to cater for drivers with a punctured tyre, at least to the extent of getting the vehicle to a repair shop.

Some of the major tyre companies are in the process of developing 'run-flat' tyres. These designs depend on some sort of lubricating fluid being released if a blow-out occurs. This lubricant, coupled with a method of supporting the tyre structure without pressurised air leads to a tyre which is only partly incapacitated after a puncture. Electronics embedded in the tyre wall warn the driver of the puncture and the driver can then reduce speed and make his or her way to a repair shop.

There may be a place for an AirBoss style tyre within this market. The AirBoss tyre cannot puncture. The tyre is naturally a super-low profile (currently , very fashionable) style. The generally low speeds that city traffic is subjected to means that problems encountered with AirBoss tyres travelling for long periods at high speed are not an issue. Prototype tyres have been designed and manufactured (figure 3.13 shows the tyres on display at a motor show). The project is ongoing. Initial response to this tyre has been very favourable.

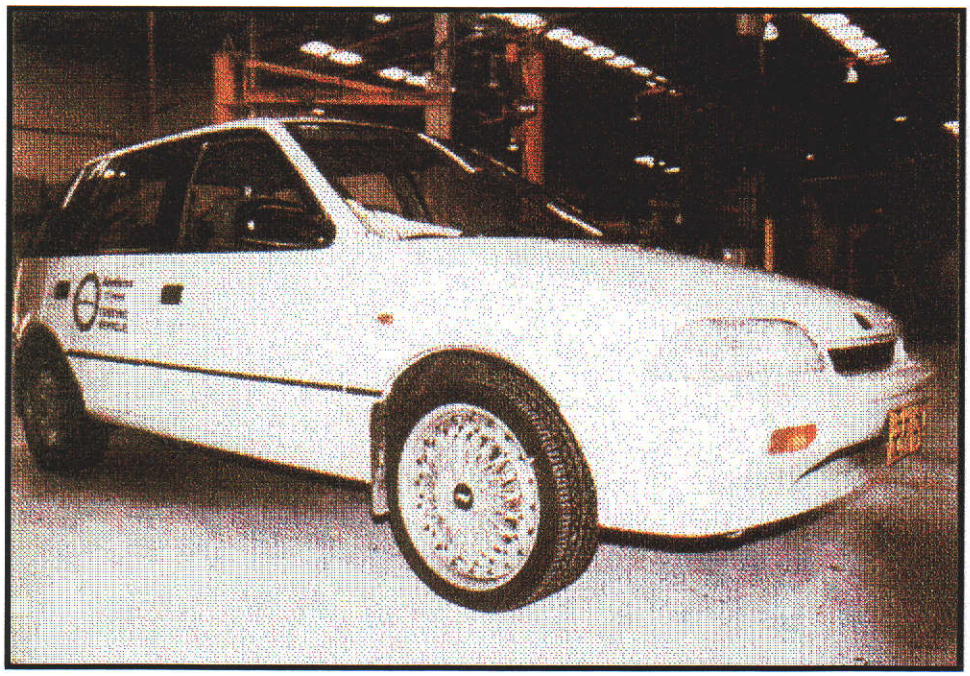

Figure 3.13 AirBoss prototype passenger car tyres.

3.3 THE '5.00 – 8' INDUSTRIAL TYRE

The tyre that has been used as the subject of this investigation into the static load bearing characteristics and thermal properties of semi-solid rubber tyres is the AirBoss 5.00-8 industrial tyre. This tyre is similar in size to the 5.00 – 8 tyres available from other sources. The '5.00' indicates that the width of the tyre is 5 inches and the '8' refers to the 8 inch rim that the tyre is fitted to.

Australian (and international) Standards require that this tyre be capable of carrying a load of 875 kilograms at a speed of 15 kilometres per hour. The tyre (depicted in figure 3.14 below) is generally used on the front axle of smaller fork lift trucks.

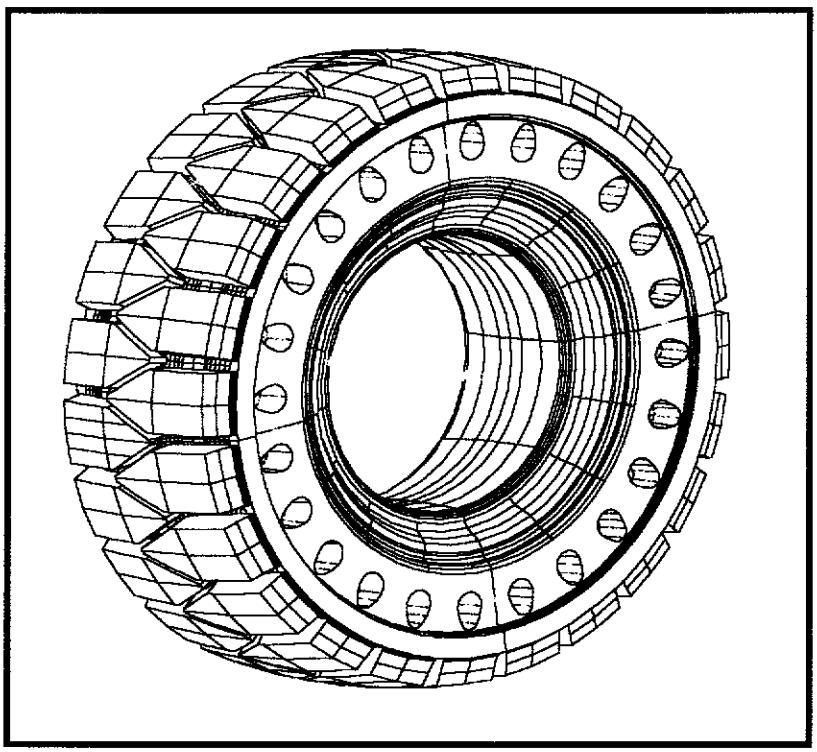

Figure 3.14 5.00 - 8, AirBoss Industrial tyre

Figure 3.15 below shows a cross-sectional view of the 5.00 – 8 tyre. The view shows the depth and arrangement of the holes. Near the innermost face of the tyre are four steel bands that clamp the tyre to the rim. Without the reinforcing steel, the tyre would stretch and lose grip on the rim.

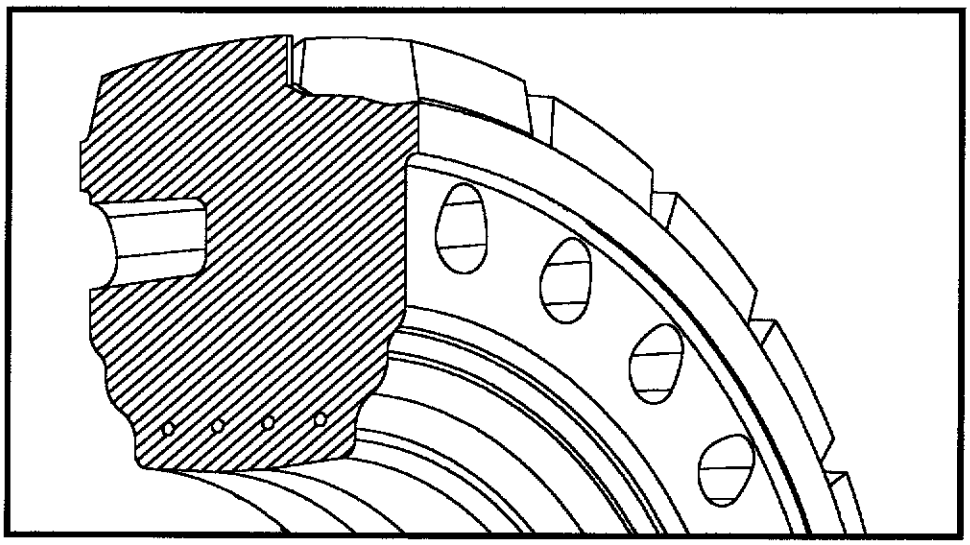

Figure 3.15 Cross-sectional view showing tyre structure

The AirBoss 5.00 – 8 tyre has been in service for some time and its performance is well understood. It may well prove valuable to work through this tyre as though it were being designed from scratch. In this way the various design stages can be confirmed. Ultimately, a prediction will be made as to the temperatures likely to be generated within the tyre structure and these will need to be confirmed by controlled testing.

After the tyre has been moulded and has cooled, it is a simple matter to determine the hardness of the rubber and hence, the static elastic modulus. For the compound developed for this tyre, the average hardness has been determined to be '71' on the 'Shore A' scale. This hardness suggests a shear modulus of 1.3 MPa (from figure 2.10). Since the value of Poisson's Ratio for rubber is 0.5 (minimal volumetric change under normal conditions) the value of elastic modulus for this compound is three times the shear modulus; 4 MPa.

With no more data from the tyre, it is possible to begin compiling data for finite element analysis of the tyre under static load conditions.

Chapter 4

MATERIAL DATA AND ANALYSES

4.1 INTRODUCTION

As will be shown during the development of this thesis, the method of predicting the static load and the heat build up characteristics in a non-pneumatic, AirBoss tyre where the material properties of the rubber are unknown and the tyre is at the design/optimisation stage, involves eleven steps:

1. Mould a current (existing design) tyre in the compound being evaluated.

2. Obtain the shear modulus of the compound using the Durometer hardness tester and graphs correlating hardness and shear modulus.

3. Generate material data to run a simulated Static (load versus deflection) analysis using Abaqus.

4. Modify the material data generated in step 3 to get an exact fit between the load-deflection curves obtained from a physical load-deflection test and the Abaqus simulation of that test.

5. Mould a small cylindrical test piece from the compound. Use it to obtain the material parameters that describe the viscoelastic characteristics of the compound. These parameters modify or generalise the static properties to include viscoelasticity.

6. Mould a cube of the rubber compound and monitor temperature changes during various tests. Use this data to determine thermal properties of the compound.

7. Perform an analysis of the cylindrical test piece (step 5) using values gained in steps 1 to 6. Simulate cyclic loading of the test piece by 'scaling up' the appropriate parameters.

8. Perform the physical test (equivalent to step 7) to obtain surface and core temperatures for the test piece.

9. Fine-tune the heat generation/dissipation parameters to obtain a good correlation between physical and simulated tests.

10. Assemble the heat parameters into the Abaqus file and solve for temperature distribution throughout a cross-section of tyre which is under design.

11. Determine whether or not the tyre design is acceptable with respect to maximum temperature likely to be reached in service.

4.2 STATIC ANALYSIS

4.2.1 MECHANICAL CONSTITUTIVE THEORY FOR RUBBER

The creators of Abaqus software suggest an extensive series of test to determine the properties of a rubber compound [Hibbitt, Karlsson & Sorensen (1997)]. The ultimate goal in determining these properties is to arrive at the Mooney-Rivlin coefficients which describe the material parameters of hyperelastic materials. Hyperelastic materials (such as natural rubber) are characterised as being highly deformable and of having a high bulk modulus [Bloch & Chang (1978)]. The high bulk modulus means the material can be regarded as incompressible unless it is in a

highly confined situation (such as an 'O' ring, restrained in a groove and subject to high pressure).

The tests are straightforward and once the apparatus is established to perform the three tests, it can be used in a routine manner. Although this method of data gathering is not used by AirBoss, it is useful to have an understanding of the way in which the Mooney-Rivlin constants can be gained. The Mooney-Rivlin form of the strain energy potential is based on phenomenological theory. Phenomenological theory, as the name implies, is concerned only with the observed behaviour of rubber. It pays no heed to molecular or thermodynamic considerations. It is work done in this area that leads directly to the method used within Abaqus finite element software for the solution of hyperelastic materials. This treatment of the problem leads to an expression for the elastic energy stored in the system. The theory was proposed by M Mooney (1940) and developed by R S Rivlin (1948, 1951). The theory lends itself quite naturally to treatment by finite element methods.

Imagine a unit cube of rubber with one corner sitting at the origin of a Cartesian grid and the three edges that make up this corner being aligned with the three orthogonal axes (1,2 and 3) as shown below.

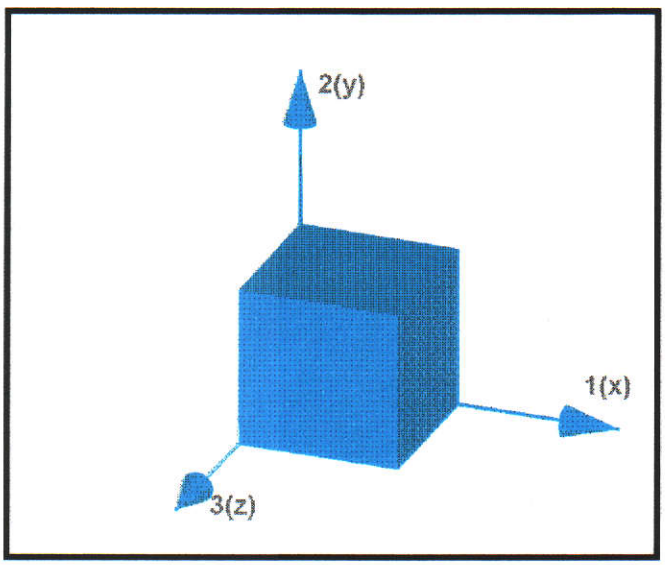

Figure 4.1 Unit cube element
Source: Hibbitt, Karlsson & Sorensen (1997) Abaqus Theory Manual

Then all strains can be expressed in terms of distortions or stretches along these axes.

Define λ_i (i=1,2,3) as the stretch ratios in the three principal directions.

In order to arrive at a state of strain for the element above, an amount of work must be done which will be stored in the element as strain energy.

$$W(\lambda) = \int_{\lambda_1=1}^{\lambda_1} \sigma_1 d\lambda_1 + \int_{\lambda_2=1}^{\lambda_2} \sigma_2 d\lambda_2 + \int_{\lambda_3=1}^{\lambda_3} \sigma_3 \lambda_3 \qquad (4.1)$$

The λs are as described above, the ratio of the element stretched in direction i to the unstretched length. The energy is a unique function of strain and, if the amount of strain in these directions is known, the elastic properties of the material can be completely defined.

Although the strain energy function, expressed in terms of the principal extension ratios, is chosen without regard for any molecular mechanisms, it must satisfy certain logical constraints to remain consistent with properties of isotropic solids. These constraints lead to the expression of W in terms of 'strain invariants'.

$$W = W(I_i) \qquad (4.2)$$

i=1,2,3

Where the I's (strain invariants) are defined as

$$I_1 = \lambda_1^2 + \lambda_2^2 + \lambda_3^2 \qquad (4.3)$$

$$I_2 = \lambda_1^2\lambda_2^2 + \lambda_2^2\lambda_3^2 + \lambda_2^2\lambda_1^2 \qquad (4.4)$$

$$I_3 = \lambda_1^2\lambda_2^2\lambda_3^2 \qquad (4.5)$$

Since the material is virtually incompressible $I_3 = 1$

The particular form of the strain energy potential proposed by Mooney and developed by Rivlin is

$$U \equiv \sum_{i+j=1}^{N} C_{ij}(I_1 - 3)^i (I_2 - 3)^j \tag{4.6}$$

Where U is the strain energy stored in the element due to elastic deformation

I_1, I_2 are the strain invariants defined above and C_{ij} are constants to be determined by experiment for a particular rubber compound.

All analysis done for this project uses N=2 for the polynomial expression. This leads to;

$$U = C_{10}(I_1 - 3) + C_{01}(I_2 - 3) + C_{20}(I_1 - 3)^2 + C_{02}(I_2 - 3)^2 + C_{11}(I_1 - 3)(I_2 - 3) \tag{4.7}$$

Further elaboration of the above equation is required so that the equation incorporates only parameters which can be directly measured; force and displacement (stress and strain) of a test piece. These parameters can then be used to solve for the C_{ij} constants.

The recommended tests are; a UNIAXIAL test, BIAXIAL test and SHEAR test. In each case, the test involves straining a test piece, taking measurements of the amount of deformation in the appropriate directions and the applied load which is causing this deformation. These load/deformations should cover the range which is likely to be encountered in service by the part to be analysed using the material data. Sufficient readings should be taken to enable a good 'best-fit' to be made from the data.

In the case of AirBoss tyres, it has been found from experience that, if a tyre is cyclically strained to more than 50%, then the tyre is likely to fail due to fatigue. Therefore, if analysis shows a maximum strain in excess of 50%, the analysis does not proceed and the design is reworked. In order to cover the strain range of interest, the measurements from strain-zero to a strain of 100%, that is, λ values of 1.0 to 2.0 should be more than sufficient. The three tests are depicted, schematically, below.

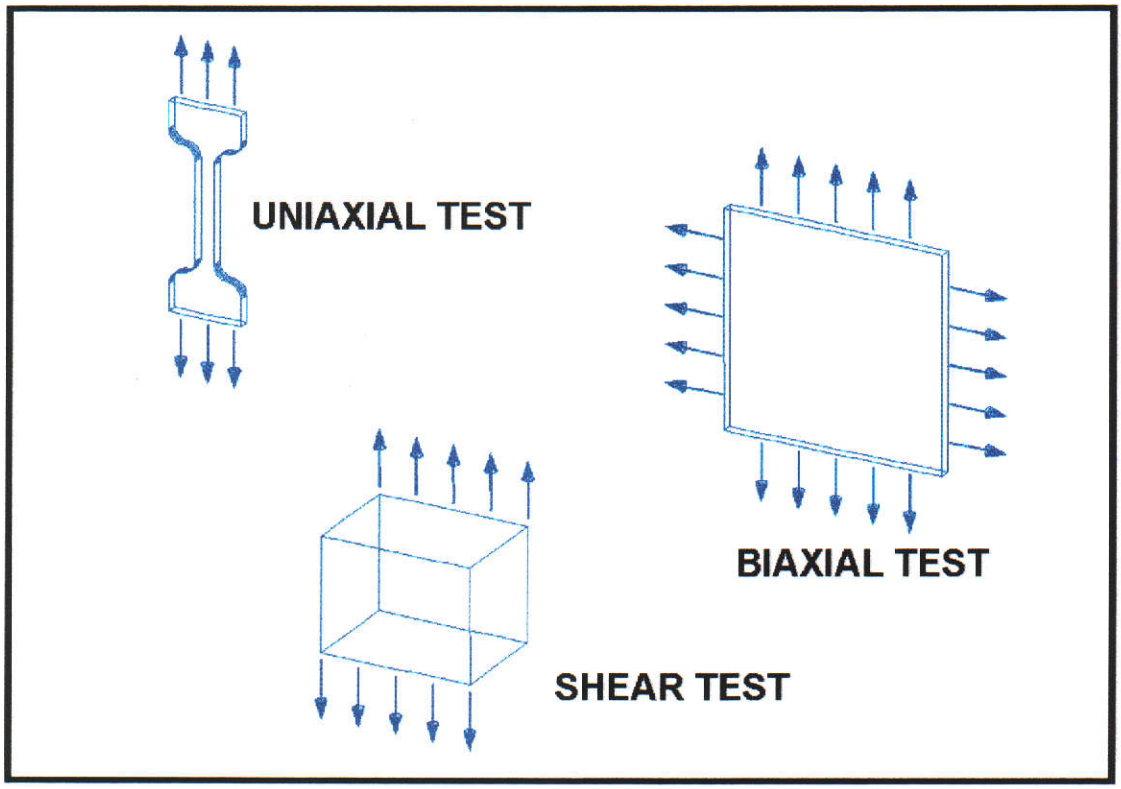

Figure 4.2 Schematic depiction of the three tests for determining the polynomial coefficients describing hyperelastic material data.

Source Hibbitt, Karlsson & Sorensen (1997) Abaqus Theory Manual

Separating strain and hence strain energy into its orthogonal components, and invoking the principal of virtual work, stress can be written as a function of strains and constant valued coefficients for each of the tests of figure 4.2. Because of the constraint of constant volume, λs can be related to each other for the different tests.

For the uniaxial test, $\lambda_1 = \lambda_U$, $\lambda_2 = \lambda_3 = 1/\sqrt{\lambda_U}$ (4.8)

Where λ_U is the stretch in the loading direction.

To derive the uniaxial nominal loading stress, T_U the principle of virtual work is invoked:

$$\delta U = T_U \delta \lambda_U \tag{4.9}$$

So that

$$T_U = \frac{\partial U}{\partial \lambda_U} = 2(1-\lambda_U^{-3})(\frac{\partial U}{\partial I_1} + \frac{\partial U}{\partial I_2}) \tag{4.10}$$

Which expands to

$$\begin{aligned} &2(1-\lambda_U^{-3})\Big[C_{10}\lambda_U + C_{01} + 2C_{20}\lambda_U(I_1-3) + \\ &C_{11}(I_1-3) + \lambda_U(I_2-3)) + 2C_{02}(I_2-3)\Big] \end{aligned} \tag{4.11}$$

For the biaxial test' $\lambda_1 = \lambda_2 = \lambda_B \quad \lambda_3 = \lambda_B^{-2}$ (4.12)

$$\delta U = 2T_B\delta_B = \tfrac{\partial U}{\partial_B}\delta_B \tag{4.13}$$

$$T_B = \frac{1}{2}\frac{\partial U}{\partial \lambda_B} = 2(\lambda_B - \lambda_B^{-5})(\frac{\partial U}{\partial I_1} + \lambda_B^2 \frac{\partial U}{\partial I_2}) \tag{4.14}$$

$$\begin{aligned} &= 2(\lambda_B - \lambda_B^{-5})(C_{10} + \lambda_B^2 C_{01} + 2C_{20}(I_1-3) \\ &+ C_{11}(\lambda_B^2(I_1-3) + (I_2-3)) + 2C_{02}\lambda_B^2(I_2-3)) \end{aligned} \tag{4.15}$$

Finally, for the shear test; $\lambda_1 = \lambda_S, \quad \lambda_2 = 1 \quad \lambda_3 = \lambda_S^{-1}$ (4.16)

$$T_S = \frac{\partial U}{\partial \lambda_S} = 2(\lambda_S - \lambda_S^{-3})(\frac{\partial U}{\partial I_1} + \frac{\partial U}{\partial I_2}) \tag{4.17}$$

$$= 2(\lambda_S - \lambda_S^{-3})[C_{10} + C_{01} + 2(C_{20} + C_{11} + C_{02})(I_1 - 3)] \tag{4.18}$$

For the three tests depicted in figure 4.2 above, data pairs can be logged of λ_i (ratio of current length in direction i to original length) versus applied load. A sufficient number of pairs would be ten for each of the tests with the values of λ ranging from 1 (no stretch) to 2 (100% stretch). The above equations can be used to determine the C_{ij} constants or they may be entered into the Abaqus input file as paired values of stress (engineering) and strain. With these values, Abaqus will compute the constants as part of the analysis.

4.2.2 THE AIRBOSS METHOD OF OBTAINING MATERIAL DATA.

The Method of obtaining hyperelastic material data as used by AirBoss Tyres relies on work done by Turner and Brennan (1987). Turner and Brennan, in turn draw on work carried out by Blatz, Sharda & Tschoegl (1974, 1978). The basic premise of the work is that natural rubber can be regarded as a linear (or hookean) material over a limited range of strain if the comparison is made between strain and true stress (force divided by current cross sectional area) as opposed to the more usual engineering stress(force divided by original cross sectional area).

With the vast majority of engineering materials, especially metals, where strain values are rarely more than a few points of a percent, the reduction in cross sectional area is so small that whether reduced or original cross sectional area is used in calculations is academic. However, for items such as the semi-solid tyres in question, strains of around fifty percent are usual. The constraint of minimal volumetric change under unconfined rubber conditions means that for the elongation of a 'dog

bone' test piece by fifty percent, the cross sectional area must reduce by 33%. Such an enormous difference between engineering stress and true stress must be taken into account.

As can be seen from the right hand graph of figure 4.3 below, for true stress versus strain, especially in the case of lightly filled or unfilled vulcanisates, there is a straight line relationship between stress and strain up to a strain of about eighty percent (corresponding to a λ of 1.8). Since no analysis proceeds where the strain in an AirBoss tyre exceeds fifty percent, it can be stated that, in the region of interest the relationship between true stress and strain may be considered linear.

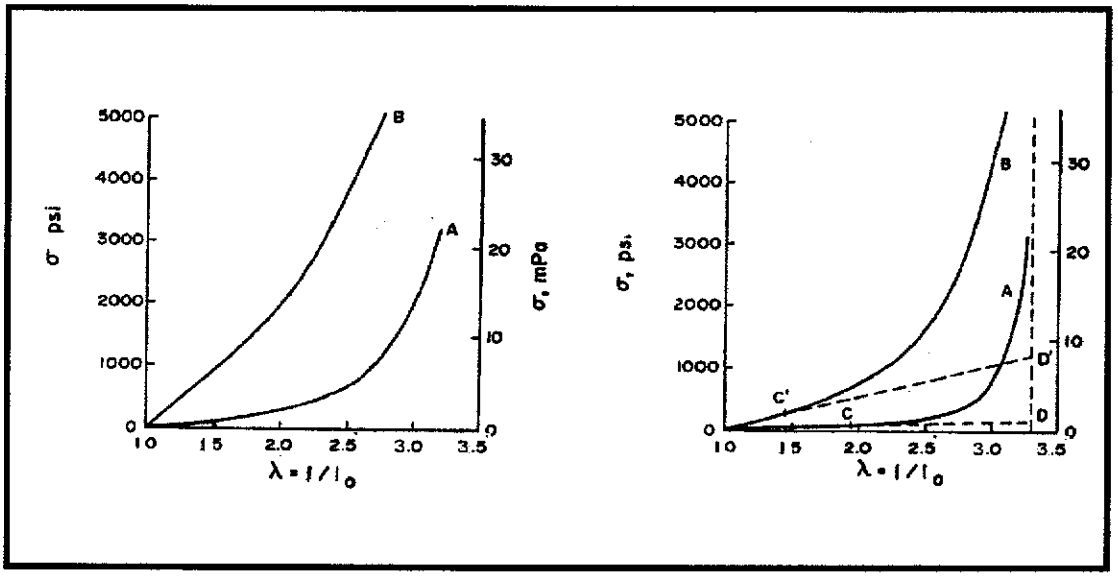

Figure 4.3 Graphs of stress and strain for rubber with and without filler. Left is engineering stress, right is true stress

Source: Shaw & Young, Transactions of the ASME (July 1988)

For any compound, an elastic modulus can be assigned. The modulus is the rate of change of true stress with strain or the point where the straight line portion of the true stress - strain curve (if extrapolated) crosses the line strain = 1.0.

With knowledge of the curve relating rubber hardness to modulus, it is now possible to define a compound from a simple hardness (Durometer) test. With the compound thus defined, data can be generated to enable the calculation of the Mooney - Rivlin coefficients upon which the analysis of components, made from hyperelastic materials depend.

The method of generating material data is taken from work carried out by D Turner and M Brennan (The Multiaxial Behaviour of Rubber: Plastics and Rubber Processing and Applications Volume 14(3)). Turner and Brennan refer to the method for generation of test data as a "Poisson's Ratio Method' the procedure is outlined below.

Beginning from standard engineering equations describing strain in terms of Young's modulus, stress and Poisson's ratio;

$$\sigma_2 = E(\lambda_2 - 1 + \upsilon(\lambda_1 - 1))/(1-\upsilon^2) \tag{4.19}$$

$$\varepsilon_1 = {}^{1}\!/_{E}[\sigma_1 - \upsilon(\sigma_2 + \sigma_3)] \tag{4.20}$$

$$\varepsilon_2 = {}^{1}\!/_{E}[\sigma_2 - \upsilon(\sigma_1 + \sigma_3)] \tag{4.21}$$

In the three tests in question (uniaxial, biaxial, and shear) σ_3 is zero. Neglecting σ_3 and replacing ε , with λ-1, the above equations can be rearranged to give:

$$\sigma_1 = E(\lambda_1 - 1 + \upsilon(\lambda_2 - 1))/(1-\upsilon^2) \tag{4.22}$$

$$\sigma_2 = E(\lambda_2 - 1 + \upsilon(\lambda_1 - 1))/(1-\upsilon^2) \tag{4.23}$$

$$\upsilon = (\lambda_2\lambda_1 - 1)/(\lambda_2\lambda_1(\lambda_1 + \lambda_2 - 1) - 1) \tag{4.24}$$

The above equations can now be used to generate values for the uniaxial, biaxial and shear tests.

For the uniaxial test, the constraint of constant volume dictates that

$$\lambda_2=\lambda_U^{-½}$$

hence $$T_U=\lambda_U-1+\nu=(\lambda_U^{-½}-1)/(1-\nu^{-2}) \quad (4.25)$$

For the biaxial case:

$$\lambda_2=\lambda_B$$

and $$T_B=\lambda_B-1+\nu=(\lambda_B-1)/(1-\nu^{-2}) \quad (4.26)$$

For the shear test

$$\lambda_2=1$$

and $$T_S=(\lambda_S-1)/(1-\nu^{-2}) \quad (4.27)$$

For each of the three cases and for λ=1 to λ=2 in steps of 0.1, the value of ν is generated (using a spreadsheet). From the values of ν and λ, the above equations are used to generate ten values of stress, corresponding to each increment of λ as shown below. These stresses are true stress and are converted to engineering stress by dividing each stress by the corresponding λ.

Table 4.1 below shows the test data in the form required by Abaqus for determination of the constants defining the hyperelastic material. These values of stress and strain are entered into the Abaqus input file as shown . The nominal value of the elastic modulus for this case is 3.5MPa. That is, if the linear section of the

(true) stress strain curve were to be extrapolated to cross the line strain = 100% , then the y value at this point would be 3.5Mpa .

```
HYPERELASTIC,N=2,TEST DATA
INPUT
** Note
**(a) SHEAR=Pure Shear
**(b) BIAXIAL=Equi-biaxial
**(c) ENG.STRESS(Pa),STRAIN
**
**
**
**
**
*UNIAXIAL TEST DATA
.3182E+06, .10
.5833E+06, .20
.8077E+06, .30
.1000E+07, .40
.1167E+07, .50
.1313E+07, .60
.1441E+07, .70
.1556E+07, .80
.1658E+07, .90
.1750E+07,1.00
*SHEAR TEST DATA
.4115E+06, .10
.7352E+06, .20
.9960E+06, .30
.1210E+07, .40
.1389E+07, .50
.1540E+07, .60
.1670E+07, .70
.1783E+07, .80
.1882E+07, .90
.1969E+07,1.00
*BIAXIAL TEST DATA
.5943E+06, .10
.1029E+07, .20
.1357E+07, .30
.1612E+07, .40
.1815E+07, .50
.1979E+07, .60
.2114E+07, .70
.2228E+07, .80
.2324E+07, .90
 .2406E+07,1.00
```

Table 4.1 Generated stress and corresponding strain as it appears for compilation into the Abaqus input file.

Source: AirBoss Tyres Limited

Below is a set of plots for uniaxial, biaxial and shear test for a compound that has been put through the suggested physical tests (by the Akron Rubber Research Center) together with data generated by the Turner Brennan method. As can be seen , stresses generated by the Poisson's ratio method agree very well with data provided by the Akron Research Center

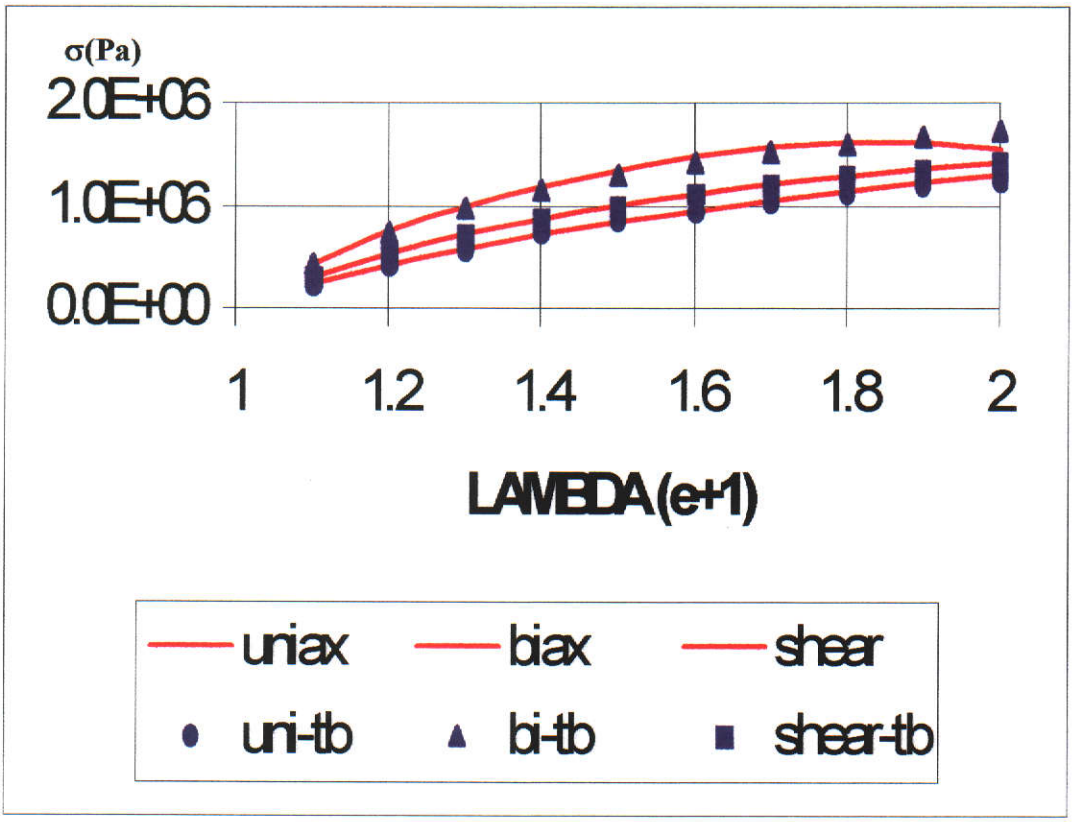

Figure 4.4 Comparison of data generated by the Turner-Brennan method and data obtained by physical testing

Source: AirBoss Tyres Pty Ltd and the Akron Rubber Research Institute.

At this stage, there is material data, sufficient for solution of a static analysis, that is where boundary conditions are applied slowly or where transient effects are allowed to reduce to zero. This is analogous to the cases of a rubber component being strained suddenly and then left until the force becomes constant or where a load is suspended from a test piece and the elongation has ceased to change. Analysis performed using a static procedure is important for two reasons:

The prediction of the load versus deflection curves are the prime concern of equipment manufactures when comparing AirBoss tyres with both solids and with pneumatic tyres. A small value of deflection for a given load means not only a harsher ride for the operator but also the possibility of premature failure of running gear such as axle bearings, steering joints, axles and so on. The aim in optimising the

tyre design is to achieve a static load deflection curve which is as close as practicable to the curve of an equivalent pneumatic tyre without inducing strain of greater than fifty percent in the area of the core holes.

The second reason for the necessity of material data for static load conditions is that this data is the foundation of the viscoelastic and hence heat generating aspect of rubber. Before the material properties can be extended or generalised to include these properties there must be an accurate evaluation of the stresses and strains caused by a load applied in a static test.

4.2.3 BUILDING THE INPUT FILE FOR ABAQUS SOLVER.

Once the material data has been prepared, the remaining data required for a static analysis is node and element data and boundary condition data. The procedure for obtaining the geometry data for compilation into the Abaqus input file and the method of describing the boundary conditions are outlined below. Once the Abaqus solver has been run with this data, the same file can (and will) be used to solve for the heat generation and dissipation characteristics of the tyre by adding the additional information required and re-running.

- **A model of the tyre** under design is created using the software package I-deas from the Structural Dynamic Research Corporation.

- **This model is then discretised** to create a finite element model. The model is closely approximated by a number of small bricks each joined to its neighbour at the nodal points or vertices.

- **Node and element data are exported** from I-Deas in the format which is required for input into Abaqus. The nodal data consists of an integer label (999 in the case shown below) which uniquely defines each node and the x,y and z co-ordinates of the nodal point in Cartesian space.

```
*NODE, NSET=ALL
999,  .01234,  .54321,  .77777
```
(4.28)

The element data consists of an integer label for each element plus the nodes which define the element. There are eight nodes used to define the eight vertices of each brick. The order in which the node labels appear must be consistent so that the element is described as a brick in three-dimensional space.

```
*ELEMENT,TYPE=C3D8H  ,ELSET=TYRE
 973,  1202,  1201,  1469,  1470,  1208,  1207,  1472,  1473
```
(4.29)

The remaining data needed from the model are groups or lists of element or node labels which can be used to refer to any number of nodes or elements by a single name. In the data lines (4.29) above, the keyword (indicated by *) declares that the data following is to describe elements. The 'TYPE=C3D8H" declares the type of element (continuum, three-dimensional, eight-node-brick, hybrid solution). The "ELSET=TYRE" states that, wherever elements are referred to by the name 'TYRE' all the elements defined after the keyword (which could be many thousands) are referred to.

In the case in question here, a group is created for nodes which may come into contact with a plane defining the ground and nodes which are clamped so that they remain fixed in space during the analysis. These nodes represent the part of the tyre adjacent to the rim. The only other groups exported from the I-Deas model are elements which can be referred to by their group name for the purpose of viewing in the Abaqus viewer. In this case they are 'slices' of tyre which will enable a cross section of the tyre to be viewed.

- **Boundary conditions**. For the static analysis, the enforced condition is that a model of the tyre under analysis be held rigidly at the points where it contacts the rim and that a geometric plane which represents the road or floor be pushed against the tyre with a force which represents the load which must be borne by the wheel in

service. The rigidly held tyre centre is accomplished by naming the nodes, grouped for the purpose followed by the degrees of freedom and their movement;

```
*BOUNDARY
FIXED,1,3,0.
```
(4.30)

The keyword *BOUNDARY states that the following lines are boundary conditions. FIXED refers to a group of nodes gathered under this label. '1,3' refers to translational degrees of freedom 1,2 and 3 (movement along any axis). The ',0.' Is the permitted amount of movement along these axes (none).

The ground or floor is described within Abaqus by giving the co-ordinates of the start and end points of a line in space and the direction in which this line is swept to create a geometric plane. This plane is then given a label and associated with single node (say 9999) created for the purpose. The plane is moved by applying a force to the node;

```
*CLOAD
9999,2,50000.
```
(4.31)

The keyword indicates that a description of a concentrated load follows. '9999' refers to the node which in turn controls the rigid plane representing the ground. '2' is the 'Y' direction and 50000. is the force applied to the node. This boundary condition will cause the ground to move in the positive Y direction and press against the tyre with a force of 50000 (Newtons in this case).

The group of nodes which may make contact with the ground have been designated. Once a node from this group comes within a specified proximity to the plane, its movement is limited to sliding on the plane, it is constrained from penetrating the plane.

Other information required for the Abaqus input file relate to the way loads are to be applied and the information required from Abaqus (stresses, strains, displacements and so on).

The Abaqus input file is a text file. Data generated from I-deas software needs to be cut and pasted into the file. Generally, there is an existing file which can be used as a template. The Abaqus solver is run by typing in the path and the name of the executable file (Abaqus) followed by the name of the input file containing the data.

Due to constraints of disk size and time considerations, model data is kept to about ten thousand elements. A job of this size would take about four hours to run on the workstations in use at AirBoss Tyres.

4.2.4 RESULTS FROM THE ABAQUS SOLVER FOR LOAD-DEFLECTION

Once the Abaqus input file has been run. The information in the Results File can be viewed graphically or as X-Y plots.

Figure 4.5 below is a plot from the Abaqus post processor showing the AirBoss 5.00 - 8 Industrial Tyre deformed by a 2000 kg load.

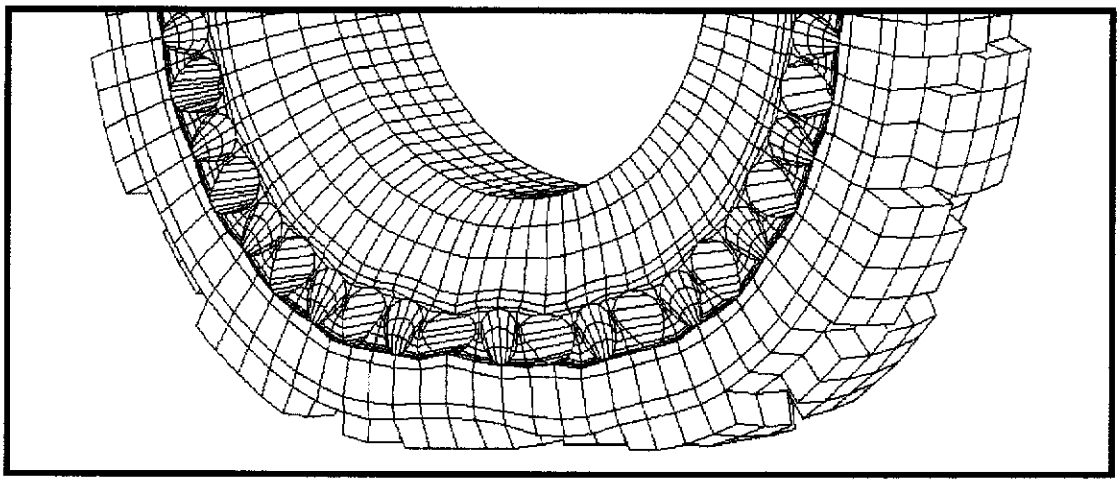

Figure 4.5 Deformed model of AirBoss 5.00 - 8 tyre.

Figure 4.6 below is a comparison of Load deflection curves for both simulation of a 35 millimetre deflection of the 5.00-8 tyre and a deflection of the same size imposed by a hydraulic test rig.

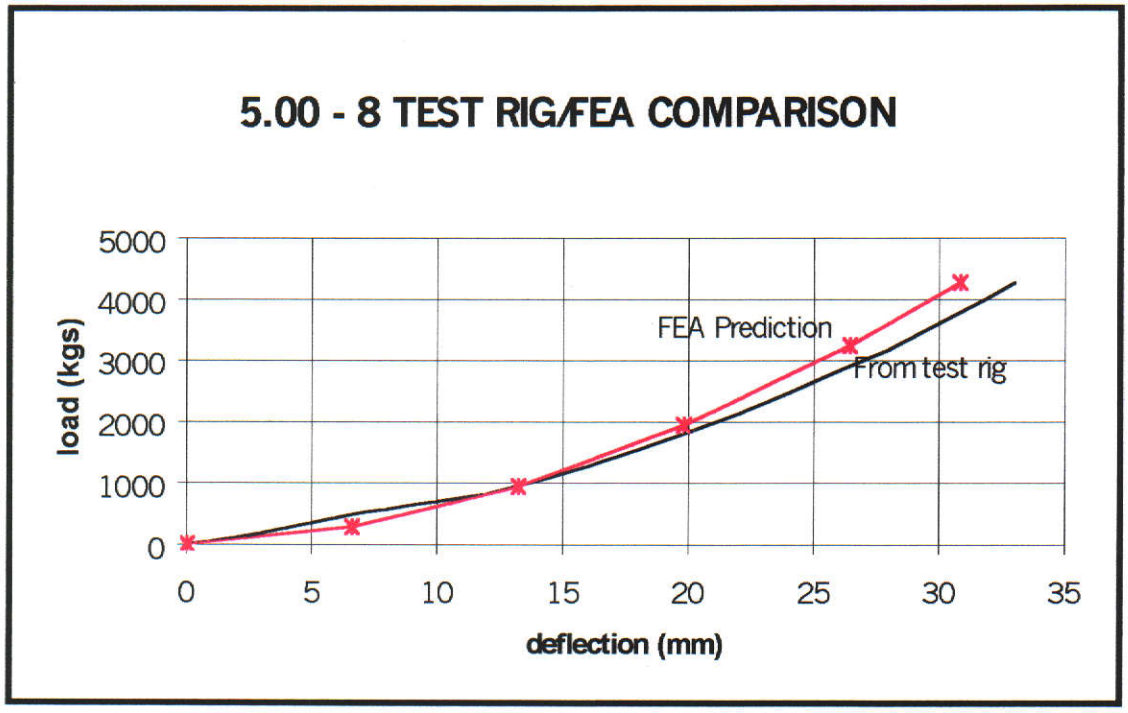

Figure 4.6. Graph comparing predicted and measured load-deflections

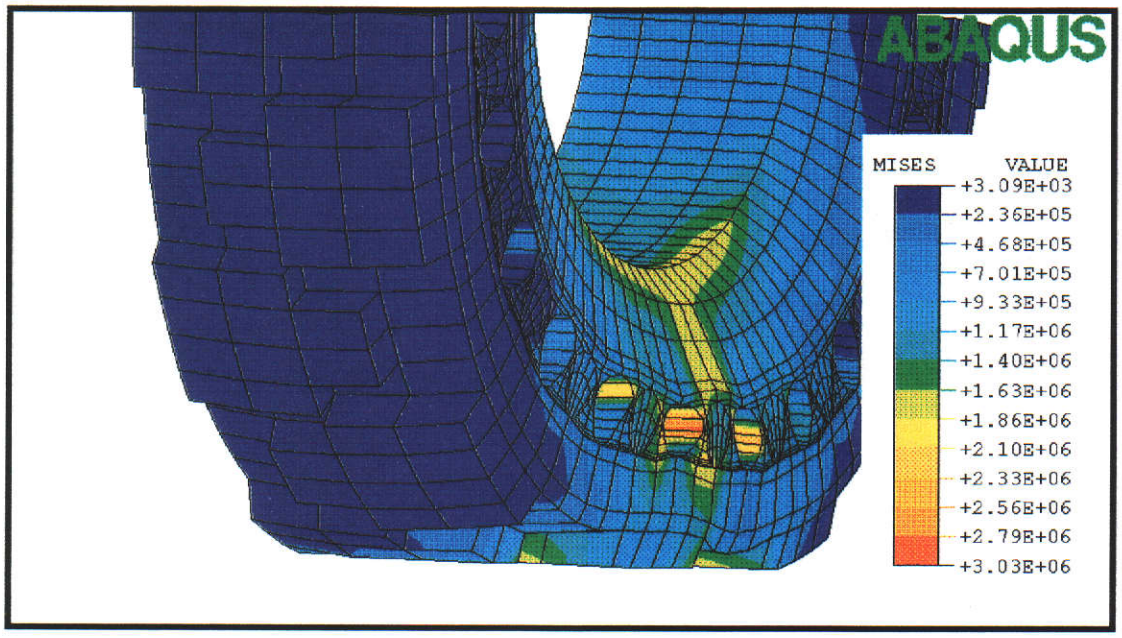

Figure 4.7. Deformed model showing stress (Mises) contours

4.3 VISCOELASTIC ANALYSIS

The information gathered from the static load versus deflection analysis is valuable insofar as it is data which can be readily compared to data available for other brands of tyre. For a more complete picture of the behaviour of a tyre (especially a solid or semi-solid tyre) data is required to determine the dynamic properties.

The most important characteristic of a tyre, as far as operator comfort is concerned, is the degree to which the tyre deflects to accommodate bumps and irregularities in the ground. Since the tyre has a fairly small amount of time to deform to the ground contours, the viscoelastic properties of the rubber compound become important.

The ultimate goal of this thesis is to arrive at a method of predicting heat build up throughout an AirBoss tyre. The energy lost due to viscoelasticity is the source of this heat energy and so a viscoelastic analysis is essential as a second step towards a fully coupled temperature-deformation analysis.

4.3.1 THE VISCOELASTIC PROPERTIES OF RUBBER.

A test rig has been designed and built to squash an AirBoss tyre in a manner which simulates the tyre bearing an increasing load, varying from zero to the maximum load the tyre is expected to withstand. The rig is basically a frame in which a tyre (or test piece) can be mounted. A flat plate (which represents the ground) is forced upwards by an hydraulic ram. A force transducer, between the plate and the ram, gives a digital readout of the force being applied to squash the tyre. A displacement measuring device gives a simultaneous readout of the amount of deflection that the tyre has experienced.

By applying the increasing force (or, equivalently, advancing the hydraulic ram) over a predetermined time, a measure of the viscoelastic nature of rubber can be determined. For the graph of Figure 4.10 the time taken to load the tyre was sixty seconds. If the time for loading were to be decreased, then the endpoint of the graph would be higher. That is, it takes a greater force to deflect a rubber component a given amount in a shorter time. When it comes to the case of impact loading (such as hitting a bump or kerb at speed) a completely solid rubber tyre will resist undergoing any significant deflection.

Figures 4.8 and 4.9 below show the test rig.

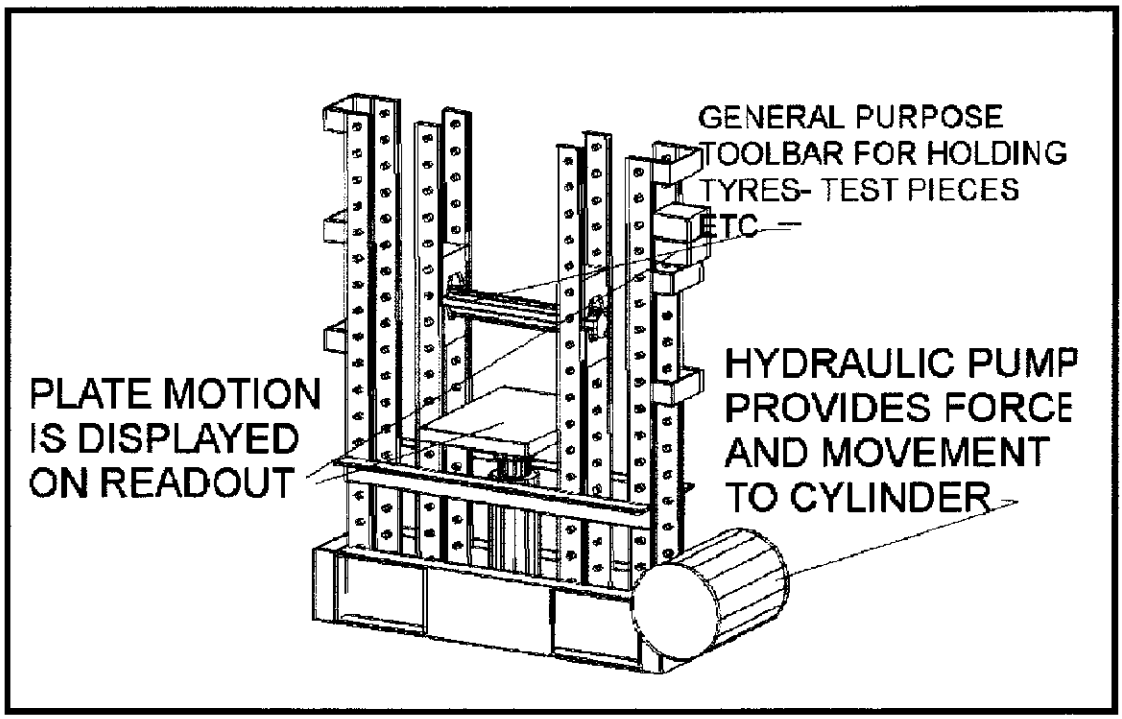

Figure 4.8 Schematic of the load - deflection test rig

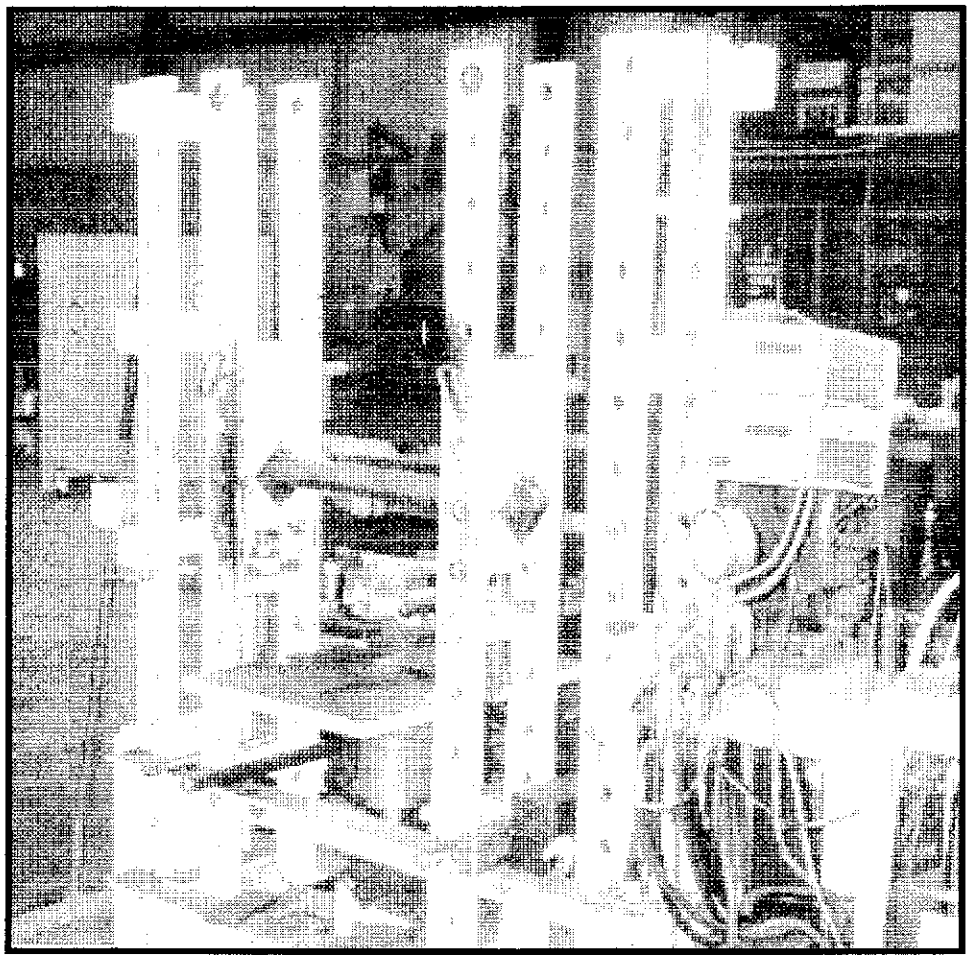

Figure 4.9 Photograph of the load - deflection test rig

If the load and deflection of the tyre or test piece are monitored while the load is being progressively removed, then curves similar to those shown at Figure 4.10 will result. Figure 4.10 shows the graph of data for two complete cycles of loading and unloading of the AirBoss 5.00 – 8 Industrial tyre. Both the loading and the unloading cycles were for periods of sixty seconds.

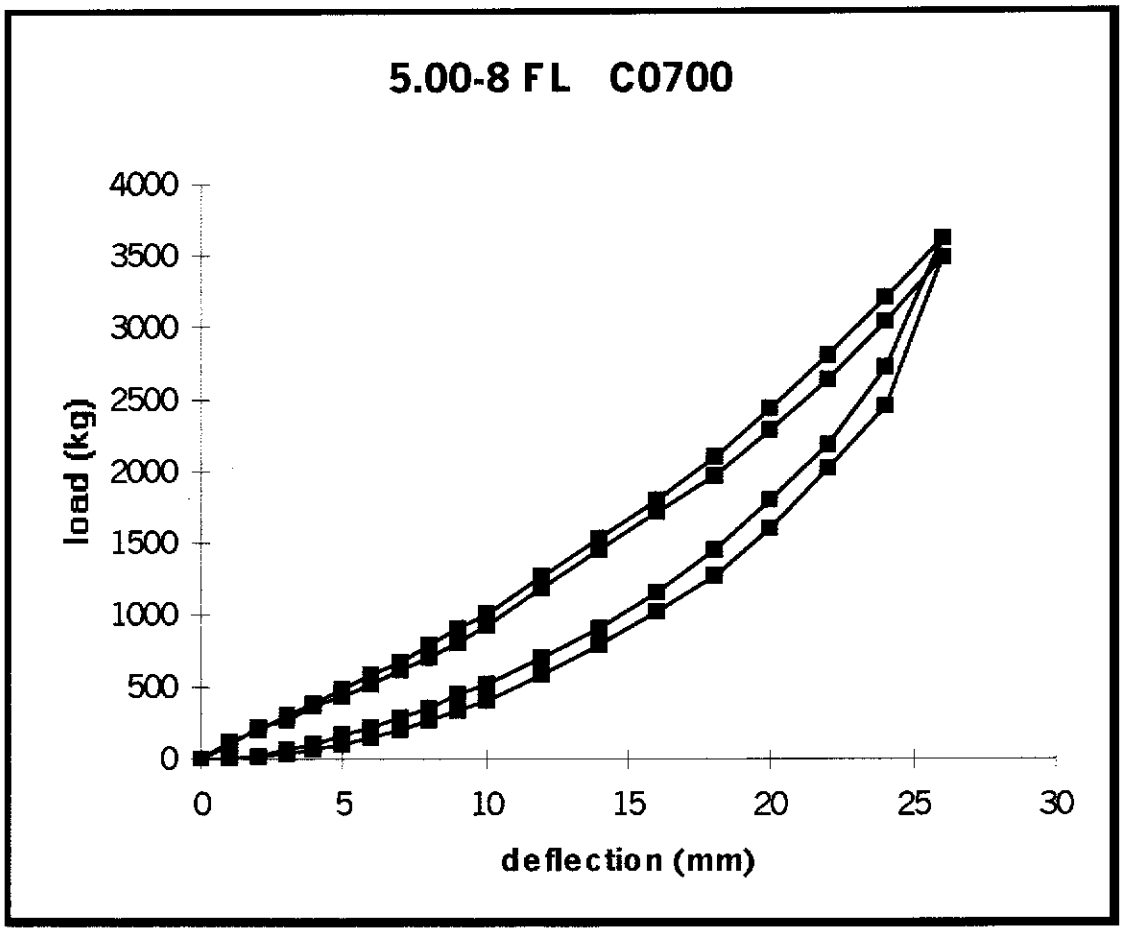

Figure 4.10 Load - deflection curves taken from a 5.00-8 industrial tyre using the rig shown in figures 4.8 and 4.9

The upper curves represent the loads versus deflection values recorded during the time the load was being applied. The lower curve is from data recorded during unloading. Since the area under each curve is the product of stress and strain or energy stored in the deformed structure, the area enclosed by the loop represents energy which is not returned to system during one loading-unloading cycle [Ferry (1961)]. Virtually all of this energy is converted into heat.

4.3.2 DETERMINATION OF CONSTANTS FOR VISCOELASTIC ANALYSIS.

The second stage of the process for determining heat generated by the tyre is to generalise the Mooney-Rivlin coefficients, describing hyperelastic behaviour, to include a viscoelastic response to strain. As has been described earlier, the spring and dashpot model of rubber elements give rise to a transient response to a step strain and a complex (in-phase and out-of-phase) response to a steady, harmonic strain.
The viscoelastic properties are described by a Prony series expansion of the relaxation modulus [Hibbitt, Karlsson & Sorensen (1997)].

$$G_R(t) = G_0(1 - g_1^P(1 - e^{-\frac{t}{\tau}})) \tag{4.32}$$

In this case, the time dependent material behaviour is approximated with a single term Prony series for the shear relaxation modulus

The dimensionless term ;

$$1 - g_1^P(1 - e^{-\frac{t}{\tau}}) \tag{4.33}$$

Is equal to $$1 - \frac{G_R}{G_0} \tag{4.34}$$

Where G_0 is the instantaneous shear modulus and

G_R is the long term (stable) shear modulus.

In the case under consideration, with the rubber unconfined, value of Poisson's ratio can be taken as 0.5 (no volumetric strain). Hence, G=E/3 [Green & Zerna (1968)].

4.3.3 VISCOELASTIC ANALYSIS OF A TEST CYLINDER

The required data to determine the viscoelastic parameters for input into Abaqus can be obtained using the load/deflection test rig shown in figures 4.18 and 4.9 The additional item needed is a cylindrical test-piece. The test piece, moulded from the compound under investigation, is shown in figure 4.11 below.

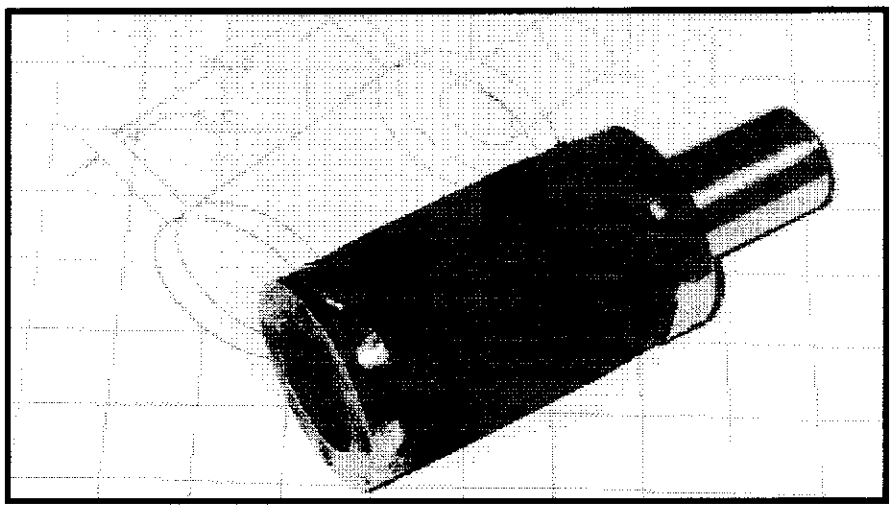

Figure 4.11 Test cylinder.

The test piece, shown above, has been used for obtaining viscoelastic and temperature related parameters. It is a cylinder of rubber moulded from the compound under investigation. The undeformed cylinder has a diameter of 50 mm and a length of 75 mm. Steel discs are bonded to the test piece cylinder during moulding so that the test piece can be clamped in the load-deflection rig (and, later, in a rig designed to determine the heat generation properties) During testing for viscoelastic parameters, the cylinder is squashed to a height of 65 mm and data pairs are recorded for elapsed time and force applied. Figure 4.12 below shows the test cylinder mounted in the load/deflection rig.

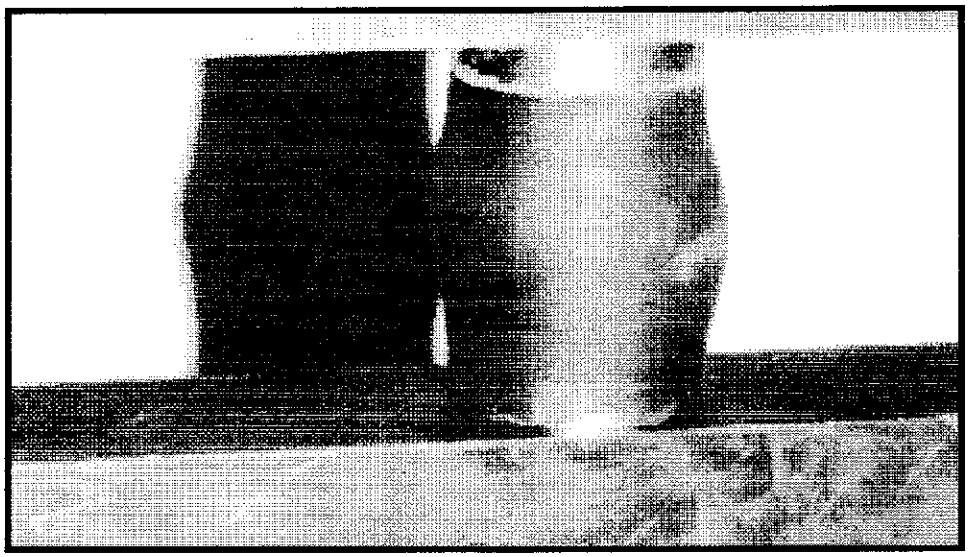

Figure 4.12 Deformed test cylinder.

The value of force applied to the test piece is initially high but drops away over a period of several seconds until a final steady force can be read from the readout. The values of force applied to maintain this constant strain are recorded (together with the corresponding time) from time = zero to the time when the final force is achieved.

Time (s)	Force (kgf)
0	2
8	15
16	13
24	9
32	8.7
40	8.5
48	8.35
56	8.22
64	8.2

Table 4.2 Data logged using test-cylinder

The values of force and corresponding time are shown in table 4.2 (above)
As might be expected, they show a declining force which stabilises (at 8.2 Kgf.)

The expected form of the governing equation is;

$$F = K_1 + K_2 e^{\frac{t}{\tau}} \tag{4.35}$$

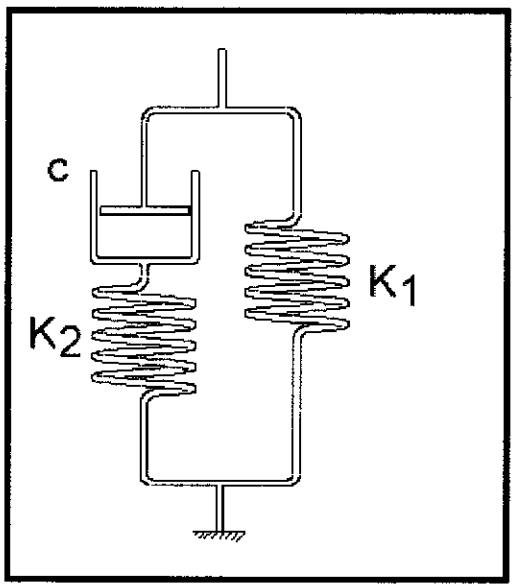

Figure 4.13 Maxwell Voigt model

Source: Ward & Hadley (1993), Properties of Solid Polymers

Using the spring and dashpot model, repeated at figure 4.13, and the data table of 4.2, it can be seen from inspection that K_1 (the long term or residual force) is 8.2 Kgf.

The initial or 'glassy' modulus is $K_1 + K_2$ (25 Kgf), making K_2 = 16.8 Kgf.

The term τ in equation 4.34 describing the decaying force is C/K_2 where C is the dashpot damping coefficient.

The value of τ can be determined by a 'best fit' method. In this case, Microsoft Excel's built in solver has been used.

The data from the load-deflection rig is assembled into an Excel spreadsheet. Column 1 has the data for elapsed seconds. Column 2 is the corresponding force, read from the rig's digital readout. An initial guess at the time constant (in this case, the initial value was 1.0) is added to a cell at the foot of column 1. From equation 4.34, a third column of smoothed data is generated. A fourth column is generated, containing the squares of the difference between columns 2 and 3. The cell at the foot of column 4 is the sum of squared differences between actual data and smoothed. The Excel Solver is asked to minimise the sum of squares by altering the value of the time constant. As can be seen in table 4.3 below, the computed value is very close to 10 seconds.

Time (s)	Force (kgf) from rig	Force (kgf) Calc	Square of Difference
0	25	25	0
8	15	15.75195	0.565432
16	13	11.59476	1.974697
24	9	9.726016	0.5271
32	8.7	8.885976	0.034587
40	8.5	8.508361	6.99E-05
48	8.35	8.338615	0.00013
56	8.22	8.26231	0.00179
64	8.2	8.22801	0.000785
10.00534			3.10459

Table 4.3 Data used to determine the viscoelastic decay constant.

With $K_1 = 8.2$, $K_2 = 16.8$ and $\tau = 10$, the graphs of actual and smoothed data are shown below.

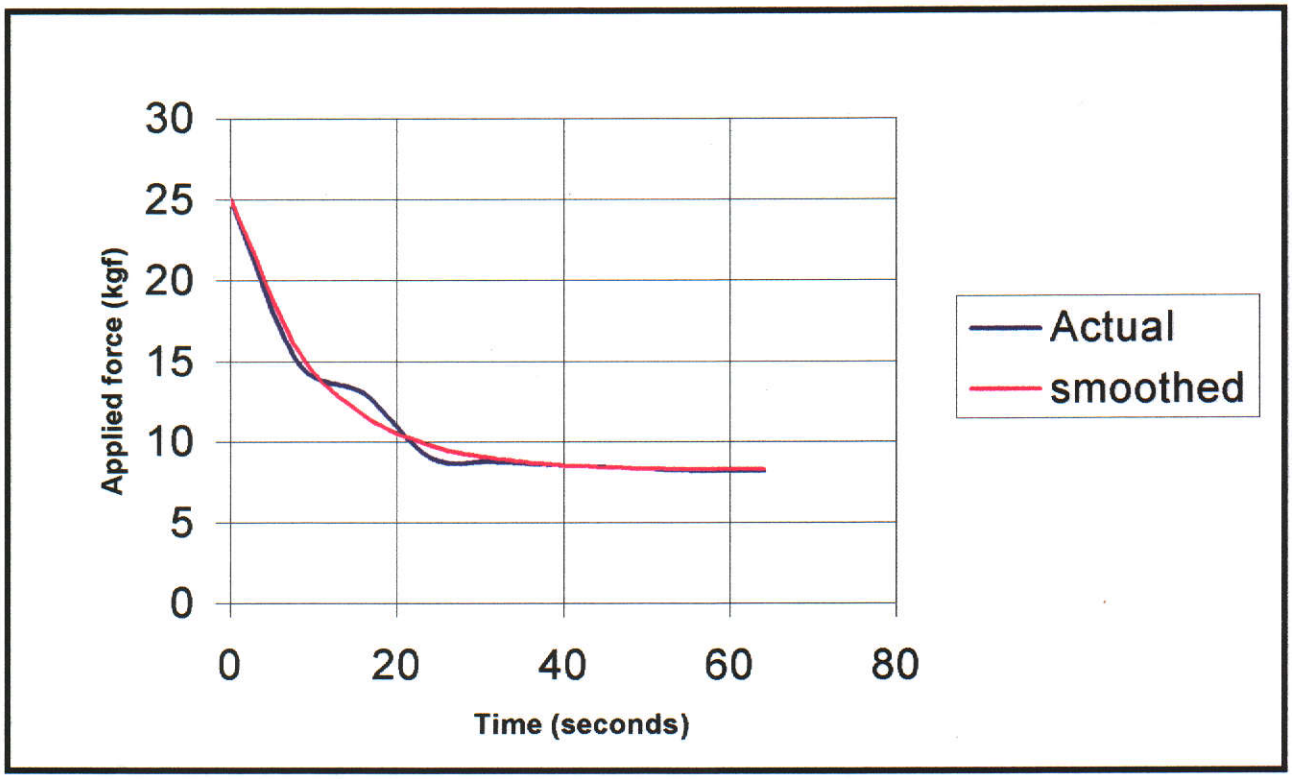

Figure 4.14 Comparison of actual and smoothed data from 'best fit'

If this process involved time-dependent volumetric change, then a similar procedure would need to be carried out to determine the Prony series value for the dimensionless bulk relaxation modulus and its time constant. However, as was stated earlier, for unconfined rubber the volumetric change can be taken as zero.

We now have the data required by Abaqus to generalise the HYPERELASTIC material parameters to include VISCOELASTICITY.

The form of entry in the Abaqus input file is "*Keyword" (in this case VISCOELASTIC) and on the following line, the single Prony term describing the stress relaxation

$$1 - \frac{finalstress}{initialstress} \qquad (4.36)$$

Followed by a similar term to describe bulk relaxation (in this case zero)
And lastly, the decay constant; 10.0

The data line is;

```
*VISCOELASTIC, TIME=PRONY                                    (4.37)
0.672,0.0,10.0
```

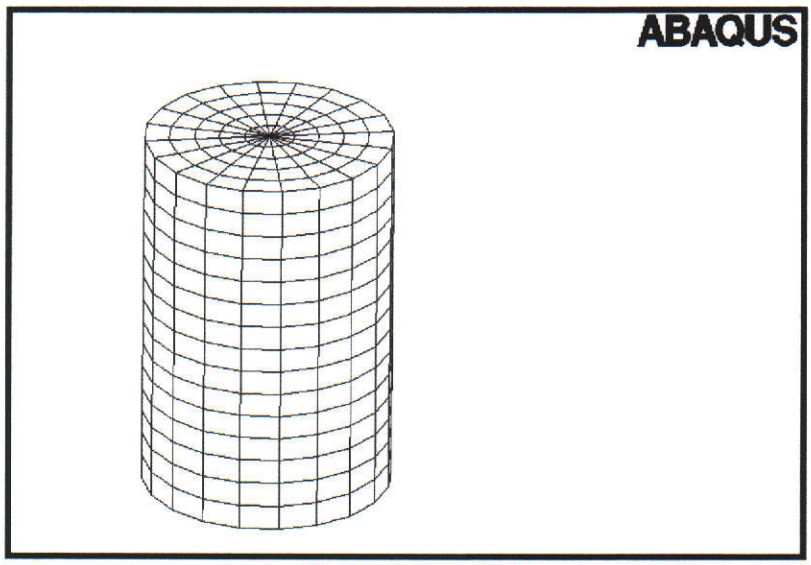

Figure 4.15 F. E. Model of cylindrical test piece.

The F.E. model has been run with the additional data and the results compared. The graph of figure 4.16 shows the comparison.

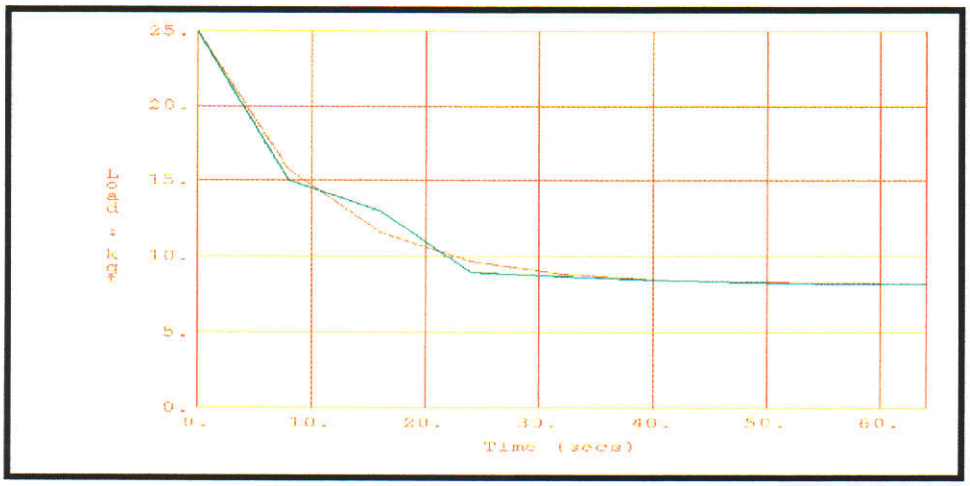

Figure 4.16 F. E. Analysis curve (red) and measured curve.

4.4 COUPLED TEMPERATURE – DISPLACEMENT ANALYSIS

At this point, there is sufficient data available to perform an analysis of the AirBoss tyre under static and transient loading conditions. Graphs of load versus displacement can be produced for any given rate of loading. Stresses and strains within the structure of the tyre can be visualised as contour plots on the model.

The final step in the finite element analysis of the AirBoss tyre is to predict the temperature contour within the tyre. The rubber compound used to manufacture the 5.00 - 8 Industrial tyre degenerates rapidly at temperatures in excess of 130°C. If an analysis of the tyre suggests such temperatures are likely to be reached then the design must be reworked to either reduce the amount of heat generated or to improve the ability of the tyre to dissipate heat.

All the data gathered and compiled into the Abaqus input file is used in the final, coupled temperature-displacement analysis. The file is completed by the addition of data to generalise the procedure to include heat generation and dissipation.

4.4.1 MATERIAL DATA FOR PREDICTION OF HEAT GENERATION

The remaining material properties required to perform a heat analysis are:

- Conductivity
- Specific heat
- Density
- Film coefficient and
- Inelastic heat fraction

The properties; specific heat and film coefficient will be assumed to be 'average' values, taken from literature which will then be modified in light of experimental data obtained from the cylindrical test piece. Density is readily obtained for any compound by weighing a block of known dimensions.

4.4.1.1 CONDUCTIVITY

The problem of rubber being able to generate heat by hysteresis is further exacerbated by the fact that rubber is a very poor conductor of heat. Steel is almost 400 times as efficient as rubber at transferring heat. Table 4.4, below, shows some comparisons between conductivity for various materials.

Material	Conductivity (W/mK)
Silver	420
Copper	395
Mild steel	51
Building brick	.63
Natural rubber	.13
Asbestos	.12
Cork	.046

Table 4.4 Comparison of thermal conductivities for various materials.

Source: Nagdi (1993), Rubber as an Engineering Material.

The value of 0.13 $W.m^{-1}.K^{-1}$,given as the conductivity of natural rubber, is for 'unfilled' compound. Once carbon black has been added in significant quantity, the conductivity rises appreciably. To determine the thermal conductivity of any particular compound, a simple procedure has been devised. A simple mould tool

(shown in figure 4.17) is used to mould a block of rubber 150 x 150 x 150 millimetres with thermocouple wires embedded at positions shown. The tool is loaded with rubber by layers with the thermocouple wires embedded between. With the tool and rubber at ambient temperature, the bottom platen of a moulding press is heated to 160°C . The tool/rubber assembly is placed on the hot platen.

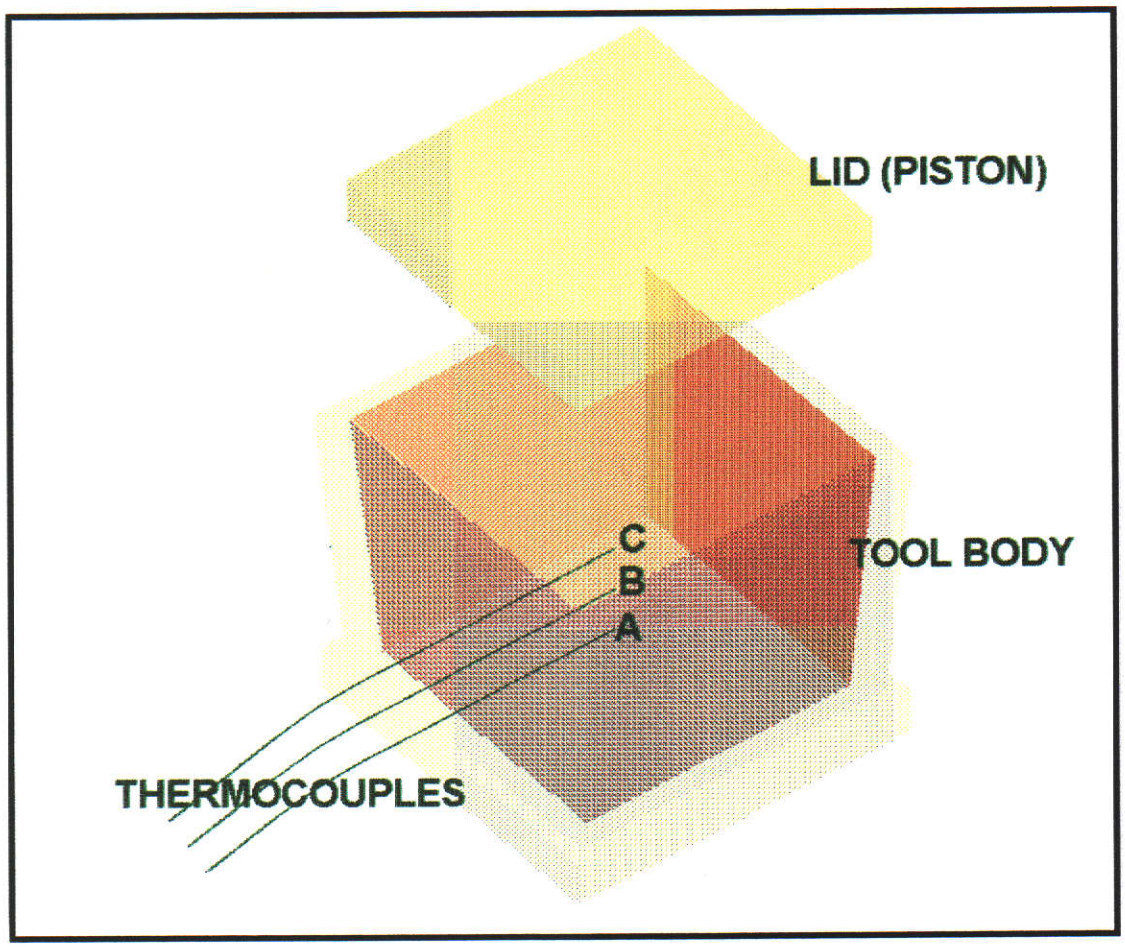

Figure 4.17 Mould tool with thermocouple inserts

The lower face of the rubber quickly reaches 160°C. Temperatures are monitored at points A,B and C until a stable temperature is reached.

Once data pairs have been logged, the assembly is removed from the press and allowed to cool to ambient. The procedure is then repeated with the tool inverted, as shown in the photograph of figure 4.18.

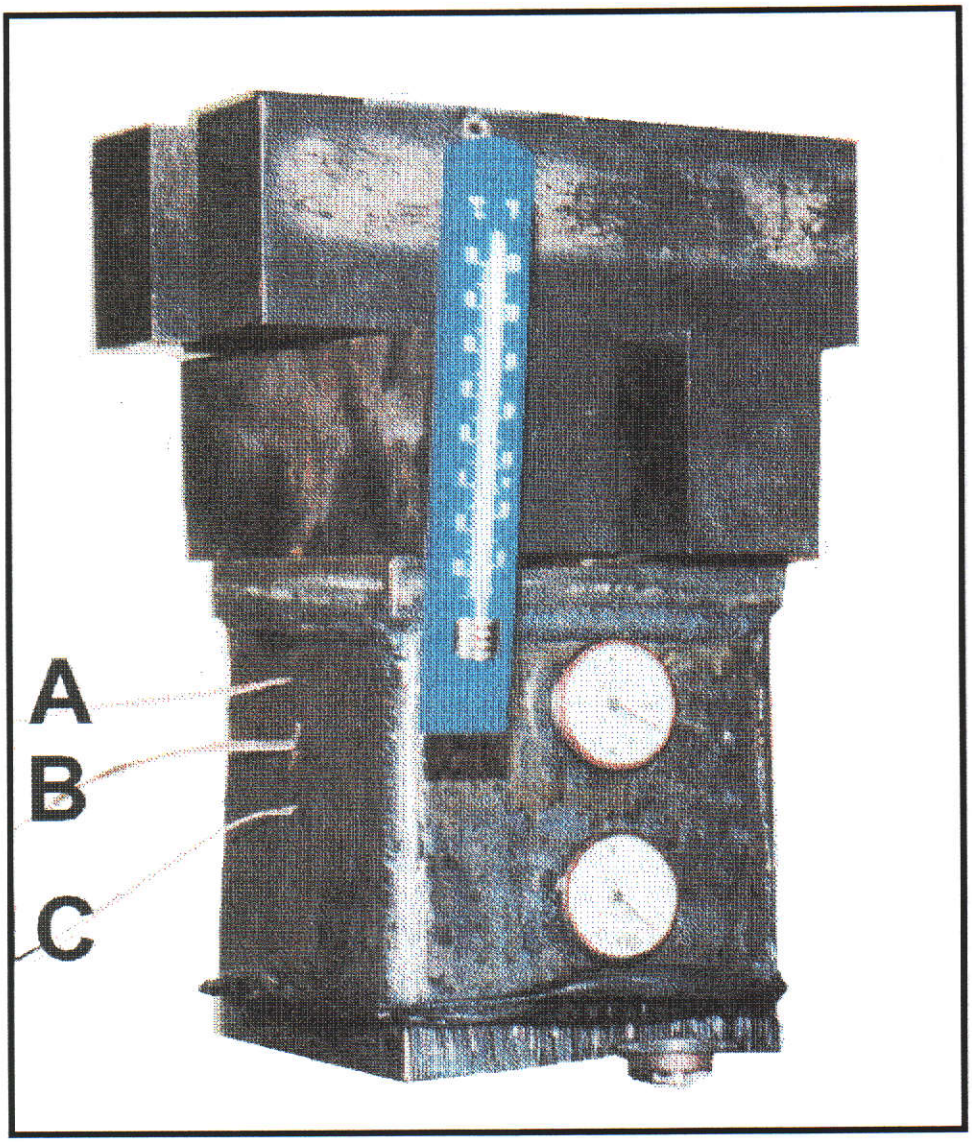

Figure 4.18 Photograph of the mould tool in the inverted position.

The block is modelled with brick elements (one quarter is modelled due to symmetry) and the above procedure is simulated. The only material data required for the heat transfer analysis are; density, specific heat (both of these values are available from Natural Rubber Engineering Data Sheets.) and thermal conductivity (which is the data sought). The value for conductivity is entered as a 'best guess', initially, and then modified, using the results of simulation and experiment, as described below.

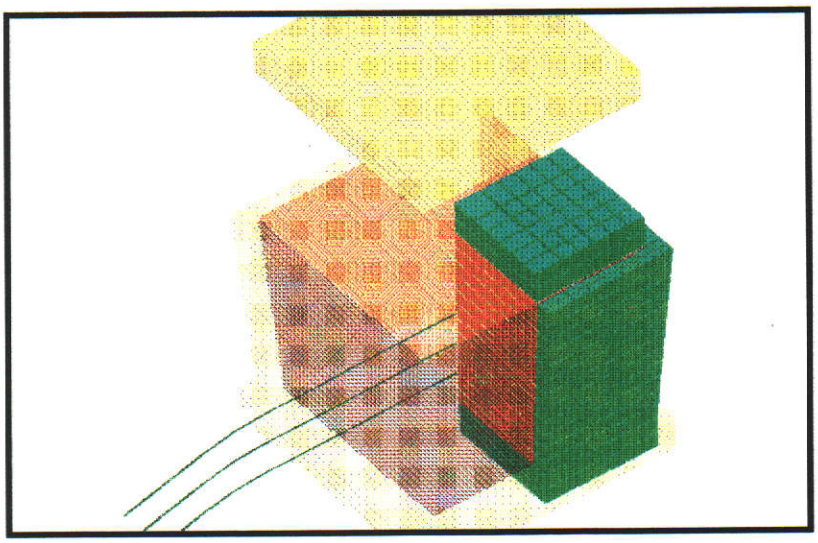

Figure 4.19 FEA model of moulded block.

The temperature rise at the three thermocouples is a function of specific heat and thermal conductivity. It would be preferable to isolate conductivity but, because data sheets quote the value of specific heat as 1900 $J.kg^{-1}.K^{-1}$ over a wide range of compounds, it was decided to take the given value as being correct.

X-Y plots are produced to compare temperatures obtained from the physical test with those obtained from simulation. The value of thermal conductivity, used in the simulation, is modified until an acceptable correlation is obtained between physical and simulated testing. The FEA plots of figure 4.20, below, were obtained using a value of thermal conductivity of 0.86 $W.m^{-1}.K^{-1}$ This value of thermal conductivity will be taken as the correct value for the compound under investigation.

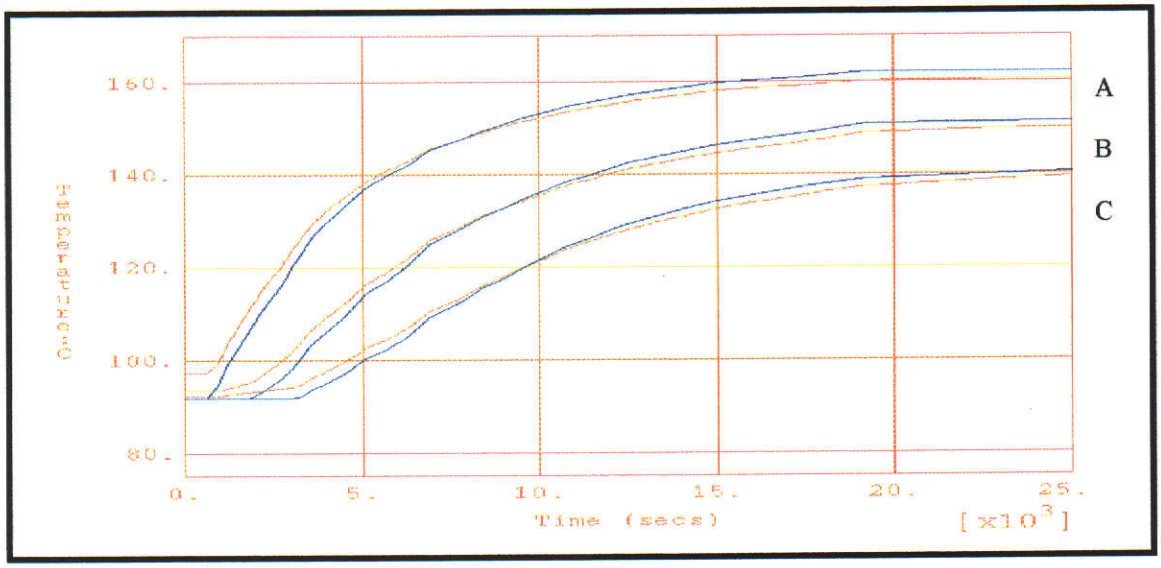

Figure 4.20 Comparison of measured and predicted temperatures.
(Blue lines are physical measurements)

4.4.1.2 SPECIFIC HEAT

As mentioned above, Engineering Data Sheets (Malaysian Rubber Research Association (1980) give the value of specific heat as 1900 $J.kg^{-1}.K^{-1}$ For this investigation, the value of 1900 $J.kg^{-1}.K^{-1}$ has been taken as correct. The good correlation between simulation, using this value, and experiment suggest the given value for specific heat is valid.

4.4.1.3 DENSITY

This value is supplied, as a matter of course, by the rubber compounders. It would also be the simplest of material parameters to obtain, by weighing a piece of rubber of known dimensions. The value of the density of the compound used here is 1.12 kilograms per litre.

4.4.1.4 FILM COEFFICIENT

The value of the film coefficient governs the rate at which heat energy is transferred across the rubber/air interface. The value is multiplied by the difference in temperature between the rubber surface and the ambient temperature of the surrounding air (the 'sink' temperature). The procedure for obtaining this parameter makes use of the rubber block moulded in the test to determine thermal conductivity. Once the mould and rubber temperatures have stabilised, the rubber cube is removed from the mould and a temperature probe is inserted into the cube centre (the embedded thermocouples are, unfortunately, destroyed in removing the cube from the tool). The cube was supported at corners only so that all faces were exposed to ambient temperature air.

With the thermal conductivity of the compound determined from experiment as 0.86 $W.m^{-1}.K^{-1}$, the film coefficient is readily determined by running a simulation of the block cooling in air and modifying the film coefficient to obtain an acceptable

correlation between the cooling curve measured from the embedded thermocouple and that predicted from FEA It was found that a film coefficient of 0.63 $W.m^{-2}.K^{-1}$ gave a good correlation between measured and predicted curves.

4.4.1.5 INELASTIC HEAT FRACTION

There is already enough data to hand for Abaqus to calculate the amount of energy stored and lost during a single squashing of a component made from the hyperelastic material. The Mooney – Rivlin expression is for total strain energy (stored and lost) within a deformed element of rubber. The final piece of information needed to evaluate the heat produced within the rubber structure is the percentage of the energy lost which appears as heat. If the keyword "*INELASTIC HEAT FRACTION" is not included in the input data file, a figure of 0.95 (95%) is assumed. In some processes, it could be imagined that energy appears as sound or light. Since neither of these phenomena seem to be produced by rubber tyres, a figure of 0.99 is ascribed. The final stage of the process for determining material parameters provides an opportunity to 'fine tune' some of the material parameters obtained thus far.

4.4.2 PROCEDURE FOR OBTAINING THE FINAL MATERIAL PARAMETERS

The test piece used for fine tuning the material parameters is the rubber cylinder shown at figure 4.26 This test cylinder has already been modelled, compiled and run for an analysis of the viscoelastic behaviour of the test piece, subjected to a step strain. The final stage of the AirBoss procedure for the determination of material parameters to predict heat behaviour is as follows. Using the input file for the cylinder.

- Add the keywords and values of conductivity, specific heat, film coefficient, density and inelastic heat fraction (scaled up by a factor of 10,000 where necessary). Modify the input file so that a fully coupled, heat transfer - stress analysis is performed by Abaqus.

- Run the analysis using a single step but with the appropriate parameters scaled up to simulate a test duration of 10000 cycles.
- Perform the same test, physically, on the test-piece cylinder, monitoring the temperatures at the core of the test piece and at the surface.
- Modify the key parameters; Film coefficient, conductivity and inelastic heat fraction so that a second run of the analysis produces results that match those from the physical test.

Once this stage of the procedure has been carried out, it is assumed that accurate material data for the complete analysis of AirBoss tyres made from the compound in question is to hand.

4.4.3 THE HYSTERESIS TEST RIG.

In order to cyclically deform the test piece cylinder and thus monitor temperature rise due to hysteresis, a simple procedure has been set up.

- A three tonne inclinable press was purchased. (This is a piece of equipment normally used for stamping out small items, say washers, from sheet metal).

- The brake and activating system was removed such that, once switched on, the ram of the press would simply move up and down at a fixed rate.

- The test cylinder had plates bonded to each end, specifically so that it could be bolted into the inclinable press.

- A 'K' type thermocouple was inserted into the centre of the cylinder for monitoring of the core temperature.

- An infra-red thermometer, held near the surface of the test cylinder, enabled recording of the surface temperature.
- The test was run for ten thousand cycles and temperatures read at appropriate intervals to enable the data to be plotted for comparison with Abaqus predictions.

Figure 4.21 below, shows the cylindrical test piece used with the hysteresis test rig. The test-piece, originally 75 mm high, is squashed 16 mm then extended 9.4 mm. The total deformation is 25.4 mm.

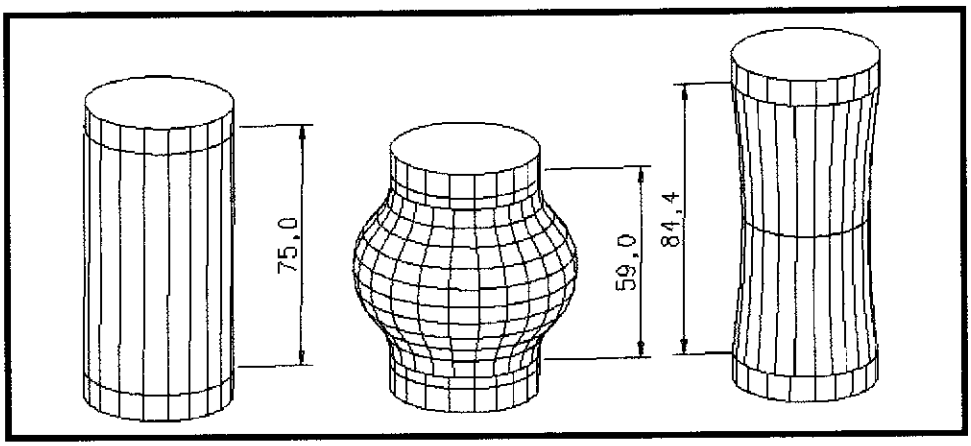

Figure 4.21 The test cylinder in the (left to right) undeformed, maximum compressed and maximum extension states.

Figure 4.22 (right) shows the inclinable press used to repeatedly deform the cylindrical test piece. The ram of the press travels 25.4 mm (one inch) at a rate of 180 cycles per minute.

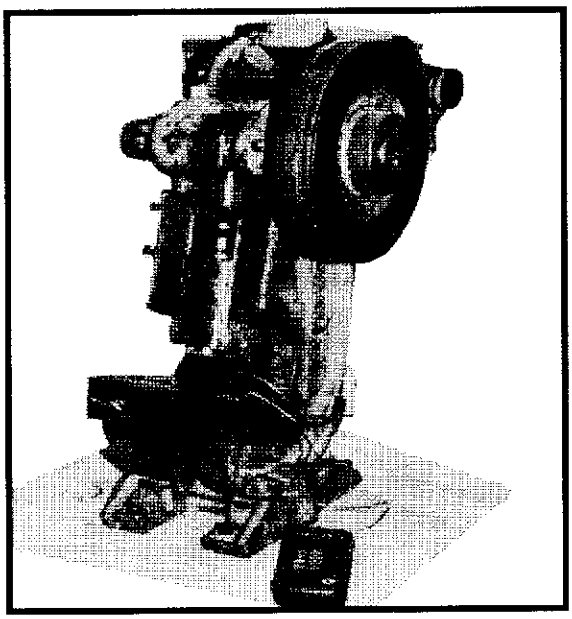

The cylindrical test piece is bolted into the press. The ambient temperature is recorded, as is the initial temperature at the centre of the cylinder. The press is switched on. The temperature at the centre of the cylinder rises quickly during the first few minutes and then rises more slowly with increasing time. After a period of about forty-five minutes, the temperatures and the centre of the cylinder and at the outside surface become stable. At this point, the heat energy flowing across the air/rubber interface is equal to the heat energy being produced within the rubber cylinder.

The test is terminated after 10,000 cycles have been completed (fifty-five minutes). A graph of temperature rise at the two monitored positions (centre and surface) is shown below.

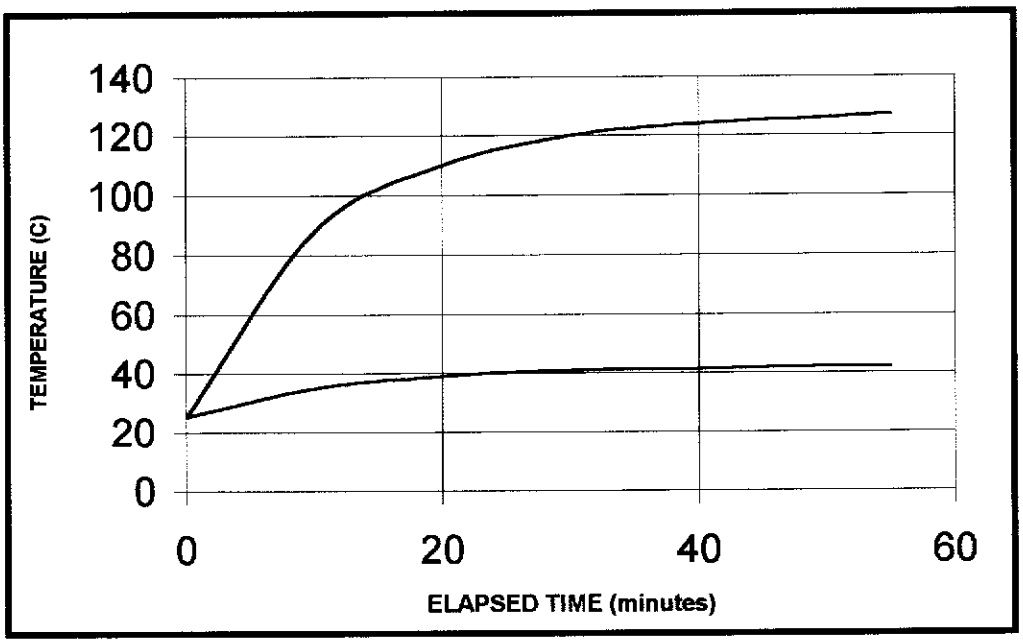

Figure 4.23 Graph of results taken from Hysteresis test Rig. (Upper curve is centre temp. Lower curve is surface temperature.)

The results from the coupled temperature displacement analysis can now be compared with the results obtained from the hysteresis test rig. The results shown below are from a second analysis performed after modification of the relevant material parameters. The predicted temperature rise at two nodal points (one at the centre of the model and at the surface) is shown in figure 4.24 below.

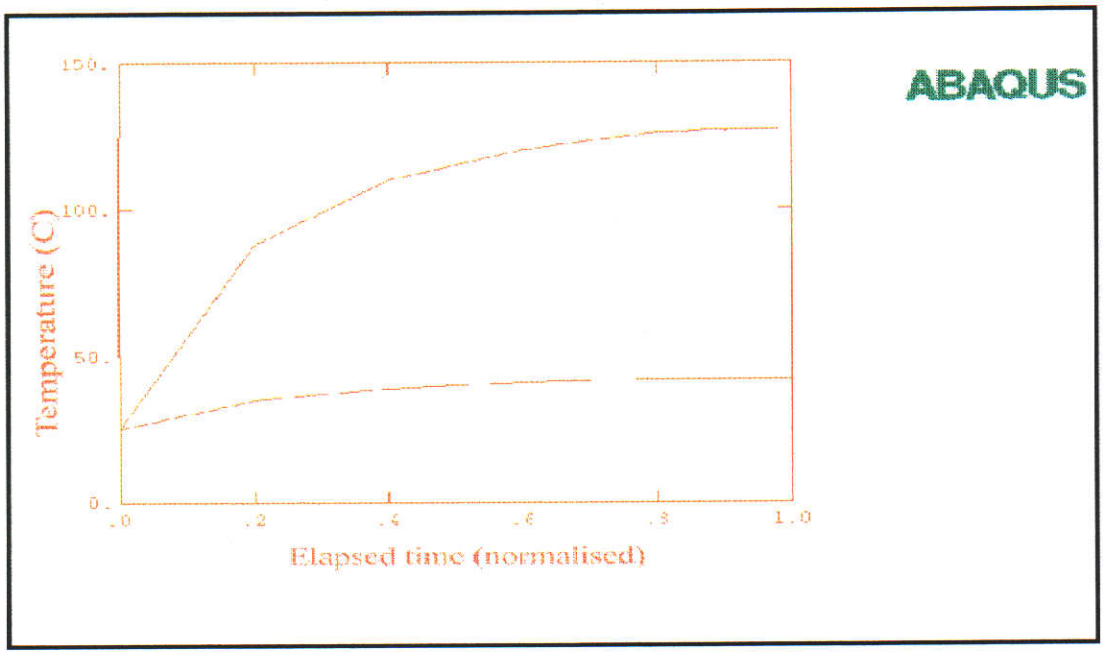

Figure 4.24 Temperature curves predicted by Abaqus, upper cure is core temp Lower curve is temperature at cylinder surface in central region.

As can be seen from the Excel chart Figure 4.25 (below) comparing the two sets of data, there is a fair correlation between the predicted (after data modification) and the actual test data for the centre - point of the test piece. It was found that modification of the film coefficient in an attempt to match surface temperatures (Actual and predicted) led to a far less accurate match of the core temperature.

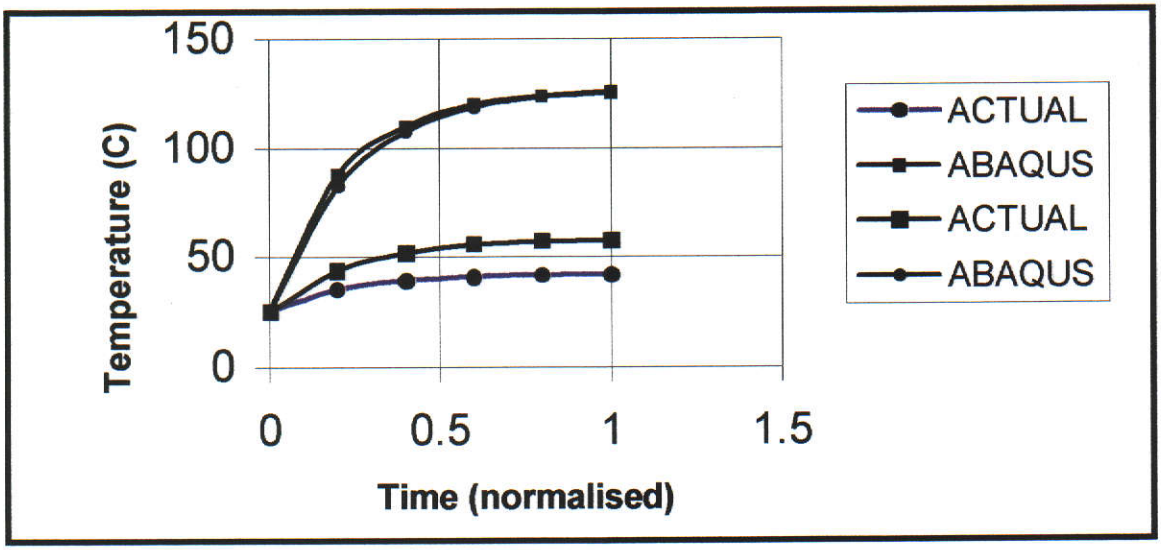

Figure 4.25 Comparison between predicted and actual temperatures.

Since it is the hottest point of the tyre which is likeliest to fail (hence is of greatest interest) it would seem more important to have this temperature accurately predicted than any other.

The map of predicted temperatures is shown on a section of the model at figure 4.26 below. The material parameters that have been adjusted are: specific heat (adjusted from 1900 $J.kg^{-1}.K^{-1}$ to 1860 and film coefficient (adjusted from 0.06 $J.s^{-1}.m^{-2}.K^{-1}$ to 0.063 $J.s^{-1}.m^{-2}.K^{-1}$) These modifications give near coincident figures of temperature at the centre of the cylinder (but a poorer match for the surface temperature)at the end of the fifty-five minute test cycle.

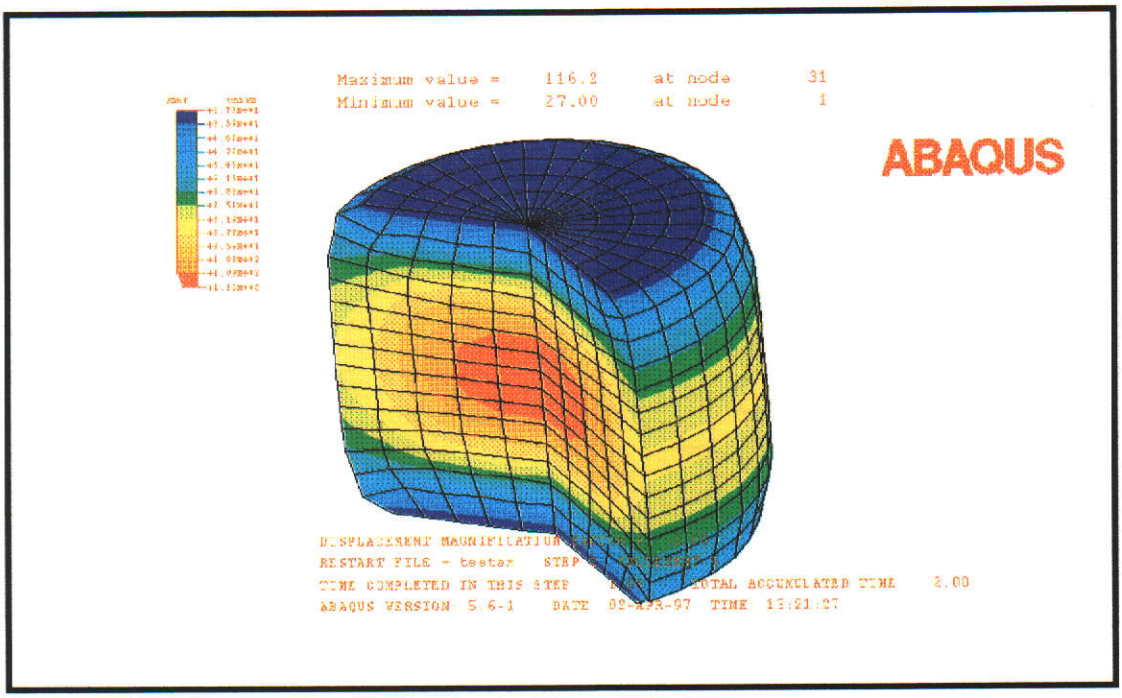

Figure 4.26 Contour plot of temperature within the test piece.

Chapter 5

VALIDATION OF PROCEDURE.

5.1 INTRODUCTION

The material data, the scaling of key material parameters and the procedure for temperature prediction have been verified using the cylindrical test piece. The proof of the pudding now lies in the ability to use the material properties and the procedure to predict the temperature distribution in an AirBoss tyre.

The exercise will use the 5.00 – 8 Industrial tyre which was moulded from the compound under investigation. This tyre was used to obtain hardness measurements and hence the elastic modulus of the compound used.

The tyre was also modelled and analysed for static load/deflection behaviour. Hence all the geometry data (nodal coordinates, element definitions and contact surface definition) are to hand. The Mooney – Rivlin coefficients have been estimated and fine-tuned after performing a load – deflection test on the tyre. Viscoelastic properties have, likewise, been estimated and then refined to give a good correlation for the step-strain/creep test of the cylindrical test piece. The heat dissipation properties have been obtained from the rubber cube tests. The heat generation properties have been obtained and refined using the Hysteresis Test Rig.

Three FE models of the 5.00-8 tyre have been created with varying mesh densities. It is important to repeat simulations, using varying mesh densities, to ensure that a poor quality mesh has not produced incorrect results.

5.2 COMPILING THE COUPLED TEMPERATURE DISPLACEMENT FILE.

Because of all the Abaqus input data compiled so far, the compilation of an input file to produce a temperature map of a cyclically squashed 5.00 – 8 tyre involves no

more than a moderate amount of 'cut and paste' text editing of the input files used so far. The file used for temperature predictions in the cylindrical test piece was used as a template. The node and element data was cut out and replaced by the node/element data for the 5.00 –-8 tyre. The geometry and contact conditions for the rigid plane which simulates the road were transferred from the 5.00 – 8 model to the template. The boundary condition of 10 millimetres of squash was replaced by 28 millimetres and the newly formed input file submitted to the Abaqus solver.

Because the model uses three-dimensional elements and because of the large amount of computation needed to solve for displacement and temperature generation and dissipation at the same time, the run to solve for temperature distribution in the finest mesh model took a total of nine hours. At the end of this time, all stress strain and temperature data were available.

The procedure described here is not identical with the real life situation of a tyre, under load, moving along the ground at speed. Under such conditions the entire tyre would develop a series of hot spots, corresponding to the number of times the geometric features of the tyre were repeated. The simulation seeks to apply the load conditions to a relatively small area of the tyre. An assumption is made that this gives information which correlates to the tyre in service.

5.3 THE A-FRAME TEST RIG

In order to assess the correlation between the predicted temperatures and temperatures generated in a physical test, the A-Frame test rig was built. This test rig is capable of holding a tyre/wheel assembly, up to 1100 millimetres in diameter and deforming the tyre by forcing a flat plate against it in a cyclic manner. The amount of deflection, that the tyre is forced to undergo, is adjustable and, in this case, set to 28 mm (to match the simulation).

The test – rig in question is shown, schematically, in figure 5.1 below and also in figure 5.2.

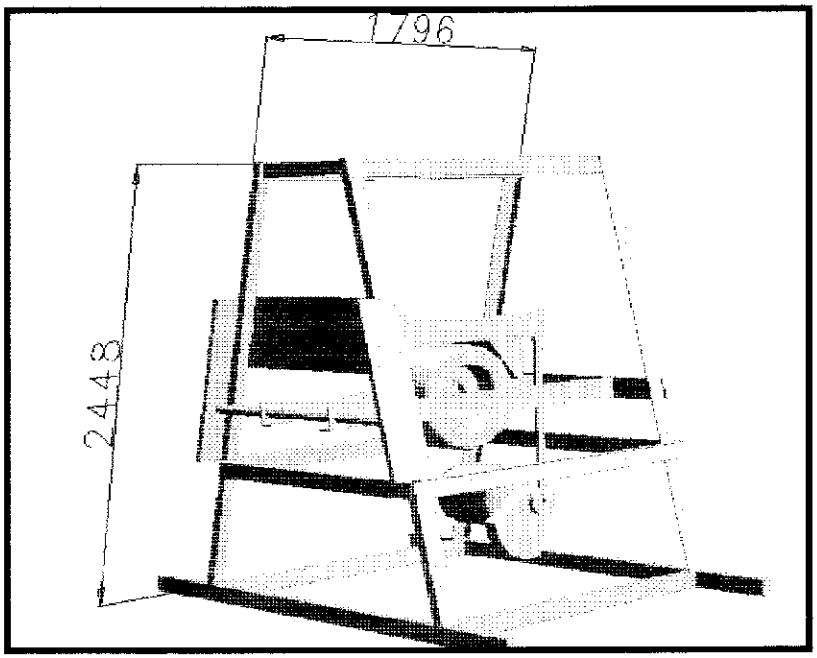

Figure 5.1 The 'A' Frame Test Rig for cyclically deflecting the 5.0008 tyre

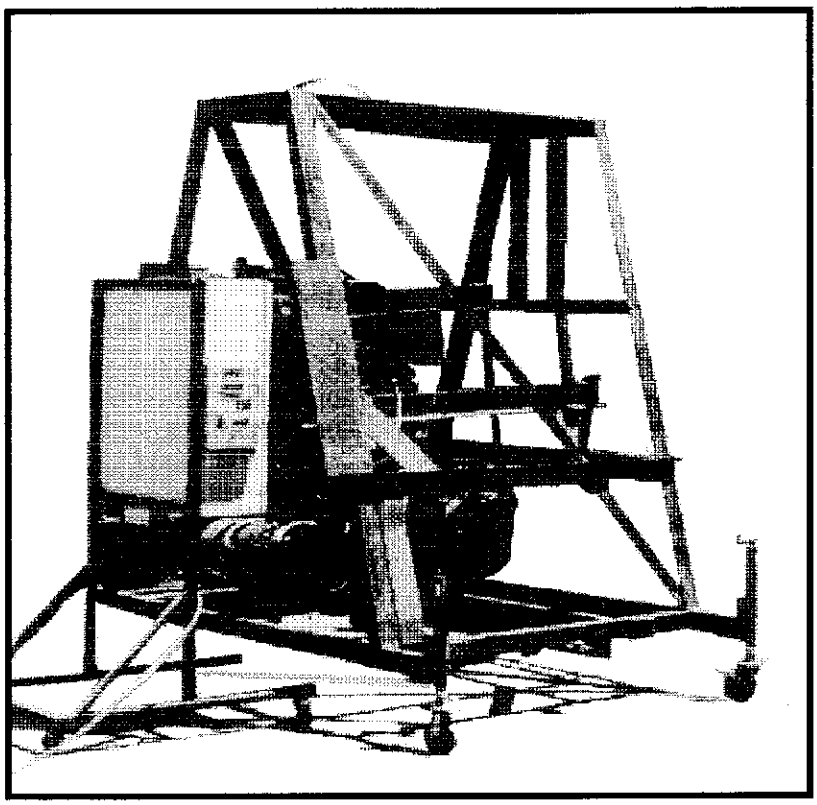

Figure 5.2 Photograph of 'A' Frame test rig

As can be seen from figures 5.1 and 5.2, the rig comprises an 'A' frame in which the test tyre can be rigidly mounted. A near-rigid arm which, carries a flat steel plate, is pivoted at one end of the rig. The other end of the pivoting arm is fixed to a crank-arm which is pinned, eccentrically, to a fly-wheel. The fly wheel and crank are driven by a variable speed electric motor. The arrangement causes the crank-arm to pull the plate onto the tyre, and deform it. The speed and amount of deflection are adjusted to match that of the likely conditions of the tyre in service which, in this case, have been determined to be 28 millimetres of deflection at a rate of 180 events per minute.

The temperature of the tyre, in the region being squashed by the plate, is read by pushing a thermocouple into the tyre to various depths at various time intervals.

5.4 RESULTS FROM THE A-FRAME RIG

Using the technique, described above, the basic temperature map shown at figure 5.3 has been created. Figure 5.4 is the temperature map predicted by Abaqus for this tyre.

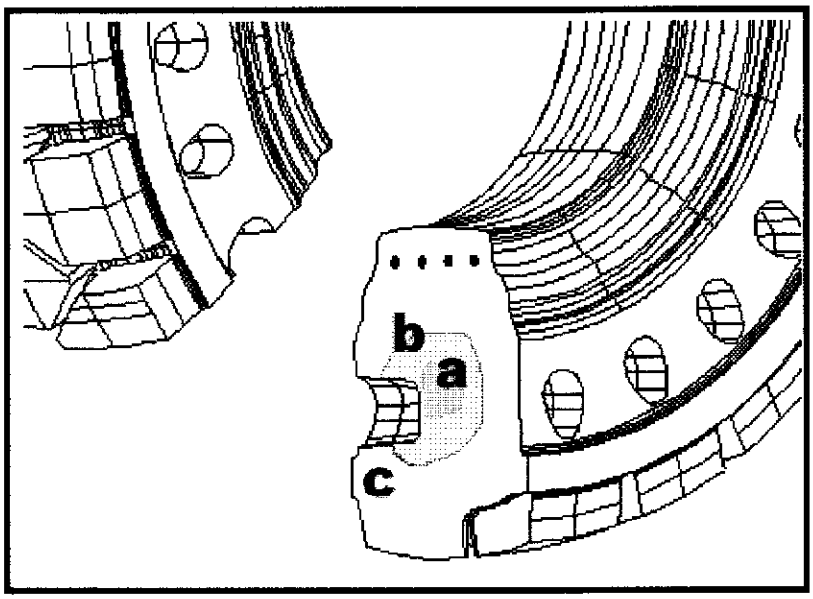

Figure 5.3 Contour plot of temperatures taken from the 5.00-8 tyre on 'A' frame test rig.

The temperature of the three regions, indicated by letters in figure 5.3 are;

(a) 125°C
(b) 112°C
(c) 52°C

The results from the Abaqus run, simulating the A-Frame test on the 5.00-8 tyre are shown below.

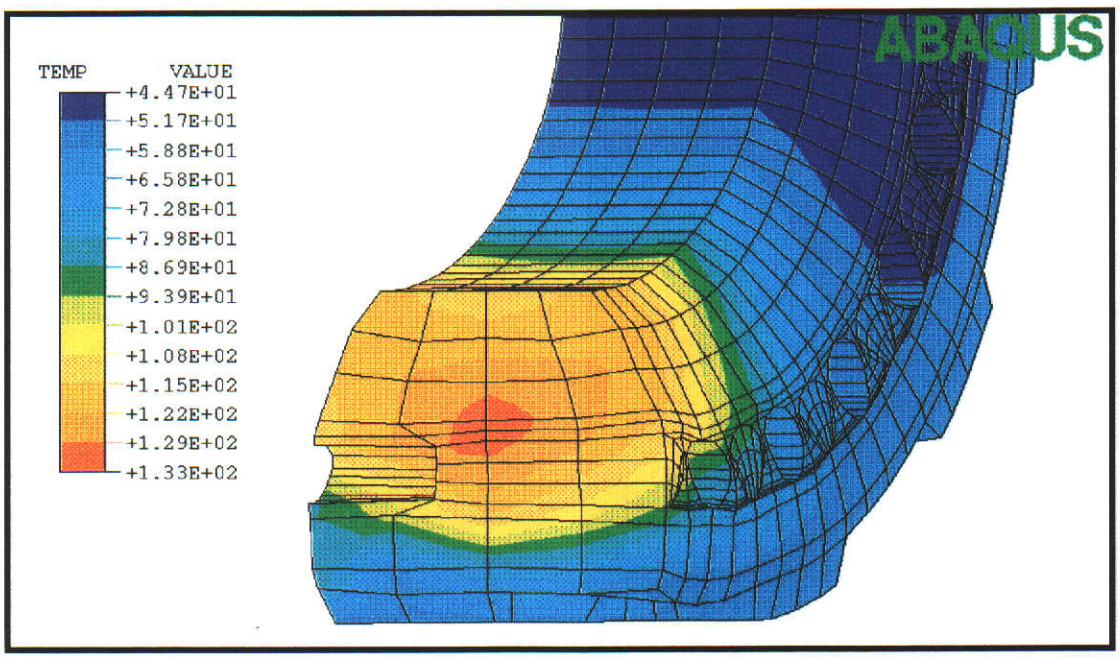

Figure 5.4 Temperature map produced by Abaqus

As can be seen by comparing the data from the physical test with those on the Abaqus contour plot legend;

Abaqus prediction of highest temperature is 6% higher than actual.
Prediction of mid temperature is about 4% lower than actual.
Prediction of temperature in coolest region is about 15% lower than actual.

Chapter 6

CONCLUSION AND DISCUSSION.

The eight-degree discrepancy between predicted maximum temperature and the temperature measured at the hottest spot on the 'A frame' test rig is within the tolerance accepted for other aspects of analysis for rubber. In practice, the properties of rubber compound vary by five percent from batch to batch, hence there is little hope of obtaining solutions that are nearly exact for all batches of compound. There are several reasons for coming to the conclusion that this method of predicting temperature distribution in the semi-solid AirBoss tyre is valuable as a design tool.

The exact final temperature is not needed in order to decide if a design is acceptable. An approximate figure will enable a design to be classified as 'hot' or otherwise. If there is a hot spot, then the design will be reworked to reduce it. If the design still appears to be borderline, then other methods can be used to check whether the predicted temperature is sufficiently in error to enable the tyre to be progressed to production. Methods such as moulding a tyre from an inexpensive mould, capable of producing two or three tyres can be used to decide whether or not an optimised design is suitable for production. A second method which has been employed to determine whether finite element analysis has produced results that are in error is to mould a tyre without the intended apertures or voids. After the tyre has cooled, it is part machined and then finished with hand tools to approximate the intended design. Both of the above methods are time consuming and hence, costly. Neither could be used to progressively optimise a tyre design.

On the other hand, once a tyre model has been meshed, it can be modified quickly and only the new node co-ordinates need to be put into the Abaqus input file. All other data in the file can remain as is. The checking methods mentioned earlier would only be used when a tyre design has been optimised and the results indicate that more information is needed to determine whether or not the design is acceptable.

Natural rubber varies in its properties. Chain lengths vary between 300 and 10000 monomer units. The amount of ash and other impurities also varies from batch to

batch. These variations make it impossible to predict the behaviour of components made from natural rubber with great accuracy.

Once a tyre has been analysed, if the amount of heat generation is too high the design can be modified by either reducing the amount of heat generated or by improving the heat dissipation properties of the design. In both cases the improvements can be made by alteration to either or both of the geometry of the design or the properties of the rubber compound.

The modifications that can be made to geometry of a tyre in order to reduce the amount of heat generated is to reduce the amount of strain and hence strain energy in the area of the tyre where the maximum heat is occurring. This is done, for example, by making the apertures or holes smaller. The limit to this method is that the overall deflection of the tyre under load becomes too small and hence the tyre becomes too stiff.

Heat dissipation can be improved by altering geometry so that the distance from the hot spot to a surface is minimised. It has been found that where a heat problem exists it is invariably in a thick section of the tyre. The very low heat conduction properties of rubber mean that in thick sections even moderate amounts of heat generation lead to a significant temperature rise. It is interesting to note that heat generation is minimised by making geometric sections thicker and heat dissipation is maximised by making sections thinner.

In a similar way heat generation can be reduced and heat dissipation can be increased by modifications to the natural rubber compound. The rubber compound becomes more resilient when the amount of carbon black filler is reduced. Unfilled rubber is the most resilient of all. However other properties of rubber are so enhanced by the use of fillers that its inclusion is vital. Resistance to tearing, to wear, to the tendency of cracks to propagate through the structure are all improved dramatically by the inclusion of particulate fillers. The use of higher structure (that is greater surface area per gram) carbon black means that lower amounts of the filler can give acceptable properties while keeping the resilience high.

Fillers other than carbon black can be used. Replacing a portion of the carbon black filler with silica can make the compound more heat tolerant. Silica does not form natural bridges with radical sites on the hydro carbon chain as does carbon black. For this reason the silica has to be surface coated and this means that the cost of using silica is high.

Zinc oxide can be added to improve the dissipation of heat in the compound. At inclusion rates of much more than ten percent other properties mentioned earlier can be compromised. For this reason six to ten parts per hundred of zinc oxide are included.

6.1 FUTURE DIRECTIONS

In general, further work needs to be done to refine the various tests used to obtain material parameters for compounds. There may be some scope for reducing the number of tests by obtaining, for example, the film coefficient and heat generation and dissipation properties during the Hysteresis test, rather than performing the additional test of moulding the rubber cube to measure film and conduction properties. It may be found that properties such as film coefficient do not vary from compound to compound and test for this property could be dropped altogether.

The ultimate aim must be a continual improvement in methodology leading to consistently high accuracy in predicting all aspects of a tyre's performance while it is at the design stage. There is a need to simplify and document the testing procedures so that shop floor personnel can conduct the tests in a routine manner whenever a new compound first arrives.

References

Hibbitt, Karlsson and Sorensen (1997) ABAQUS STANDARD USERS MANUAL, VERSION 5.6, pub. HKS Inc., Rhode Is., New York.

Aklonis J., MacKnight W., Mitchell s., (1972) INTRODUCTION TO POLYMER VISCOELASTICITY. Pub. Wiley Interscience, New York.

Bhowmick, A.K. & Stephens, H.L. (editors) (1988) HANDBOOK OF ELASTOMERS, pub. Marcel Dekker Inc., New York

Blatz, P.J., Sharda, S.C. & Tschoegl, N.W. (1974) "Strain Energy Functions for Rubberlike Materials Based on a Generalised Measure of Strain", *Journal of Rheology 18, pp145-161*

Bloch, R., Chang, W.V. & Tschoegl, N.W. (1978) "The Behaviour of Rubberlike Materials in Moderately Large Deformations", *Journal of Rheology 22, pp1-32.*

Cook, R.D., Malkus, D.S. & Plesha, M.E. (1989) CONCEPTS AND APPLICATIONS OF FINITE ELEMENT ANALYSIS – 3rd EDITION, pub. John Wiley and Sons Inc., Singapore.

Crandall, S.H. Dahl, N.C. & Lardner, T.J. (1978) AN INTRODUCTION TO THE MECHANICS OF SOLIDS – 2nd EDITION, pub. McGraw-Hill, New York

Ferry J. D. (1961) VISCOELASTIC PROPERTIES OF POLYMERS. Pub. John Wiley and sons. New York.

Gent A., (1992) ENGINEERING WITH RUBBER, HOW TO DESIGN RUBBER COMPONENTS. Pub. Hanser Publishers, New York.

Gent, A.N. & Thomas, A.G. (1958) "Forms for the Stored (Strain) Energy Function for Vulcanised Rubber", *Journal of Polymer Science 28 (108), pp.625-628*

Green, A.E. & Zerna, W. (1968) THEORATICAL ELASTICITY – 2nd EDITION, pub. Oxford Clarendon Press, London

Hofmann W., (1988) RUBBER TECHNOLOGY HANDBOOK. Pub. Hanser Publishers, New York.

Mooney, M. (1940) "A Theory of Large Elastic Deformation", *Journal of Applied Physics 11, pp.582-592.*

Mullins, L. (1987) "Engineering with Rubber", *Chemtech, Dec. 87, pp.720-727.*

Nagdi K. (1993) RUBBER AS AN ENGINEERING MAT ERIAL, GUIDELINES FOR USERS. Pub. Hanser Publishers, New York.

Obata, Y., Kawabata, S. & Kawai, H. (1970) "Mechanical Properties of Natural Rubber Vulcanizates in Finite Deformation", *Journal of Polymer Science Part A-2 8, pp903-919.*

Osswald T.A. and Menges G., (1995) MATERIALS SCIENCE OF POLYMERS FOR ENGINEERS. *Pub. Hanser Publishers, New York.*

Rivlin, R.S. (1948) "Large Elastic Deformation of Isotropic Materials. IV. Further Developments of the General Theory", *Philosophical Transactions of the Royal Society of London Series A 241, pp379-397.*

Rivlin, R.S. . & Saunders, D.W. (1951) "Large Elastic Deformation of Isotropic Materials. VII. Experiments on the Deformation of Rubber", *Philosophical Transactions of the Royal Society of London Series A 243, pp251-288.*

Rosen, P.J. (1971) PRINCIPLES OF POLYMERIC MATERIALS FOR PRACTISING ENGINEERS, pub. Barnes and Noble Inc., New York.

Spyrakos C.C. (1994) FINITE ELEMENT MODELING IN ENGINEERING PRACTICE, Pub. West Virginia University Press., Morgantown. USA

Turner D.M. (1988) "A Triboelastic Model for the Mechanical Behaviour of Rubber", *Plastics and Rubber Processing and Applications 9* (4), pp 197-201.

Turner D.M. & Brennan M. (1990) "The Multiaxial Behaviour of Rubber", *Plastics and Rubber Processing and Applications 14* (3), pp 183-188.

Ward I.M. and Hadley D.W. (1993) AN INTRODUCTION TO THE MECHANICAL PROPERTIES OF SOLID POLYMERS. Pub. John Wiley and Sons. Chichester, England .

Zienkiewicz, O.C. & Taylor, R.L. (1989) THE FINITE ELEMENT METHOD 4th EDITION, VOLUME 1: BASIC FORMULATION AND LINEAR PROBLEMS, pub. McGraw-Hill Book Co., London.

Zienkiewicz, O.C. & Taylor, R.L. (1990) THE FINITE ELEMENT METHOD 4th EDITION, VOLUME 2: SOLID AND FLUID MECHANICS, DYNAMICS AND NON-LINEARITY, pub. McGraw-Hill Book Co., London.

Bibliography

The Texts listed below were used to obtain much of the background material for this thesis. They are not quoted directly within the body of this thesis.

Alexander, H. (1968) "A Constitutive Relation for Rubber Like Materials", *International Journal of Engineering Science 6, pp.549-563.*

Arruda, E.M. & Boyce, M.C. (1993) "A Three-Dimensional Constitutive Model for the Large Stretch Behaviour of Rubber Elastic Materials", *Journal of the Physics of Solids 41(2), pp389-412.*

Babuska, I. (1990) "The Problem of Modelling the Elastomechanics in Engineering", *Computer methods in Applied Mechanics and Engineering 82, pp155-182*

Bubuska, I. & Rank, E. (1987) "An Expert-System-Like Feedback Approach in the hp-Version of the Finite Element Method", *Finite Element Analysis and Design 3, pp127-147.*

Bauer R.F. & Crossland, A.H. (1990) "The Resolution of Elastomer Blend Properties by Stress-Strain Modelling. An Extension of the Model to Carbon-Black-Loaded Elastomers", *Rubber Chemistry & Technology 63 pp.779-791*

Beringer, C.W., Kwon, Y.D. & Pevorsek, D.C. (1987) "Sensitivity of Temperature Rise in a Rolling Tire to the Viscoelastic Properties of the Tire Components", *Tire Science and Technology 15 (2), pp123-133.*

Blakey, K. (1989) "Getting the Best Designs with FEA" , *Machine Design, 20 July 89, pp89-93*

Blatz, P.J. & Ko, W.L. (1962) "Application of Finite Elastic Theory to the Deformation of Rubbery Materials"", *Transactions of the Society of Rheology 6, pp223-251.*

Brown, R.P. (1986) THE PHYSICAL TESTING OF RUBBER – 2nd EDITION, pub. Elsevier Applied Science Publishers Ltd., Barking, Essex

Cheung, Y.K. & Chen, W. (1989) "Hybrid Element Method for Incompressible and Nearly Incompressible Materials", *International Journal of Structures and Solids 25(4) pp483-495*

Courant, R. & Hilbert, D. (1953) METHODS OF MATHEMATICAL PHYSICS, pub John Wiley and Sons Inc., New York

Dawson, P.R. & Thompson, E.G. (1978) "Finite Element Analysis of Steady-State Elast-Visco-Plastic Flow by the Initial Stress-rate Method", *International Journal of Numerical Methods in Engineering 12, pp.47-57*

Dillon, O.W. Jnr (1962) "A Non-linear Thermoelasticity Theory", *Journal of Mechanics of Physical Solids 10, pp.123-131*

Doyle, M.J. (1988) "How Elastomers Fail in Fatigue", *Machine Design, 10-Mar-1988, pp.135-139*

Finney, R.H. & Kumar, A., (1988) " Development of Material Constants for Non-linear Finite Element Analysis", *Rubber Chemistry & Technology 61, pp.879-891.*

Fong, J.T. & Penn, R.W. (1975) "Construction of Strain-Energy Function for an Isotropic Elastic Material", *Transactions of the Society of Rheology 19(1), pp99-113*

Freakley, P.K. & Payne. A.R (1978) THEORY AND PRACTICE OF ENGINEERING WITH RUBBER, pub. Applied Science Publishers, London

Fried, I. (1974) "Finite Element Analysis of Incompressible Material by Residual Energy Balancing", *International Journal of Solids and Structures 10, pp.993-1002*

Fried, I. & Johnson, A.R. (1988) "A Note on Elastic Density Functions for Largely Deformed Compressible Rubber Solids", *Computer Methods in Applied Mechanics and Engineering 69, pp53-64*

Fried, I. & Johnson , A.R. (1988) "Non-linear Computation of Axisymmetric Solid Rubber Deformation", *Computer Methods in Applied Mechanics and Engineering 67, pp241-253.*

Funt, J.M. (1987) "Dynamic Testing and Reinforcement of Rubber", *Paper 54, 131st Meeting of the Rubber Division, American Chemical Society, Montreal, 26-29 May 1987.*

Futamura, S. (1991) "Deformation Index – Concept for Hysteretic Energy Loss Process", *Rubber Chemistry & Technology 64, pp57-64*

Gent, A. & Hindi, M. (1988) "Heat Build-up and Blow-out of Rubber Blocks", *Rubber Chemistry & Technology 64, pp.892-905*

George, E.D. jnr., Haduch, G.A. & Jordan, S. (1988) "The Integration of Analysis and Testing for the Simulation of the Response of Hyperelastic Materials", *Finite Elements in Analysis and Design 4, pp237-247*

Golden, J.M. & Graham, G.A.C., (1988) BOUNDARY VALUE PROBLEMS IN LINEAR VISCOELASTICITY Pub. Springer-Verlag, New York.

Hart-Smith, L.J. & Crisp, J.D.C. (1967) "Large Elastic Deformations of Thin Rubber Membranes", *International Journal of Engineering Science 5 pp.1-24*

Hepburn, C. & Reynolds, R.J.W. (Editors) 1979 ELASTOMERS: CRITERIA FOR ENGINEERING DESIGN, pub. Applied Science Publishers Ltd., Barking, Essex

Hong, I., Lee, T.W., Vivic, J. & Roldan, S. (1990) "Hysteretic Heat Generation in Elastomeric Components: Experiment and Simulation", *Presented at the 137th Meeting of the Rubber Division of the American Chemical Society, Las Vegas, Nevada, May 29 – June 1 1990*

James, A.G. & Green, A. (1975) "Strain Energy Functions of Rubber, II. The Characterisations of Filled Vulcanizates", *Journal of Applied Polymer Science 19, pp.2319-2330*

Kar KK. Bhowmick AK. MEDIUM STRAIN HYSTERESIS LOSS OF NATURAL RUBBER AND STYRENE-BUTADIENE RUBBER VULCANIZATES – A PREDICTIVE MODEL. *Polymer. 40(3):683-694, 1999 Feb.*

Kong, D.C. & Meinecke, E.A. (1984) "Heat Build-up of Bonded Rubber Blocks Due to Shear Cycling", *Contribution 29, Presented at the 126th Meeting of the Rubber Division, American Chemical Society, Denver Colorado, Oct 23-26 1984*

Kraus, G. (1984) "Mechanical Losses in Carbon-Black Filled Rubbers", *Journal of Applied Polymer Science, Applied Science Symposia 39, pp75-92*

Kugler, H.P., Stacer, R.G. & Steimle, C. (1990) "Direct Measurement of Poisson's Ratio in Elastomers", *Rubber Chemistry & Technology 63, pp.473-487.*

Landau L.D. and Lifshitz E.M., (1959) THEORY OF ELASTICITY 3RD EDITION Pub. Pergamon Press, Oxford

Lau, J.H. & Jeans, A.H. (1989) "Non-Linear Analysis of Elastomeric Keyboard Domes", *Journal of Applied Mechanics 56, Dec 89, pp.751-755*

Lee, B.L. (1981) "Dynamic Mechanical Properties and Heat Build-up of Carbon Black Loaded Rubber Vulcanizates", *Society of Plastics Engineers 39th Annual Technical Conference, Boston, USA, 4-7 May 1981*

Liau WB. Cheng KC. DYNAMIC MECHANICAL RELAXATION OF LIGHTLY CROSS-LINKED NATURAL RUBBER. *Polymer.* 39(24):6007-6012, 1998 Nov.

Lindley, P.B. (1992) ENGINEERING DESIGN WITH NATURAL RUBBER – 5th EDITION, Revised by Fuller K.N.G. & Muhr, A.H., pub. Malaysian Rubber Producers Research Association, Brickendonbury, England.

Liu, G.Q. & Owen, D.R.J. (1989) "The Computer Simulation of Rubber Components and Composites", *Composite Science and Technology 36, pp.267-281*

Malaysian Rubber Producers Research Association (1980) NATURAL RUBBER ENGINEERING DATA SHEETS. Pub. Malaysian Rubber Research and Development Board., Brickendonbury, Hertford, England.

Manna AK. De PP. Tripathy DK. De SK. Chatterjee MK. CHEMICAL INTERACTION BETWEEN SURFACE OXIDIZED CARBON BLACK AND EPOXIDIZED NATURAL RUBBER. *Rubber Chemistry & Technology*. 70(4):624-633, 1997 Sep-Oct.

Medalia, A.I. (1991) "Heat Generation in Elastomer Compounds: Causes and Effects", *Rubber Chemistry & Technology 64, pp.481-492*

Meinecke, E. (1991) "Effect of Carbon Black Loading and Crosslink Density on the Heat Buildup in Elastomers", *Rubber Chemistry & Technology 64, pp269-284*

Mooney, M. (1940) "A Theory of Large Elastic Deformation", *Journal of Applied Physics 11, pp.582-592.*

Moore, E.J. (1993) HEAT GENERATION IN A SEGMENTED NON-PNEUMATIC TYRE, Final Year Project Report; K.K. Teh and D.J. Charlton (Supervisors), Department of Mechanical Engineering, Curtin University, Perth, Australia.

Morman, K.N. & Pan, T.Y. (1988) "Application of Finite Element Analysis in the Design of Automotive Elastomeric Components", *Rubber Chemistry & Technology 61, pp503-533*

Mullins, L. (1987) "Engineering with Rubber", *Chemtech, Dec. 87, pp.720-727.*

Nakajima, N., Chu, M.H. & Babrowicz, R. (1990) "Tensile Stress-Strain Measurements for Characterisation of Gum Elastomers and Filled Compounds", *Rubber Chemistry & Technology 63, pp.624-636.*

Nakajima, N., Scobbo, J.J. Jnr. & Harrell, E.R. (1987) "Comparison of Tensile and Shear Behaviour of Carbon Black Filled Elastomers", *Rubber Chemistry & Technology 63, pp624-636.*

Nicholson, D.W. & Nelson, N.W. (1990) "Finite-Element Analysis in Design with Rubber", *Rubber Chemistry & Technology 63, pp368-406.*

Obata, Y., Kawabata, S. & Kawai, H. (1970) "Mechanical Properties of Natural Rubber Vulcanizates in Finite Deformation", *Journal of Polymer Science Part A-2 8, pp903-919.*

Oden, J.T. (1972) FINITE ELEMENTS OF NON-LINEAR CONTINUA, pub. McGraw-Hill Book Co., New York,

Ogden, R.W. (1986) "Recent Advances in Phenomenological Theory of Rubber Elasticity", *Rubber Chemistry & Technology 59, pp361-383*

Peng, T.J & Landel, R.F. (1972) "Stored Energy Function of Rubberlike Materials Derived from Simple Tensile Data", *Journal of Applied Physics 43 (7), pp3064-3067*

Purushothaman, N., Heaton, B.S. & Moore, I.D. (1988) "Experimental Verification of a Finite Element Contact Analysis", *Journal of Testing and Evaluation 16, pp497-507.*

Reed, T.F. (1989) "Heat Buildup of Dynamically Loaded Engineering Elastomeric Components- I", *Elastomerics, November 1989, pp.22-28.*

Reed, T.F. (1989) "Heat Buildup of Dynamically Loaded Engineering Elastomeric Components- II", *Elastomerics, December 1989, pp.28-35.*

Roberts, B.J. & Benzies, J.B. (1978) "Relationship between Uniaxial and Equibiaxial Fatigue in Gum and Carbon Black Filled Vulcanizates", *Plastics and Rubber: Materials and Applications, May 1978, pp49-54.*

Sawczuk a. and Bianchi G., (1983) PLASTICITY TODAY: MODELLING, METHODS AND APPLICATIONS. Pub. Elsevier Applied Science Publishers, London and New York.

Seki, W., Fukahori, Y., Iseda Y. & Mutsunaga, T. (1987) "A Large Deformation Finite Element Analysis for Multilayer Elastomeric Bearings", *Rubber Chemistry & Technology 60, pp.856-869.*

Shaw, M.C. & Young, E. (1988) "Rubber Elasticity and Fracture", *Journal of Engineering materials and Technology 110, Jul. 88, pp.258-265.*

Smith, T.L. (1964) "Ultimate Tensile Properties of Elastomers. II. Comparison of Failure Envelopes for Unfilled Elastomers", *Journal of Applied Physics 35 (1), pp.27-36*

Steele, J.M. (1989) APPLIED FINITE ELEMENT MODELLING: PRACTICAL PROBLEM SOLVING FOR ENGINEERS, pub. Marcel-Dekker Inc., New York.

Sullivan, J.L. (1987) "A Nonlinear Viscoelastic Model for Representing Nonfactorisable Time-Dependent Behaviour in Cured Rubbers", *Journal of Rheology 31, pp.271-295.*

Sullivan, J.L. & Mazich, K.A. (1989) "Non-Separable Effects in Rubber Viscoelasticity", *Rubber Chemistry and Technology 62, pp.68-81.*

Swanson, S.R. (1985) "A Constitutive Model for High Elongation Elastic Materials", *Journal of Engineering Materials and Technology 107, pp.110-114.*

Tabaddor, F. (1989) "Finite Element Analysis of a Rubber Block in Frictional Contact", *Computers and Structures 32 (3,4), pp.549-562*

Teh, K.K. (1983) "A Three Dimensional Analysis of Laminated Composite Plates Using Numerical Methods", Ph.D Thesis, Department of Mechanical Engineering, University of Melbourne, Victoria, Australia.

Thomas, A.G. (1955) "The Departures from the Statistical Theory of Rubber Elasticity", *Transactions of the Faraday Society 51, pp.569-582.*

Tobisch, K. (1980) "Contribution to the Mathematical Description of Stress – Strain Behaviour of Elastomers", *Rubber Chemistry & Technology 53, pp.836-841.*

Tobisch, K. (1981) "A Three-Parameter Strain Energy Density Function for Filled and Unfilled Elastomers", *Rubber Chemistry & Technology 54, pp.930-939.*

Treloar L.G.R. (1958) THE PHYSICS OF RUBBER ELASTICITY – 2ND EDITION. Pub. Oxford University Press. London

Tschoegl, N.W. (1972) "Constitutive Equations for Elastomers", *Rubber Chemistry & Technology 45, pp.60-70.*

Turner D.M. & Brennan M. (1990) "The Multiaxial Behaviour of Rubber", *Plastics and Rubber Processing and Applications 14* (3), pp 183-188.

Turner, M.J., Clough, R.W., Martin, H.C. & Topp, L.J. (1956) "Stiffness and Deflection Analysis of Complex Structures", *Journal of Aeronautical Science 23, pp.805-823.*

Willet, P.R. (1973) "Hysteretic Losses in Rolling Tyres", *Rubber Chemistry & Technology 46, pp.425-441.*

Yeoh, O.H. (1990) "Characterisation of Elastic Properties of Carbon Black Filled Rubber Vulcanizates", *Rubber Chemistry & Technology 63, pp.792-805.*

APPENDIX 1. PRINTOUTS FROM THE FINAL ABAQUS RUN

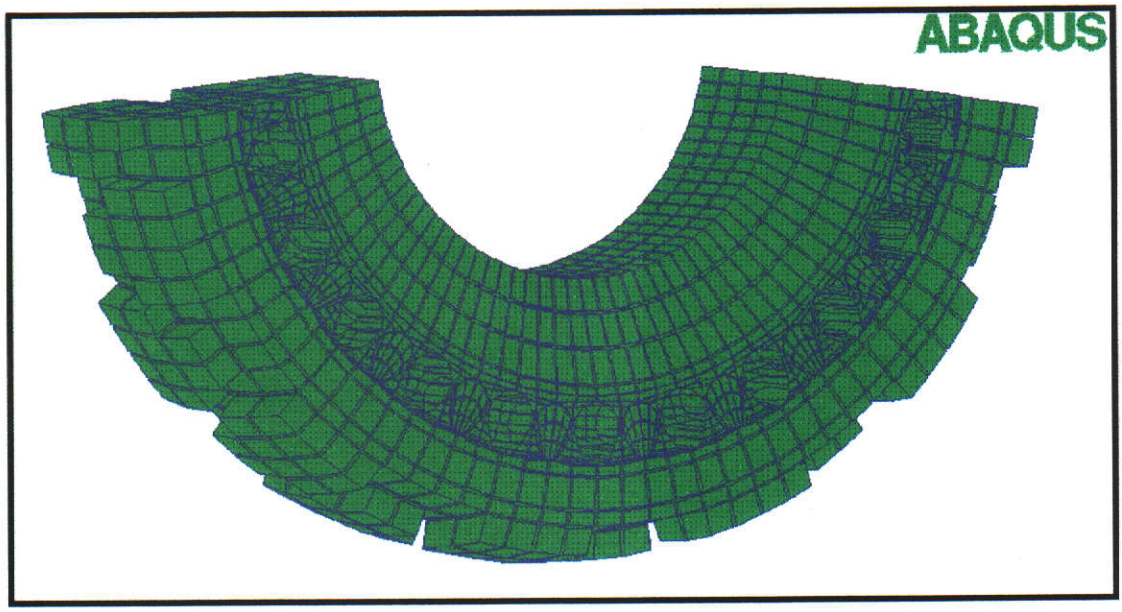

Figure A1.1. Undeformed FE Model of 5.00 – 8 Industrial Tyre

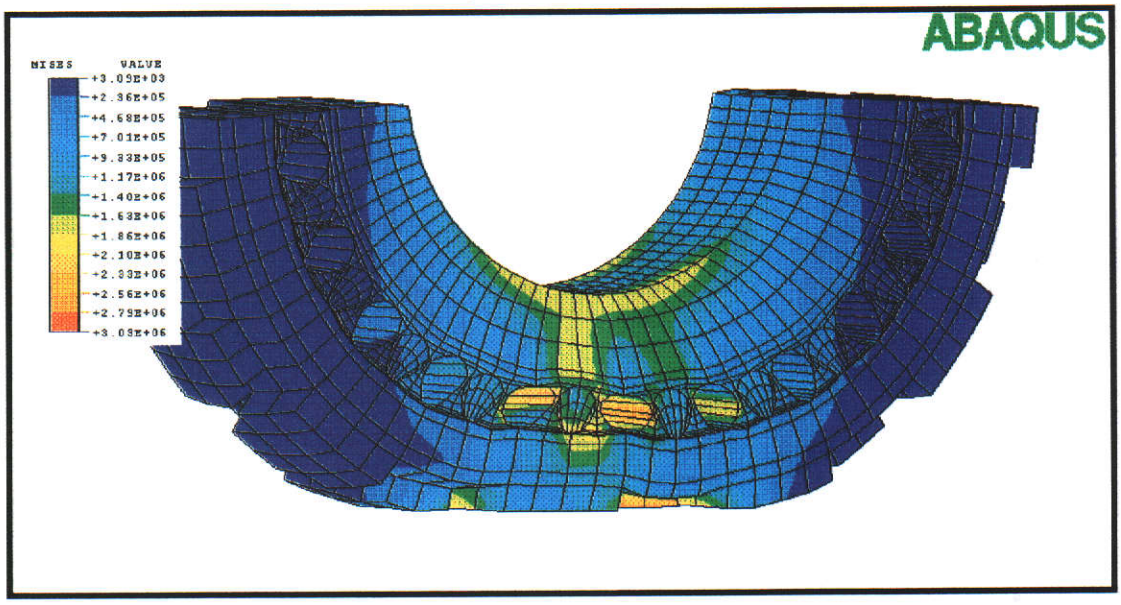

Figure A1.2. Plot of Mises stress contours on deformed tyre model

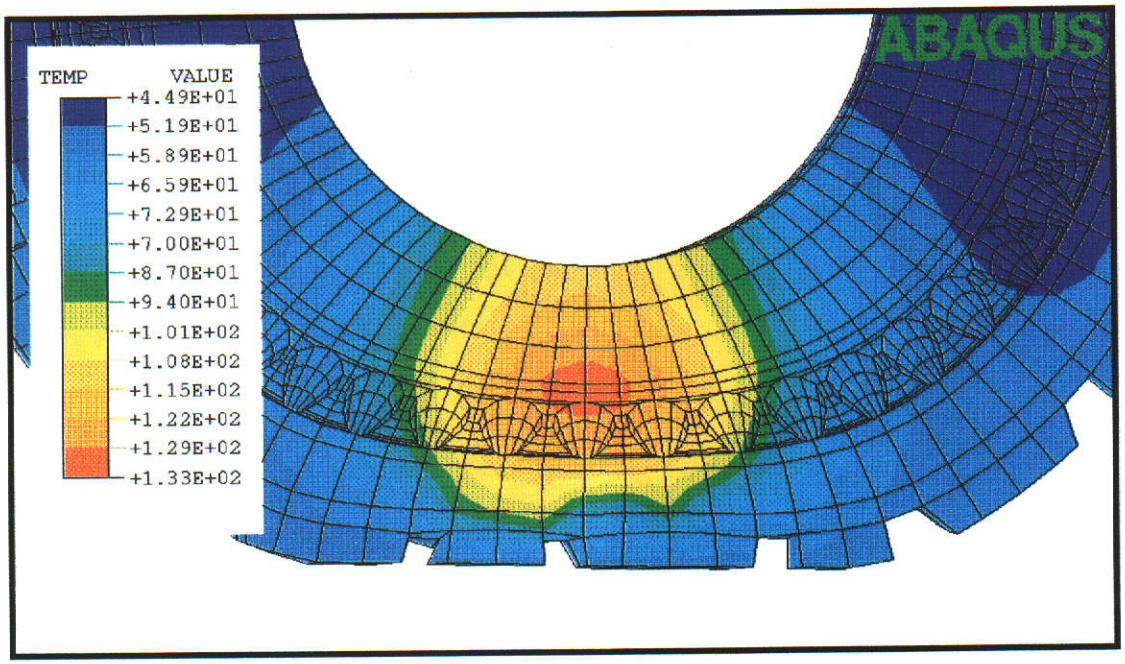

Figure A2.1 Contour plot of temperature of a slice of elements at centre of tyre

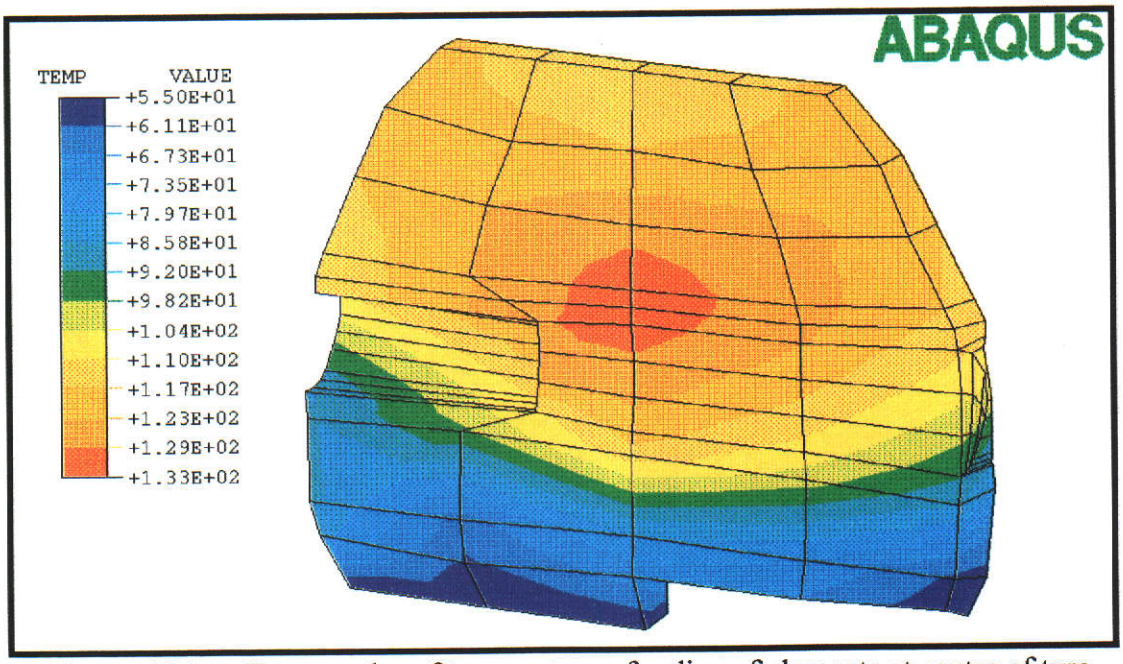

Figure A2.2 Contour plot of temperature of a slice of elements at centre of tyre

APPENDIX 3. THE ABAQUS INPUT FILE

```
*HEADING
THE ABAQUS INPUT FILE FOR ANALYSIS OF HEAT GENERATION
IN A 5.00 - 8 AIRBOSS INDUSTRIAL TYRE
*NODE,NSET=REF
     99999,0.00000E+00,0.00000E+00,0.00000E+00
*NODE,NSET=NALL
       1, 4.2423623E-04,-1.4865161E-01, 1.5000001E-01
       2, 4.2423623E-04,-1.4865161E-01, 1.0000000E-01
       3, 4.2423623E-04,-1.4865161E-01, 5.0000001E-02
**       Remaining nodal data removed
*ELEMENT,TYPE=C3D8HT,ELSET=BRICKS
    1,    1,    2,    6,    5,   41,   42,   46,   45
    2,    2,    3,    7,    6,   42,   43,   47,   46
    3,    3,    4,    8,    7,   43,   44,   48,   47
Remaining element data removed
*NSET,NSET=FIXED
   12,   11,   10,    9,    8,    7,    6,    5,    4,    3,    2
    1,  161,  162,  163,  164,  165,  166,  167,  168,  297,  298
** These nodes are fixed in space
*ELSET,ELSET=FILM
    5,   10,   15,   20,   25,   30,   35,   40,   50,   55,   60
**       The above elements have faces which are on the surface of the tyre
*CONTACT NODE SET,NAME=TYRE
   32,   31,   30,   29,   33,   34,   35,   36,   37,   38,   39
   40,  169,  170,  171,  172,  173,  174,  175,  176,  325,  326
** Nodes named here may make contact with the rigid surface
*RIGID SURFACE, TYPE=CYLINDER,NAME=ROAD,REF NODE=99999
0.,-0.216,0.,0.1,-0.216,0.
0.,-0.216,-0.1
START,+.25,0.
LINE,-.25,0.
**       Above lines describe a rigid plane
*CONTACT PAIR,SMALL
SLIDING,INTERACTION=ROADTYRE,ADJUST=.001,HCRIT=.012
TYRE,ROAD
*SURFACE INTERACTION,NAME=ROADTYRE
*SURFACE CONTACT
3.E-4,1.E01
*FRICTION,ROUGH
**       Above lines define and control contact between the
**       rigid surface and the contact nodes
**
**
**
**
*SOLID SECTION,ELSET=BRICKS,MATERIAL=RUBBER
```

```
*MATERIAL,NAME=RUBBER
*HYPERELASTIC,N=2,TEST DATA INPUT
**
**     (a) ENG.STRESS(Pa),STRAIN
**     (b) Scale factor = 5.0 MPa
**
*UNIAXIAL TEST DATA
.4545E+06, .10
.8333E+06, .20
.1154E+07, .30
.1429E+07, .40
.1667E+07, .50
.1875E+07, .60
.2059E+07, .70
.2222E+07, .80
.2368E+07, .90
.2500E+07,1.00
*SHEAR TEST DATA
.5878E+06, .10
.1050E+07, .20
.1423E+07, .30
.1729E+07, .40
.1984E+07, .50
.2201E+07, .60
.2386E+07, .70
.2547E+07, .80
.2688E+07, .90
.2813E+07,1.00
*BIAXIAL TEST DATA
.8490E+06, .10
.1470E+07, .20
.1939E+07, .30
.2303E+07, .40
.2593E+07, .50
.2827E+07, .60
.3021E+07, .70
.3182E+07, .80
.3320E+07, .90
.3438E+07,1.00
*VISCOELASTIC,TIME=PRONY
.672,0.0,10
*INELASTIC,HEAT FRACTION
9900.
*CONDUCTIVITY
.86E+04
*DENSITY
1130.
*SPECIFIC HEAT
1860.
*RESTART,WRITE
*STEP,NLGEOM,INC=10
```

```
*COUPLED TEMPERATURE-DISPLACEMENT,DELTMX=100
0.2,1.0,0.01,1.0
*BOUNDARY,OP=NEW
FIXED,1,3,0.
REF,1,1,0.
REF,3,3,0.
REF,2,2,0.028
*FILM
FILM,F2,25.,630.
*NODE FILE,NSET=NALL
NT
RF
U
*NODE PRINT,FREQUENCY=1
NT
RF
U
*EL PRINT,FREQUENCY=1
TEMP
E
S
*END STEP
**********************************************
```

APPENDIX 4 THE ROLLING DRUM TEST RIG

Once a tyre has been produced, before it is subjected to field trials, its performance is tested on a rolling drum test rig. The rig consists of a 1.7 metre diameter drum which is free to rotate. A heavy duty axle, which is driven from a variable speed electric motor, is fitted with the tyre under test. The tyre is forced against the drum and then rotated at speed. The normal procedure is to gradually increase the speed and applied load in order to arrive at set of circumstances at which the tyre will fail due to either fatigue or the rubber reverting (degrading dramatically due to excessive heat).

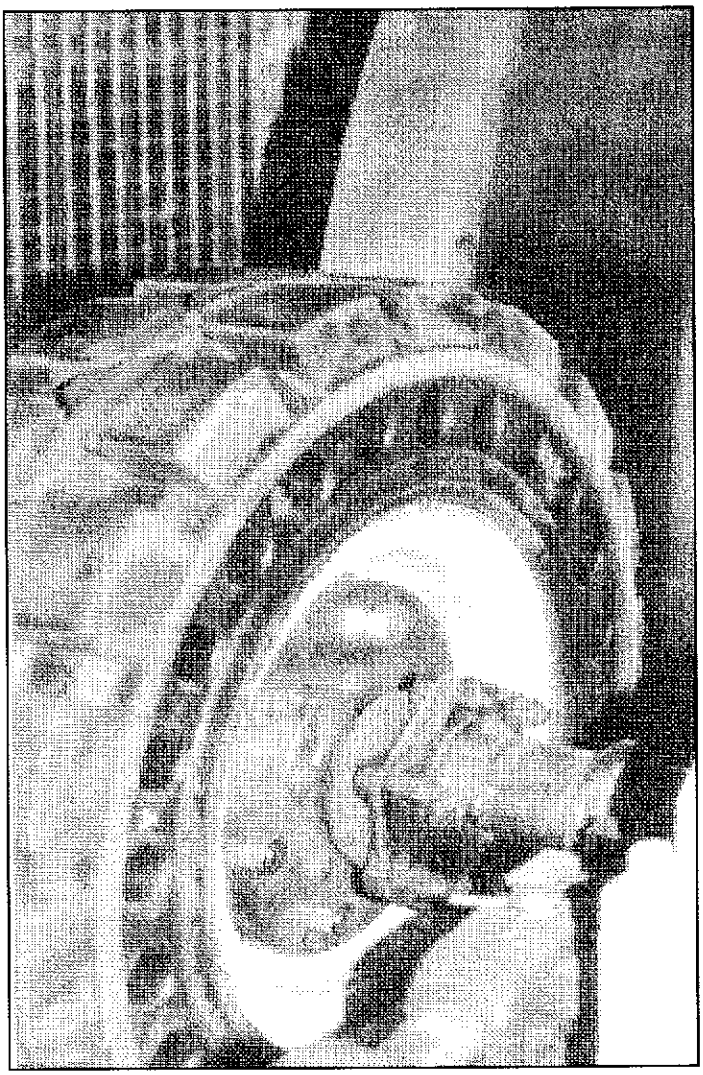

Figure A4.1 The 5.00 – 8 AirBoss Industrial tyre being tested on the drum rig.

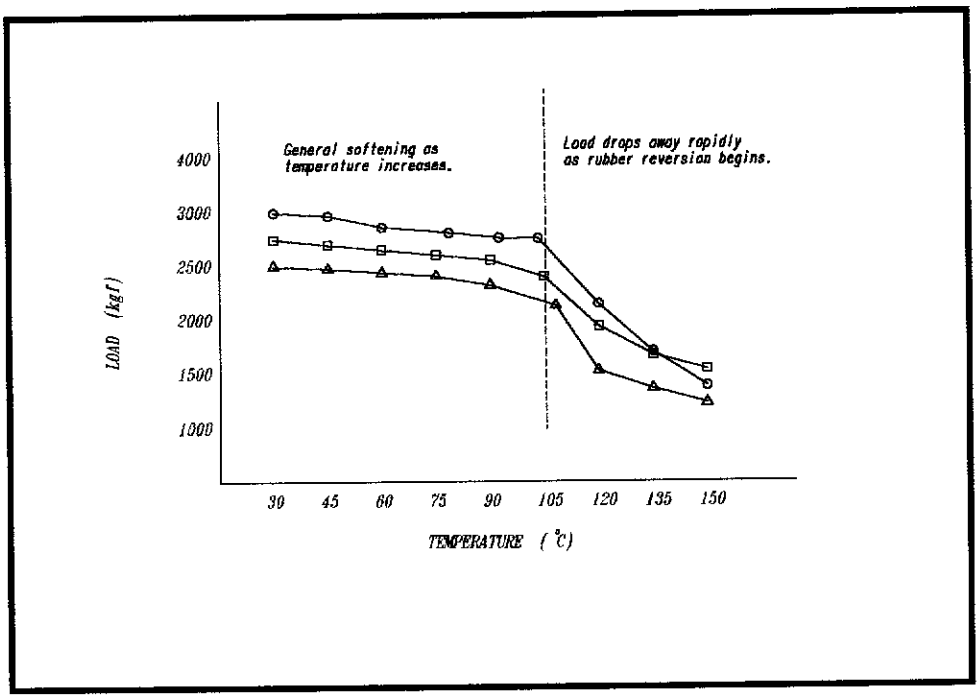

Figure A.4.2 Load Bearing Capacity of Test Tyre Vs. Temperature

The figure shows results from rolling drum tests on three tyres. All three are the same design. The variation in data is due to three different grades of carbon black filler being used in the compounds.

As can be seen from the plotted data, once the rubber temperature climbs above about 110°C, the tyre's ability to bear a load decreases dramatically. This phenomena is termed reversion. The rubber becomes a near liquid.

APPENDIX 5 THE CYLINDRICAL TEST PIECE MOULD TOOL

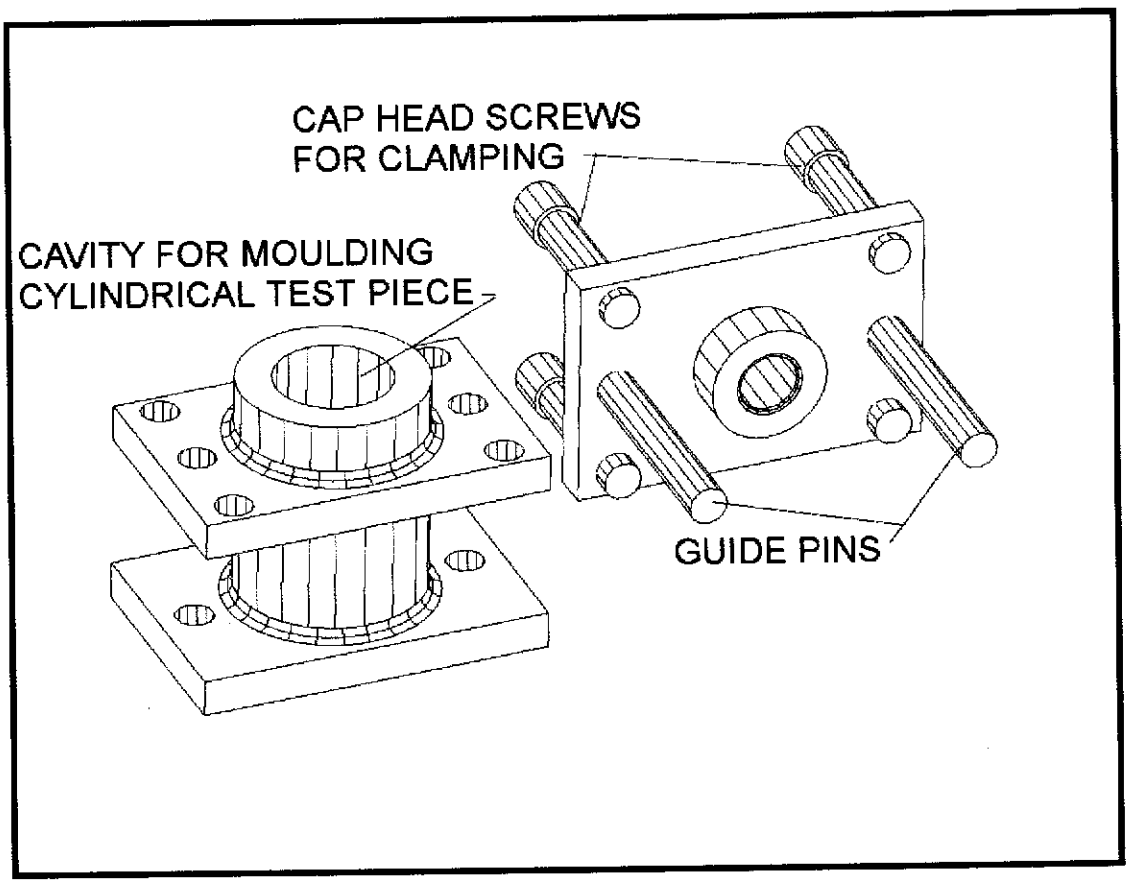

Figure A5.1 The simple mould manufactured to produce cylindrical test-pieces In the Hysteresis Test Rig.